Transport properties of selected polymer films.

Wickham, M. D.

Award date:
1983

Awarding institution:
University of Bath

TRANSPORT PROPERTIES OF SELECTED POLYMER FILMS

Submitted by M. D. Wickham
for the degree of Ph. D. of the
University of Bath
1983

M D Wickham

M. D. Wickham

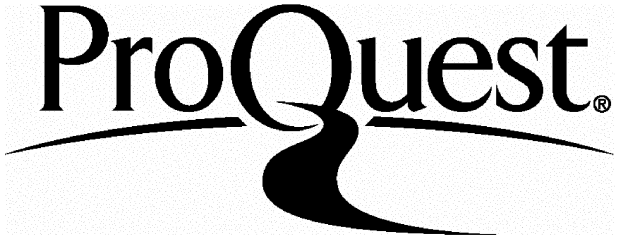

To my Mother and Father

ACKNOWLEDGEMENTS

The author would like to thank the following people for their contribution towards the preparation of this thesis.

Dr. A. J. Ashworth and Professor F. S. Stone, my supervisors for their help and advice throughout this work.

Mr. J. Stainer for technical assistance.

Mr. G. J. Price for assistance with the vacuum microbalance work.

Mrs. M. J. Riggans for typing the thesis.

The Ministry of Defence for the award of a Research Grant.

The members of laboratory 4W.05 who made my working time lively and eventful.

MEMORANDUM

The work described in this thesis was conducted in the Department of Physical Chemistry of the University of Bath during the period October 1979 and October 1982 and has not been submitted for any other degree. All the work described is the original work of the author except where specially acknowledged.

SUMMARY

A dynamic system has been developed for measuring permeability and diffusion coefficients for the transport of gases and vapours through polymer films. Activation energies determined for the permeation of methane through low density PE film using this system were found to agree well with values from the literature.

The permeation of tetrachloroethylene, nitroethane, dichloromethane and methane through poly(tetrafluoroethylene-co-hexafluoropropylene) (FEP) film was investigated over the temperature range 20 - 100 °C. Linear Arrhenius plots were found for permeability and diffusion coefficients with a change in gradient and therefore activation energies for permeation and diffusion below the glass transition temperature. This effect was more pronounced for the larger permeant molecules. Permeability and diffusion coefficients were also measured for nitroethane and dichloromethane permeation through poly(ethylene terephthalate) over the temperature range 60 - 140 °C. Once again linear Arrhenius plots were found with a change in gradient at the glass transition temperature.

Differences were found between the activation energies for permeation and diffusion of methane in samples of FEP that were annealed at different temperatures, namely 100 °C and 200 °C. Measurements using several techniques showed that the polymer annealed at the higher temperature had greater levels of crystallinity. Sorption isotherms were obtained for dichloromethane uptake in FEP samples in the as-received state, annealed at 100 °C and annealed at 200 °C. The isotherms were all found to show a downward curvature indicative of a dual-mode type sorption. The isotherms obtained with FEP in the as-received state and annealed at 100 °C were very similar

whereas the uptake of dichloromethane by the sample annealed at 200 °C was significantly lower. Isotherms obtained for the sorption of nitroethane and tetrachloroethylene showed very little dual-mode characteristics.

Solubility coefficients for dichloromethane, nitroethane and tetrachloroethylene sorption in FEP at 30 °C were obtained from static measurements. These were compared with values obtained from the dynamic method and found to be in reasonable agreement. Much larger solubilities were found for tetrachloroethylene than nitroethane despite the two permeants having similar vapour pressures at the measurement temperatures.

CONTENTS

TABLES

CHAPTER 1 INTRODUCTION

1.1 Objectives

In this research project there was an initial need to find a polymer film that had a low permeability to oxygen and favoured the transport of organic nitro-compounds relative to organic chloro-compounds. Essentially permeation is a function of solubility and diffusion. Solubility determines the amount of permeant which can be accommodated by the film and diffusion relates to the speed with which the permeant moves through the film. In general diffusion is governed by the size of the permeant molecule; the larger the molecule the slower the diffusion process. Thus, if a film is to provide selective permeation between two permeants of similar size it must have a greater attraction for one of the permeants resulting in the permeant having a greater solubility in the film than the other permeant.

The solubility and permeability tables in the Polymer Handbook[1] were examined to discover polymers having the following properties:-

(i) low oxygen permeability

(ii) high solubility in organic nitro-compounds

and

(iii) low solubility in organic chloro-compounds.

This showed poly(ethylene terephthalate) (PET) to be worthy of investigation. Furthermore, it had the advantage of being commercially available in a variety of film thicknesses.

Permeability and diffusion coefficients were determined for nitroethane and dichloromethane through PET film. These permeants were chosen as being representative of organic nitro- and chloro-compounds.

During the course of the project the interest changed from finding a polymer film that had a low permeability to oxygen and favoured the transport of organic nitro-compounds relative to organic chloro-compounds, to finding a polymer film that showed other permeability characteristics. The new requirements were:-

(i) a low permeability to water,

(ii) a high permeability to carbon dioxide relative to oxygen.

The selectivity to organic nitro-compounds relative to organic chloro-compounds was now less important.

A survey of the literature showed that the polymers poly(tetrafluoroethylene) (PTFE) and poly(tetrafluoroethylene-co-hexafluoropropylene) (FEP) showed a low permeability to water and a high general permeability. The permeability ratio of carbon dioxide to oxygen was found to vary little between different polymer films. Since PTFE and FEP fulfilled two of the permeability requirements and were available commercially as films in several thicknesses, they were both considered worthy of investigation. Permeability and diffusion coefficients were determined at different temperatures for the permeation of dichloromethane and nitroethane through PTFE film and dichloromethane, nitroethane and tetrachloroethylene through FEP film. Permeability coefficients were also determined for the permeation of methane through poly(ethylene) (PE), PTFE and FEP.

Work was continued with FEP film which was found to be the most suitable for investigation in this project. A vacuum microbalance was used to determine sorption isotherms for FEP film samples and several different absorbates. Other work involved determining changes in the crystalline content of FEP film annealed at different temperatures. The methods used to measure changes in crystallinity of the film were, differential scanning calorimetry (DSC), infrared absorption spectroscopy and density measurements.

1.2 Transport Through Polymer Films

The rate of transfer of a diffusing substance through unit cross-sectional area of an isotropic medium is given by Fick's first law of diffusion,

$$F = -D \frac{\partial c}{\partial x} \tag{1.1}$$

F is the rate of transfer per unit cross-sectional area, D is the mutual diffusion coefficient, c the concentration of diffusing substance and x the space co-ordinate measured normal to the section.

Using equation (1.1) and performing a mass balance of unit volume of an isotropic medium gives the differential equation,

$$\frac{\partial c}{\partial t} = D\left(\frac{\partial^2 c}{\partial x^2} + \frac{\partial^2 c}{\partial y^2} + \frac{\partial^2 c}{\partial z^2}\right) \tag{1.2}$$

where t is the time and x, y and z are space co-ordinates. If diffusion in one direction only is considered, such as diffusion through a plane sheet, and if that direction is along the x-axis equation (1.2) becomes,

$$\frac{\partial c}{\partial t} = D \frac{\partial^2 c}{\partial x^2} \qquad (1.3)$$

which is known as Fick's second law of diffusion.

If diffusion through a sheet of thickness l is now considered, where the concentrations of diffusing species at the two sides of the sheet are c_1 and c_2 under steady-state conditions, i.e. when $\frac{\partial^2 c}{\partial x^2} = 0$, equation (1.1) can now be integrated between the two concentrations to give,

$$F \int_{x=0}^{x=l} dx = -D \int_{c_1}^{c_2} dc \qquad (1.4)$$

In many cases when diffusion through a polymer film is being considered, the surface concentrations c_1 and c_2 are not known, but the partial pressures p_1 and p_2, of gas or vapour in equilibrium with the surface concentrations are. If it is now assumed that Henry's law, $c = S.p$ (where S is the solubility coefficient of the gas in the polymer) applies to the system, equation (1.4) can be re-written as,

$$F = \frac{DS(p_1 - p_2)}{l} \qquad (1.5)$$

A permeability coefficient, P, can now be defined as,

$$P = D.S \qquad (1.6)$$

and it is plain that the permeability of a polymer film, is dependent on both the diffusion and solubility coefficients of the gas or vapour. P may be given units of centibarrers (cB) where,

$1cB = 10^{-12}$ cm^3 (STP)cm/(cm^2 sec cm Hg)

Many polymer film/permeant systems do not show ideal diffusion and solution behaviour and may from this standpoint be divided into four categories[2].

(i) Systems which have a constant diffusion coefficient and obey Henry's law.

$$\frac{\partial c}{\partial t} = D \frac{\partial^2 c}{\partial x^2}; \quad c = S.P$$

Polymer/permeant systems that fall into this category are normally permanent or inert gases in rubber and synthetic elastomers[3-5], or polymers well above the glass transition temperature, T_g[6-8]. The systems show almost ideal behaviour, mainly because of the low concentrations encountered at normal pressures and also because there is very little interaction between the simple gases and the polymer. Since the interaction is small the permeability coefficient can be expressed as a simple function of polymer and gas terms, together with an interaction parameter, γ, which approximates to unity[9-10].

$$P = V(\text{polymer } i)\ W(\text{gas } k)\ \gamma(i, k)$$

For any given pair of gases (or polymers) the appropriate ratio of permeability constants is given by the equation,

$$\frac{Pi,k}{Pi,l} = \frac{W(\text{gas } k)\ \gamma(i,k)}{W(\text{gas } l)\ \gamma(i,l)}$$

or

$$\frac{Pi,k}{Pj,k} = \frac{V(\text{polymer } i)\ \gamma(i,k)}{V(\text{polymer } j)\ \gamma(j,k)}$$

The first ratio is almost independent of the gas and the second ratio is almost independent of the polymer.

(ii) The second category of polymer/permeant systems shows a diffusion coefficient that is dependent on the concentration of the diffusing species, but obeys Henry's law.

$$\frac{\partial c}{\partial t} = \frac{\partial}{\partial x}\left(D \frac{\partial c}{\partial x}\right); \; D = f(c), \; c = S.P$$

This category is exhibited by C_4 and C_5 paraffins diffusing and dissolving in rubber, and many organic vapours in polymers well above their T_g[11-12].

(iii) A third category can be recognised where D is a function of concentration and Henry's law is no longer obeyed.

$$\frac{\partial c}{\partial t} = \frac{\partial}{\partial x}\left(D \frac{\partial c}{\partial x}\right); \; D = f(c); \; c = f(p)$$

Systems which typify this section are higher molecular weight hydrocarbons diffusing in rubbery polymers.

(iv) The final category contains systems where D is a function of both concentration and time, and Henry's law is not obeyed.

$$\frac{\partial c}{\partial t} = \frac{\partial}{\partial x}\left(D \frac{\partial c}{\partial x}\right); \; D = f(t,c); \; c = f(p)$$

Glassy polymers (below their T_g) and hard polymers show this behaviour[13-14], which is known as anomalous or "non-Fickian". The time dependence of the diffusion coefficient causes the deviation from Fick's law. Rubbery polymers tend to react rapidly to changes in their condition, such as changes in temperature or exposure to a diffusing species. Glassy polymers react much more slowly, and the time dependence of their

properties is associated with the finite rate at which the polymer structure changes on sorption or desorption of a permeant. The time taken to react to a change, known as the relaxation time, varies widely between polymers and the different structural changes associated with the same polymer. All of the various relaxation times decrease as temperature or permeant concentration is increased, and the motion of the polymer segments enhanced.

Three useful classifications have been proposed by Alfrey et al[25], according to the relative rates of diffusion and polymer relaxation. These three classes are:-

(i) type one or Fickian, in which the rate of diffusion is much less than that of relaxation;

(ii) type two where diffusion is very rapid compared with the relaxation process;

(iii) non-Fickian or anomalous diffusion, which occurs when the diffusion and relaxation rates are comparable.

1.3 Temperature Dependence of the Transport Parameters

The diffusion of gases and vapours in rubbery polymers has been shown to be an activated process[3,6,11], with a constant activation energy for diffusion over narrow temperature ranges. The temperature dependence of the diffusion coefficient is given by the Arrhenius equation,

$$D = D_o \exp (- E_d/RT) \qquad (1.7)$$

where E_d is the activation energy for diffusion and D_o is the pre-exponential factor. Measurements of the permeability coefficients at different temperatures have shown that they too can be represented by an Arrhenius expression[6,11,26,27].

$$P = P_o \exp(-E_p/RT) \quad (1.8)$$

From the definition of P = D.S it follows that,

$$S = S_o \exp(-\Delta H_s/RT) \quad (1.9)$$

and, $$E_p = E_d + \Delta H_s \quad (1.10)$$

P_o and S_o are pre-exponential factors, E_p is the activation energy for permeation, and ΔH_s is the enthalpy of solution.

1.4 Changes in E_d and D_o for Different Polymer/Permeant Systems

E_d is associated with the energy needed for 'hole' formation against the cohesive forces of the polymer, plus the energy necessary to force the diffusing molecule through the surrounding structure. It might therefore be expected that E_d would increase with increasing size of the diffusing molecule, since larger holes have to be formed. This is found to be true for every case.

Attempts to correlate E_d with the gas diameter, d, date back to 1946 when van Amerongen[6] found that E_d increased linearly with d, for a selection of gases in several rubbery polymers. Later, Brandt and Anysas[28] and also Paul and DiBenedetto[29] observed that E_d was a non-linear function of d^2 for several different polymers. Work performed by Kumins and Roteman[30] on poly(vinyl chloride) - poly(vinyl acetate) copolymer showed that d is not linearly related to d, d^2 or d^3. Recently Ash et al[31] found that E_d is approximately linear with d^3 for three different polymers. There does not therefore seem to be any consistent relationship between E_d and the diameter of the gas molecule. However, the treatment presented

by Brandt[32], based on the activated zone theory of Barrer[33], does help to explain this apparent lack of correlation. The energy of activation was found to be composed of an intermolecular term, E_i, and an intramolecular term, E_b. Stannett[34] uses Brandt's[32] treatment, as follows, to explain the dependence of E_d on the gas diameter.

The intermolecular term was shown to depend on the permeant molecule diameter, d, the average diameter of the high polymer molecule, h, the dimension associated with the free volume per unit length of chain molecule ($\phi^{\frac{1}{2}}/2$) and the segment length, l_s. The intramolecular term was shown to be a function of the permeant molecule diameter, the dimension associated with the free volume, the segment length and the length of one backbone chain bond, Λ, measured along the chain axis. Stannett[34] then considered the case when the permeant size is large compared to the free volume dimension and $l_s \gg d$. Under these conditions the following proportionalities apply,

$$E_i \propto l_s.d.h$$

$$E_b \propto \frac{\Lambda d^2}{l_s^3}$$

From the above it is clear that E_i depends directly on d, h and l_s while E_b depends directly on d^2 and Λ, and inversely on l_s^3. If E_i makes a large contribution towards the total activation energy for diffusion, E_d, then it might be expected that E_d would vary directly with d. If E_b makes the

larger contribution then E_d might be expected to vary directly with d^2. For intermediate cases it will vary directly with a power of d between 1 and 2. Measurements for rubbery polymers where E_i makes the greater contribution, do tend to correlate with the first power, whereas stiffer chained polymers correlate with the second power of the permeant molecule diameter.

Michaels and Bixler[35] made an allowance for possible orientation effects during the diffusion of unsymmetrical molecules. The value they use for d is given by the following relationship,

$$d = d_g^2 / d_m$$

where d_g is the gas molecular diameter estimated from viscosity measurements and d_m is the maximum dimension of the molecule as determined from Stuart models. Although completely empirical, the allowance for orientation effects improved the correlation of the energy of activation for diffusion with a molecular diameter term. With larger molecules the effect of molecular shape becomes more pronounced. It has been found by various authors[36,37] that the diffusion coefficients for a series of paraffins in poly(isobutylene) level off to an essentially constant value after five carbon atoms, whereas the branched and cyclic compounds have much lower values. Kokes and Long[38], have found a large dependence on permeant size and shape for diffusion in poly(vinyl acetate) at temperatures above T_g. Park[19] has found a similar dependence for the diffusion of halogenated hydrocarbons in polystyrene at temperatures well below T_g.

1.5 Relationships Between E_d and D_o

It has been pointed out by Barrer and Skirrow[4] that the temperature dependence of the diffusivity can be written as,

$$\log_{10} D_o = \log_{10} D + 0.22\, E_d/T \qquad (E_d \text{ in cal mol}^{-1}) \quad (1.11)$$

If it is assumed that log D is constant, i.e. the range in E_d/T is much larger than log D, then a linear relationship might be expected for a plot of log D_o against E_d/T. Stannett[34], using various sources of data for different polymer/permeant systems found a linear relationship on plotting log D_o against E_d/T with a slope of 0.14. This is in fair agreement with the theoretical value predicted by Barrer[4].

According to Barrer[2], D_o is equal to m^2k_o where m is the average distance jumped by the diffusing molecule per unit diffusion process, and k_o is analogous to the pre-exponential factor in first order velocity constants.

Since plots of log D_o against E_d/T are linear over a wide range, Stannett[34] considers them to be approximately the same function of the appropriate variables.

1.6 Effect of Polymer Nature on Diffusion

The diffusivity of a gas in a series of polymers is known to be a function of the ease of hole formation in the polymer. This in turn depends on the segmental chain mobility and the cohesive energy of the polymer. Factors which change the mobility of the polymer chains are known to affect the diffusivity of polymer/permeant systems. Auerbach et al[39] compared the diffusivity of octadecane in several polymers with different degrees of saturation. The saturation was found to decrease the diffusivity by about 50%, due to the greater ease

of chain rotation with more unsaturation in the polymer backbone. Van Amerongen[11] found that adding methyl groups to polybutadiene leadsto lower diffusivities and a greater energy of activation. The methyl groups have the effect of reducing the chain flexibility. Work carried out by Kumins et al[40] showed that adding plasticisers increased the diffusivity of certain polymers. The plasticiser increased the segmental mobility which had the effect of increasing the diffusivity and reducing the activation energy. Other work by Barrer et al[4], and Aitken et al[5], on the effect of vulcanizing natural rubber to varying degrees also showed changes in the activation energy. Vulcanizing the rubber increases the cross-linking of polymer chains which reduces their mobility and increases the activation energy for diffusion.

The presence of pre-existing holes in the polymer structure might also be expected to aid the diffusion process. This is especially so below the glass transition temperature where holes and imperfections are 'frozen' into the polymer structure, normally producing a reduced activation energy below T_g. This effect is discussed in more depth later in the Introduction.

1.7 Changes at the Glass Transition Temperature

Most polymers show a second order transition temperature externally characterised by a change from a glassy to a rubbery state. The first systematic study of changes in diffusion behaviour near the glass transition temperature, T_g, was carried out by Meares[41,42], on the transport of gases through poly(vinyl acetate) films. Heats of solution in the transition region were found to reverse sign from negative to positive as the temperature increased, the activation energy for diffusion

being small over the transition region and larger above than below it. Meares[42] suggested that the holes necessary for the activated diffusion process were formed by loosening of van der Waals bonds between neighbouring chains below T_g, rather than by segmental rotation. The activation zone in the rubbery polymer, involving co-operation of polymer segments, is therefore larger than in the glassy polymer. Similar results and conclusions were reached by Michaels et al[43], on the study of gaseous diffusion in poly(ethylene terephthalate). Other work by Kumins and Roteman[30], and Stannett and Williams[44], has shown that some polymer/permeant systems do not show a glass transition effect, this generally being so with smaller gas molecules. Kumins and Roteman[30] suggested that the number of holes already present in the polymer structure did not change greatly above T_g, but that the size did. If the permeant molecules are small enough only minor changes would be seen since the probability of a molecule encountering a hole would remain approximately the same.

Brandt[32], and Frisch[45] have also proposed explanations for the change in the activation energy at T_g. Brandt[32] suggested that it could be understood as a consequence of the change in thermal expansion coefficient at this point. Frisch[45] suggested that the amount of free volume in the polymer affects the diffusion process for larger molecules, which show a transition effect because the rate of change of free volume changes at T_g. More recently Yasuda[46], using data from the literature and his own measurements, has proposed that a break point occurs in the Arrhenius plot of permeability coefficients only if the value of the diffusion coefficient at T_g is smaller than 5×10^{-8} cm^2 s^{-1}.

1.8 The Solubility of Gases and Vapours in Polymers

The solution of simple gases in rubbery polymers is well known to follow Henry's law and the temperature dependence to follow an Arrhenius relationship.

$$S = S_0 \exp(-\Delta H_s/RT)$$

The enthalpy of solution, ΔH_s, is composed of the enthalpy of condensation and the enthalpy of mixing.

$$\Delta H_s = \Delta H_{con} + \Delta H_{mix} \qquad (1.13)$$

The enthalpy of condensation is always negative and is quite small for most gases. The enthalpy of mixing is also small and usually positive. As a consequence the overall enthalpy of solution can be either positive, or negative.

Organic vapours often show marked deviations from Henry's law. Rogers et al[47], working with polyethylene, obtained isotherms for which the solubility was an exponential function of concentration.

$$S = S(0)\ \exp(G\,C)$$

Where S(0) is the intercept at zero concentration , G is a constant characterising the concentration dependence of the solubility coefficient and C is concentration.

The enthalpy of mixing is influenced by the interaction between the permeant and the polymer. To illustrate this, van Amerongen[11] found that increasing the nitrile content of a series of butadiene-acrylonitrile copolymers had the effect of decreasing the solubility of hydrogen and oxygen, and increasing the solubility of carbon dioxide and ammonia. The former are non-polar and therefore interact less with the increasingly polar polymer, whereas the latter pair are polar and hence interact more.

The enthalpy of condensation is related to the tendency of the gases to condense, of which the boiling point T_b, critical temperature T_c, and the Lennard-Jones force constant are all measures. The logarithm of the solubility has been found to be a linear function of T_b and T_c[11], and of the Lennard-Jones force constant[8]. Since all three parameters are measures of the van der Waals interaction forces of the gases, they differ only by approximately constant factors.

Sorption in polymers below T_g has been shown by many authors[48-59] to occur by two separate mechanisms; standard dissolution in the polymer, as above T_g, and sorption in microvoids frozen into the structure of the polymer as it is cooled through T_g. Free segmental rotation of the polymer chains are thought to be restricted in the glassy state, resulting in fixed microvoids throughout the polymer. The presence of microvoids was first suggested by Meares[41] working with poly(vinyl acetate). Later, Barrer[60] looking at the sorption of organic vapours in ethyl cellulose proposed two mechanisms for sorption, ordinary dissolution, and Langmuir type adsorption in pre-existing microvoids. He further proposed that the total enthalpy of sorption is composed of an exothermic part, adsorption in pre-existing voids, and an endothermic part which represents ordinary dissolution.

$$\overline{\Delta H}(n_1 + n_2) = \overline{\Delta H}_{ex}\, n_1 + \overline{\Delta H}_{en}\, n_2$$

where, $\overline{\Delta H}_{ex}$ and $\overline{\Delta H}_{en}$ are the exo- and endothermic partial molar heats of dilution, for sorption in pre-existing microvoids and sorption by mixing, respectively, and n_1, n_2 are the corresponding number of moles of permeant sorbed in the two

ways. Barrer then used this interpretation to explain differences in sorption enthalpies for iso- and n-paraffins.

Michaels et al[43,61] provided the first quantitative description of the solubility of several gases in glassy poly(ethylene terephthalate). They found that non-linear isotherms could be explained in terms of a Langmuir part and a Henry's law part. The following equation was found to fit the isotherm,

$$C = C_D + C_H = k_D p + \frac{C'_H\, bp}{1 + bp} \qquad (1.14)$$

where,

C = total solubility, $cm^3(STP)/cm^3$ polymer

C_D = dissolved concentration, $cm^3(STP)/cm^3$ polymer

C_H = concentration in holes, $cm^3(STP)/cm^3$ polymer

k_D = Henry's law constant, $cm^3(STP)/cm^3$ polymer atm

C'_H = hole saturation constant, $cm^3(STP)/cm^3$ polymer

p = pressure, atm

b = hole affinity constant, atm^{-1}

At low pressures where $bp \ll 1$ the sorption isotherm reduces to the linear expression,

$$C = (k_D + C'_H\, b)p$$

At higher pressures the microvoids become saturated and will no longer sorb additional permeant. When $bp \gg 1$ sorption in the microvoids reaches the saturation limit, C'_H, and the equation again reduces to a linear form,

$$C = k_D p + C'_H$$

The model therefore predicts that an isothermal plot of C versus p will consist of a low pressure linear region and a high pressure linear region, connected by a non-linear region, as shown below.

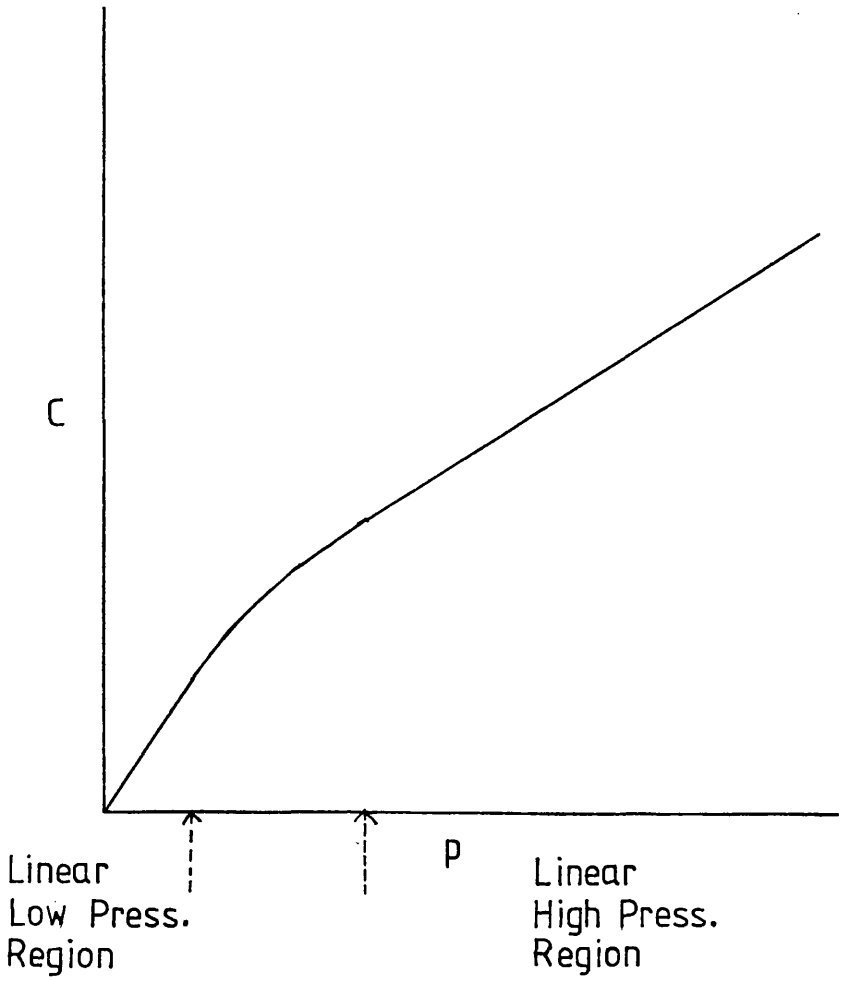

The Henry's law dissolution constant can be obtained from the slope of the high pressure region of the isotherm. This can then be used to calculate the dissolved concentration, C_D, which in turn by subtraction from the total concentration gives

the concentration in the microvoids, C_H. A plot of p/C_H versus p gives a gradient of $1/C_H'$ and an intercept of $1/C_H'b$; the remaining constants can therefore be calculated. Alternatively a non-linear regression program can be used to give the constants directly.

Veith and Sladek[62] have developed a kinetic model for the dual sorption mechanism. Their model assumes that there is immobilisation of the penetrant at a fixed number of sites, and that there is local equilibrium between mobile and immobile species. Mathematically, a material balance is first performed on a differential element of the polymer film, to obtain the unidirectional unsteady-state transport equation, as follows:

$$\partial/\partial t(C_H + C_D) = -\partial N/\partial x \qquad (1.15)$$

where N refers to the flux of dissolved gas. If it is now assumed that only the dissolved species (mobile) diffuse, the flux is given by,

$$N = -D\ \partial C_D/\partial x \qquad (1.16)$$

Substituting equation (1.16) in (1.15), with the condition that the diffusion coefficient is constant, gives

$$\partial/\partial t(C_H + C_D) = D\partial^2 C_D/\partial x^2$$

which is a modified form of Fick's second law. If it is now remembered that the mobile and immobile species are in local equilibrium, the partial pressure in the Henry's law and Langmuir isotherms can be equated to give,

$$C_H = \frac{C'_H \, b/k_D C_D}{1 + bC_D/k_D}$$

Substituting this expression in the combined isotherm eliminates the concentration of immobilised species and gives,

$$D = \partial^2 C_D/\partial x^2 = \partial C_D/\partial t \left\{ 1 + \frac{C'_H(b/k_D)}{\left[1 + \left(b/k_D\right) C_D\right]} \right\}$$

Where C_D is the concentration of the dissolved permeant, at a point x in the membrane, at time t.

The simple dual sorption theory has been extended and modified theoretically in two different ways. Both Paul[63], and Petropoulos[64] have developed equations based on a relaxation of the original assumption that adsorbed molecules are completely immobilised. Petropoulos[64] writes the unsteady-state diffusion equation as,

$$\partial C/\partial t = \partial/\partial x \left[1/RT(D_{T_1} C_D + D_{T_2} C_H) \, \partial\mu/\partial x\right]$$

Where μ denotes the chemical potential of permeant, R is the gas constant and T is the absolute temperature. D_{T_1} and D_{T_2} are the diffusion coefficients of dissolved and adsorbed permeant, respectively. C, C_H and C_D retain their usual meaning with the understanding that the permeant molecules occupying holes are now able to diffuse.

Tshudy and von Frankenberg[65] have relaxed the original assumption in the dual sorption theory that the dissolved and adsorbed molecules are always in local equilibrium. They retain the postulate of sorption by two different mechanisms, but consider the hole-filling process to be a reversible bimolecular

immobilization, ie they do not consider the hole-filling process to be extremely rapid compared to the diffusion process. They developed expressions for transient sorption, equilibrium sorption, time lag (see page 27), and steady-state permeability using the following assumptions:

(1) there are initially a fixed number of immobilizing sites uniformly distributed throughout the medium and fixed in position permanently;
(2) each site can immobilize one gas molecule;
(3) immobilization at some particular position can be represented by:

$$\text{site} + \text{gas molecule} \underset{k_2}{\overset{k_1}{\rightleftharpoons}} \text{site-molecule complex}$$

Other workers had discussed similar treatments, previous to the model described by Tshudy and von Frankenberg[65]. Goodknight and Fatt[66] and Michaels et al[67] have considered slow hole filling with the use of reversible first-order kinetics. Petropoulos[64] once again assumed slow hole filling but did not specify kinetics, and Olofsson[68] considered the case of diffusion with irreversible adsorption, where the rate of adsorption is very rapid compared to the diffusion velocity.

The previous models have been developed to explain negative deviations from Henry's law. Some cases, involving especially sorption of organic vapours and water, show positive deviations. Vieth et al[69] have postulated that the polymer network swells as

permeant is sorbed, exposing more binding sites and increasing the sorption level synergistically.

1.9.1 Crystallinity in Polymers

The first model proposed to explain the crystallinity-dependent properties observed in many polymers was the "fringed-micelle" concept. The polymer was seen as being composed of molecular chains which passed between regions of order, the crystalline parts, and regions of disorder, the amorphous parts. This concept successfully accounted for a large number of experimental observations, but became increasingly less plausible as new experimental evidence accumulated. In 1947 Bunn and co-workers studied polyethylene[70] and nylon spherulites[71], and showed that they contained molecular chains arranged in a regular manner, tangential to the radial growth elements of the spherulite. Later, in 1957 Keller[72] working with single crystals of linear polyethylene grown from solution, showed by electron diffraction that the molecular chains were oriented in a direction normal to the flat surface of the crystal. This, together with the observation that the platelets were much thinner than the polymer chain length, led Keller[72] to the conclusion that the chains must be folded, with the fold period corresponding to the thickness of the platelet. It is now widely accepted that the crystalline regions of most polymers consist of lamellae radiating from a nucleus, making up a unit known as a spherulite.

The function dependence of diffusivity on crystallinity in semi-crystalline polymers, has been explained in the literature on the basis of: (a) linear dependence of diffusivity on the

amorphous fraction[73]; (b) the concept of a transmission function; (c) a two parameter model suggested by Michaels and Bixler[35]; (d) a modification of Maxwell's equation for electrical conductivity of composite systems[74].

Laskoski and Cobbs[73] working on water permeation in poly(ethylene terephthalate), nylon and various types of polyethylene found a linear dependence of diffusivity and solubility with amorphous fraction. Since both these parameters were found to vary linearly with amorphous fraction, they give an equation for the permeability coefficient as,

$$P = P_a X_a^2$$

where P_a is the permeability of the amorphous material, and X_a is the fraction of amorphous polymer.

Klute[75] later re-examined the data of Lasoski and Cobbs[73], applied a small correction factor to their calculation of X_a, and found that the data were better represented by the equation,

$$P = P_a X_a q$$

where q is a correction factor.

Much work has been performed by Michaels and co-workers[8] on the solubility and diffusion of gases in semi-crystalline polyethylene. From this work it is postulated that a semi-crystalline polymer behaves like a two-phase system, namely a well-ordered crystalline phase dispersed in a less rigid amorphous matrix. The crystalline regions are imagined to dissolve no gas and to be quite impermeable, meaning that all gas transport takes place in the amorphous phase which is thought to have the same specific permeability, irrespective of

the extent of crystallinity. The relationship found for the solubility of gases in polyethylene was:

$$S = X_a S_a$$

where S is the solubility in the semi-crystalline polymer, X_a is the amorphous fraction and S_a is the solubility in the completely amorphous polymer. Michaels and Bixler[8] considered the crystallites in moulded polyethylene to be ribbon-like lamellae resulting from a chain folding crystallisation process. The lamellae were thought to radiate from a nucleus, in all directions, to form the secondary ordered units known as spherulites. Michaels and co-workers considered the lamellae to be the basic impenetrable units with accessible amorphous material being present in the spherulite between the lamellae. Later work by Vieth and Wuerth[76] on the solubility of gases in polypropylene showed that for annealed and slow-cooled samples the solubility is once again approximated by $S = S_a X_a$. For quenched samples the situation was complicated by the presence of a second crystal mode.

Michaels and Parker[77] proposed a two parameter model to explain the diffusivity of gases through polyethylene. In this model the diffusivity, D, is given by

$$D = D_a/\tau\beta \qquad (1.17)$$

The diffusivity is considered to be reduced from its value in a completely amorphous polymer, D_a, by the geometric impedance factor τ, reflecting the more tortuous diffusion path, and β the chain immobilization factor, initially attributed to the reduced segmental mobility of the polymer chains due to the crystallites. Later work[67], however, reassessed the significance

of β and suggested that it was a permeant size impedance to diffusion, arising from the near-molecular dimension of the amorphous channels in the spherulites. This is equivalent to making the spherulites less permeable than their surroundings, with the effect increasing for larger molecules.

1.9.2 Effects of Annealing on Crystallinity

Cooling crystallizable polymers from the melt at different rates generally produces samples with different amounts of crystallinity, the more slowly cooled samples being the more crystalline. Polymers treated in this way normally show diffusivities and solubilities that decrease with increasing crystallinity, and therefore lamellar thickness. The permeant molecules are considered to diffuse through and be absorbed only in the amorphous region, the volume of which decreases, and the tortuosity of the resulting diffusion path increases with higher crystallinity. If a polymer sample that has been quenched from the melt, and therefore has a low crystallinity and thin lamellae, is then annealed to a greater crystallinity it has been found that diffusivities increase[76,78] despite the higher crystallinity. From experiments with single crystals of polyethylene and poly(chlorotrifluoroethylene)[79] it was seen that thickening of the lamellae, produced by annealing, was accompanied by the formation of microholes with no change in the lateral dimension of the lamellae. Hoffman et al[80] considered the thickening process to proceed by the pulling of chain ends into the crystal surface, and lengthening of the fold period by migration of the molecules along their own backbones. As thickening proceeds a chain may be pulled right through a

lamella leaving behind a vacant row. This hole now formed has the effect of reducing the lateral crystal size effective as a diffusion barrier, thus reducing the tortuosity parameter. It is therefore possible for samples of high crystallinity to show higher diffusivities than less crystalline samples. The conclusion that these differences were not produced by changes in the amorphous phase, was supported by evidence from Vieth and Wuerth[76] on the diffusion of gases through polypropylene. They found no changes in either the heat of sorption, or the activation energy for diffusion on annealing to greater lamellar thickness. Changes in the amorphous phase should be reflected in changes in both of these parameters.

1.9.3 Measurement of Crystallinity

The methods chosen for the measurement of the amount of crystallinity in the present work were differential scanning calorimetry (DSC), infra-red absorption spectrometry and density determinations.

A differential scanning calorimeter measures the energy input necessary to establish a zero temperature difference between a substance and a reference material in the same environment, heated or cooled at a controlled rate. When the sample is heated through its crystalline melting temperature a peak is seen on the recorder trace, the area of which is proportional to the volume % crystallinity in the polymer. A measurement of the fraction of crystalline material present requires a knowledge of the enthalpy of fusion of a 100% crystalline sample which is sometimes not available. If the two phase model of crystalline and amorphous material is assumed,

then measuring the density of the polymer, together with a knowledge of the crystalline and amorphous densities gives a value for the crystalline fraction from the equation,

$$\text{Volume \% Crystallinity} = \frac{\rho - \rho_a}{\rho_c - \rho_a} \times 100 \qquad (1.18)$$

Measurement of crystalline or amorphous infra-red absorption band intensities can be used to detect differences in volume % crystallinity between different polymer samples. The method is based on the assumption that a polymer can be treated as a two-component mixture of amorphous and crystalline regions, and that crystalline and amorphous band intensities are linear functions of volume fraction crystallinity. To measure absolute levels of crystallinity a sample of 100% amorphous polymer is required if an amorphous band is being considered or a 100% crystalline sample if the band being considered is due to absorption by the crystalline phase.

1.10 The Measurement of Permeation Through Polymer Films

The closed volume method normally used to measure permeation through polymer membranes was first employed by Daynes[81], and later elaborated by Barrer[4]. The method involves applying a known pressure of the permeant to one side of a membrane mounted in a partition cell, and measuring the pressure build-up on the downstream side of the membrane, both sides being initially evacuated. After a gradual rise the pressure increases linearly with time when steady-state permeation is established. The permeability coefficient for the system can be calculated from the slope under steady-state conditions and the diffusion coefficient from its intersection with the time axis, known as

the 'time-lag'. If the sheet is initially free of permeant and there is negligible pressure build-up on the downstream side of the membrane, the amount of diffusant, Q_t, which passes through the sheet of thickness, l, in time, t, is given by,

$$\frac{Q_t}{lC_1} = \frac{Dt}{l^2} - \frac{1}{6} - \frac{2}{\pi^2} \sum_{1}^{\infty} \frac{(-1)^n}{n^2} \exp\left(\frac{-Dn^2\pi^2 t}{l^2}\right)$$

where n = 0,1,2,3---

As the steady state is approached, with increasing time, the graph of Q_t against t tends to the line

$$Q_t = \frac{DC_1}{l} \quad (t - \frac{l^2}{6D})$$

which has an intercept on the time axis given by

$$L = \frac{l^2}{6D} \tag{1.19}$$

The diffusion coefficient can therefore be calculated from the above equation. Knowing the diffusion and permeability coefficients the solubility can simply be calculated from S = P/D. This treatment applies only to systems with a constant diffusion coefficient, although expressions have been obtained for a concentration dependent diffusion coefficient[82-85]. This method suffers from the disadvantage of needing a membrane support due to the pressure differential between the upstream and downstream sides. Vacuum tight seals are also necessary.

An alternative dynamic method has been devised recently[86-89] which avoids these problems. The membrane is held in a permeability cell, separating upstream and downstream chambers. Penetrant gas or vapour is passed through the upstream chamber

and a carrier gas picks up penetrant permeating through the film, and carries it to the detector. The trace produced as the recorder signal approaches its steady-state value gives the diffusion coefficient. Fig. 5 shows a typical recorder trace from a permeation run.

Pasternak et al[88] proposed the following mathematical treatment for the dynamic method.

The permeation flux, F, through a membrane of thickness l is given by,

$$F(x) = -D(dc/dx)$$

where c is the concentration of the permeant in the membrane at a position x.

In their treatment it is assumed that the diffusion coefficient, D, is not a function of the concentration, that the surface concentration is proportional to the pressure of the permeant and that swelling of the membrane is negligible.

The following generalized boundary conditions are characteristic for permeation studies[88]:

$C = 0$	$x = l$	$t > 0$
$C = C_i$	$x = 0$	$t = 0$
$C = C_f$	$x = 0$	$t > 0$
$C = C_i\ (l - x)/l$	$0<x<l$	$t = 0$
$C = C_f\ (l - x)/l$	$0<x<l$	$t = \infty$

These boundary conditions represent the change from one steady-state to another, with the pressure of permeant on the downstream side of the membrane always kept at zero. Two useful solutions of the differential equation, which are obtained by generalizing expressions given in the literature, are[6]:

$$F = \frac{Dc_i}{l} + \frac{D(c_f - c_i)}{l}\left\{1 + 2\sum_{n=1,3,5}^{\infty}(-1)^n \exp\left(\frac{-n^2\pi^2 Dt}{l^2}\right)\right\}$$

$$F = \frac{Dc_i}{l} + \frac{D(c_f - c_i)}{l}\frac{4}{\sqrt{\pi}}\sqrt{\frac{l^2}{4Dt}}\sum_{n=1,3,5}^{\infty}\exp\left(\frac{-n^2 l^2}{4Dt}\right)$$

where F is the flux at x = l; Dc_i/l and Dc_f/l are the steady-state fluxes at time t = 0 and t = ∞, respectively.

Pasternak et al[88] found the second equation the most useful and give a first-order approximation as:

$$\Delta F = \Delta F_\infty (4/\sqrt{\pi})\sqrt{(l^2/4Dt)}\exp\ (-l^2/4Dt)$$

where $\Delta F = F - Dc_i/l$ represents the change in flux during the experiment. They argue that it is reasonable to retain only the first term when the second term contributes less than 2% to the sum, ie $\Delta F/\Delta F_\infty < 0.97$. The above equation is then re-written as,

$$\Delta F/\Delta F_\infty = (4/\sqrt{\pi})\ X \exp\ (-X^2)$$

where $X^2 = l^2/4Dt$

The curve given by the above equation has an extended linear range with an empirical slope of,

$$d(\Delta F/\Delta F_\infty)/d(1/X^2) = 1.42$$

When the definition of X is introduced, one obtains

$$D = 0.176\ l^2(d\Delta S/dt)\ (1/\Delta S_\infty) \qquad (1.21)$$

where $d\Delta S/dt$ is the slope of the linear part of the experimental curve, and ΔS_∞ is the maximum signal height. The diffusion coefficient, D, can therefore be obtained by measuring the gradient of the linear portion of the trace and the plateau height at steady-state permeation. Since the permeability constant can be calculated from the plateau height (provided the sensitivity of the detector to the permeant is known) the Henry's law solubility can be calculated from, $S = P/D$. A permeation trace using the dynamic method will therefore give all three transport parameters.

Ziegel et al[87] suggest another method for calculating the diffusion coefficient from the dynamic method permeation trace. Their method involves measuring the time taken to reach half the steady-state permeation rate, $t_{\frac{1}{2}}$, rather than the gradient of the transient region. The equation they derived to calculate the diffusion coefficient is based on the solution of Fick's law appropriate to the conditions of the time-lag method given by Daynes[81]. His derivation is based on an infinite sheet of thickness, l, initially at zero permeant concentration. Henry's law solubility, a linear concentration gradient, and a concentration independent diffusion coefficient are assumed. This leads to the following expression of the volume flow rate, F, per unit area of the sheet,

$$F/F_\infty = 1 + 2 \sum_{n=1}^{\infty} (-1)^n \exp\left(-n^2\pi^2 Dt/L^2\right)$$

When F is equal to $F_\infty/2$ ie at time $t_{\frac{1}{2}}$ the following equation applies[87],

$$\exp\left(-\pi^2 Dt_{\frac{1}{2}}/L^2\right) = 0.2539$$

and therefore,

$$D = L^2/(7.199t_{\frac{1}{2}}) \qquad (1.22)$$

When measuring the time-lag from an experimental trace the response of the whole experimental system to a stepwise change in permeant concentration is measured. Since it is only the membrane response that is required, corrections have therefore to be made for the time the permeant takes to travel from the switching valve to the membrane, and from the other side of the membrane to the detector.

1.11 Work Performed in this Research Project

The need to measure the permeation of gases and vapours through polymer films required the construction of a new experimental apparatus. Since it was envisaged that during the course of this project the transport properties of several polymer/permeant systems would be investigated an experimental method was needed for measuring permeability and diffusion coefficients reasonably rapidly. The dynamic permeability method described in the Introduction was thought to be the most suitable for this work. This method provided continuous monitoring of the permeation rate through the film, and because the

system was run at or near atmospheric pressure no membrane support or vacuum tight seals were required.

Permeant vapour streams of nitroethane, tetrachloreothylene and dichloromethane, chosen as being representative of organic nitro- and chloro-compounds, were produced using a gas saturator. A Ni^{63} electron capture detector was used to detect dichloromethane permeating through PET. For the other polymer/permeant systems studied a single flame ionization detector was employed.

Initially, permeability and diffusion coefficients were determined for the transport of dichloromethane and nitroethane through PET film, over the temperature ranges 60 - 130 °C for dichloromethane and 50 - 140 °C for nitroethane. Because the flame ionization detector employed for these measurements was operating at the limits of its sensitivity the experimental system was adapted to incorporate the more sensitive Ni^{63} electron capture detector. Permeability coefficients were determined for the permeation of dichloromethane through PET film over the temperature range 65 -110 °C, using the electron capture detector.

Problems with calibrating the electron capture detector and the change of interest to the much more permeable PTFE and FEP films, meant the flame ionization detector was more suitable for measuring permeation through these polymer films. Using the flame ionization detection system permeability and diffusion coefficients were determined for the systems PTFE/nitroethane over the temperature range 69 - 160 °C, and PTFE/dichloromethane

over the temperature range 81 - 151 °C. Permeability coefficients were also determined for the system PTFE/methane over the temperature range 60 - 150 °C. The FEP/permeant systems investigated to determine permeability and diffusion coefficients were, FEP/dichloromethane, FEP/nitroethane, FEP/tetrachloroethylene and FEP/methane over the temperature range 20 - 100 °C.

To determine the accuracy of results obtained using the dynamic system permeability parameters were measured for the transport of methane through the well characterized polymer low density polyethylene, samples of which were obtained from two different sources. These results were found to compare favourably with values reported in the literature.

Differences were noticed between activation energies of permeation and diffusion for FEP films annealed at different temperatures, prior to performing permeation runs. This effect was attributed to changes in the crystalline content of the FEP and attempts were made to measure changes in the crystallinity of the polymer using differential scanning calorimetry, infra-red absorption spectroscopy and density measurements.

A vacuum microbalance was used to record the sorption of nitroethane and tetrachloroethylene by FEP film samples in the as-received state. Sorption isotherms were also recorded for the uptake of dichloromethane by FEP film samples annealed at 100 °C for 24 hours, annealed at 200 °C for 24 hours and in the as-received state.

CHAPTER 2 EXPERIMENTAL

2.1 The Flow System

A schematic diagram of the flow system constructed to measure permeability and diffusion coefficients for gases and vapours through polymer films is shown in Fig. 1.

A cylinder of high purity nitrogen supplied the flush gas and saturator streams. Both lines contained brass toggle valves to enable the two streams to be switched on and off independently. Brooks flow controllers positioned beyond the toggle valves gave accurate flow control of the flush and saturator nitrogen streams.

The saturator nitrogen stream then passed from the flow controller to the gas saturator (which is described in detail in Section 2.3) and emerged saturated with permeant vapour at the temperature of the gas saturator. All tubing, couplings and valves positioned beyond the gas saturator and therefore coming into contact with permeant vapour, were constructed of stainless steel. The permeant stream then passed from the gas saturator to a three-way ball valve which enabled the vapour stream to be switched over to a methane permeant stream supplied directly from a cylinder. The permeant stream, whether methane or vapour, then passed to a Perkin-Elmer gas chromatographic sampling valve, henceforth called the flush/permeant switching valve. This enabled the stream to be switched from flush to permeant, or vice-versa, with the stream that was not passing through the permeability cell being vented to the atmosphere. This was important for the correct functioning of the gas

Fig. 1 THE FLOW SYSTEM

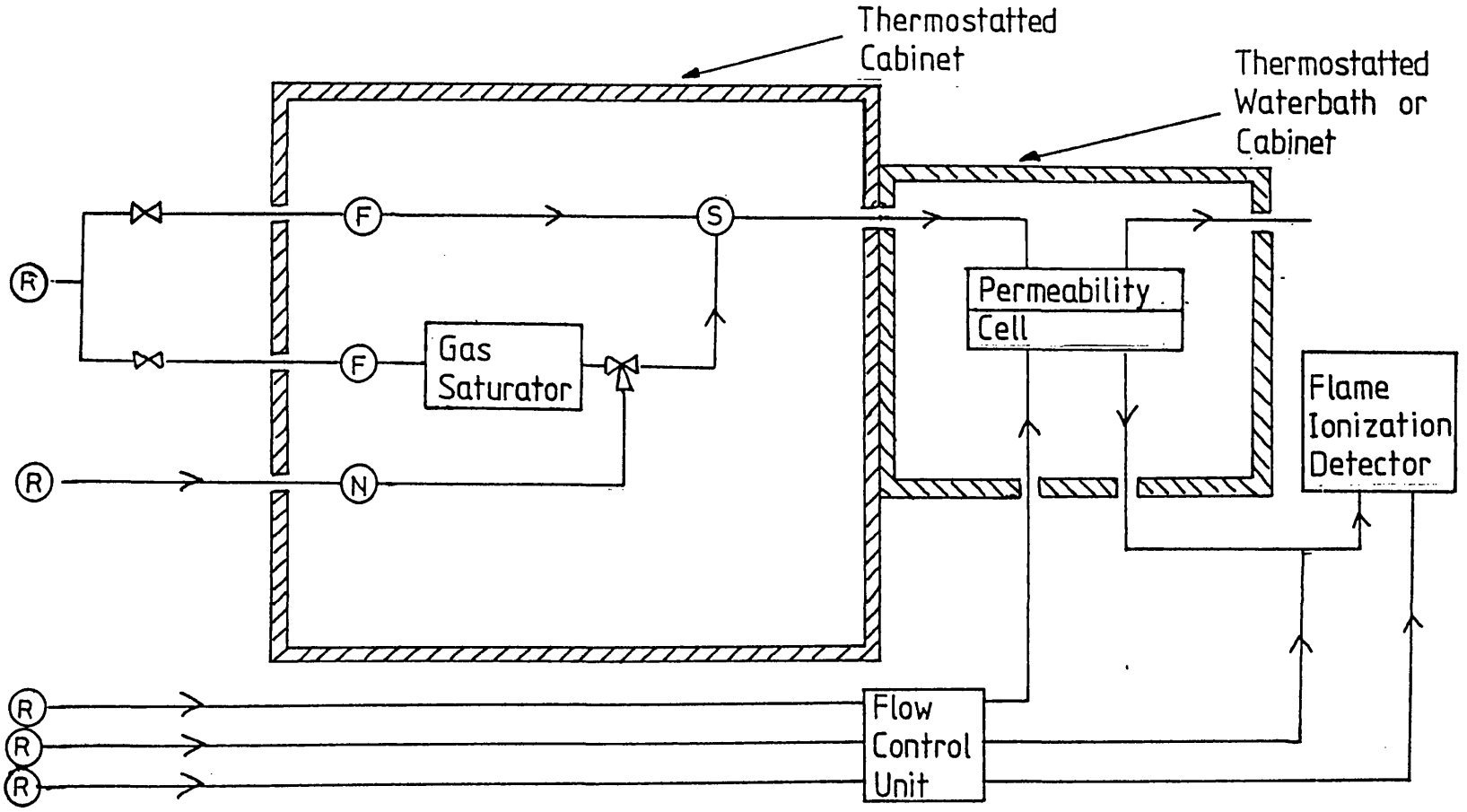

⋈ — Toggle Valve
⋈ — Three Way Ball Valve
(N) — Needle Valve
(F) — Flow Controller
(R) — Cylinder Regulator
(S) — Switching Valve

saturator since it meant that the nitrogen stream could be left passing through the saturator and vented to the atmosphere before an experiment, giving the saturator stream time to reach equilibrium concentration before switching over from flush gas and therefore beginning a run.

Gas or vapour permeating through the polymer film to the downstream chamber of the permeability cell, was carried to the flame ionization detector by a carrier gas stream of high purity nitrogen which continually flushed through the downstream chamber. A Perkin-Elmer single flame ionization detector produced a signal in response to dichloromethane or nitroethane vapour permeating through PET film; this was registered as a trace on a Bryan's chart recorder. A Pye 104 series Ni^{63} electron capture detector was used to detect dichloromethane permeating through PET film. For the other polymer/permeant systems investigated a Pye 104 series flame ionization detector was employed.

2.2 The Permeability Cell

Fig. 2 shows a diagram of the permeability cell used to hold the polymer film during permeability measurements. The cell was machined from stainless steel in two parts held together, with the polymer film in place, by six screws. The permeation chamber was designed to give a film area exposed to the permeant of 19.63 cm^2 with the upstream and downstream chambers having a depth measured from the film of 0.02 inch. The depth measurement was deliberately made small so as to reduce the chamber volume and therefore facilitate the rapid flushing through of a permeant on switching over gas streams.

Fig. 2 THE PERMEABILITY CELL

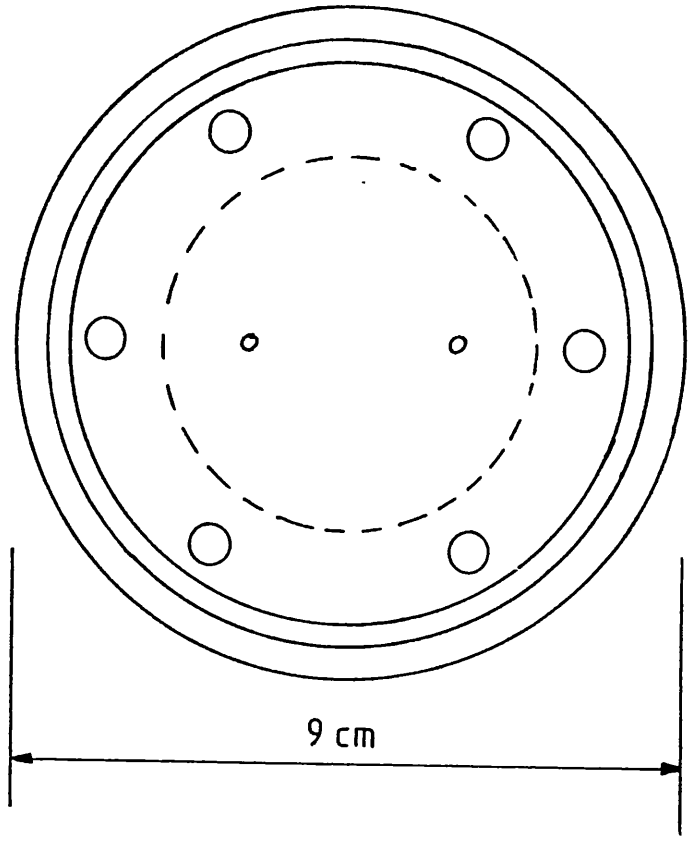

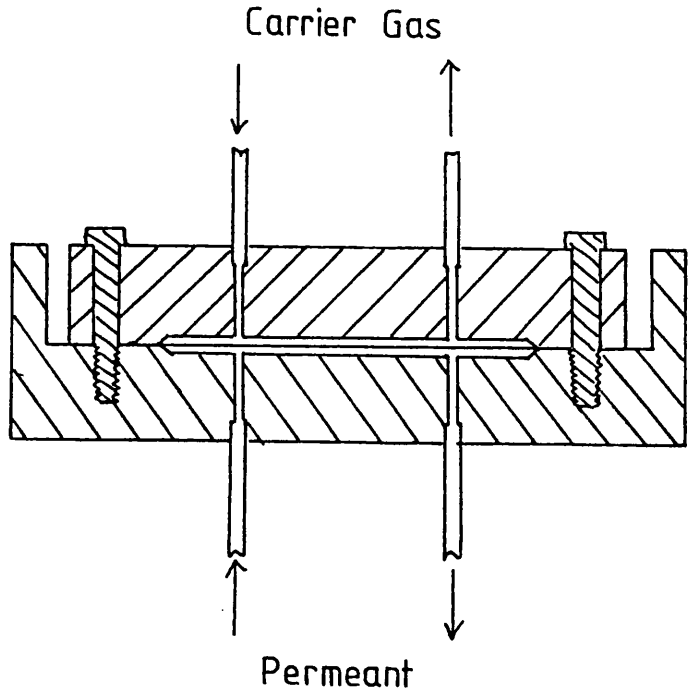

With the polymer film in place between the two sections of permeability cell and the six screws tightened, the outer rim of the film clamped between the flat cell surfaces behaved like a gasket and sealed the permeation chamber. This sealing method provided a well-defined surface area exposed to the permeant (unlike a rubber O-ring seal) but required the film to be of sufficient thickness and have the right texture to act as a sealing gasket. All the films used in the present work fulfilled these criteria making this a satisfactory sealing method.

For the high temperature permeation measurements (60 - 100 °C) the permeability cell was housed in a Pye 104 series gas chromatograph oven which controlled the temperature to ±0.05 °C. Mercury-in-glass thermometers graduated to 0.1 °C were used to measure the temperature of the oven. Because the gas chromatograph oven temperature could not be controlled precisely enough below 60 °C, for the low temperature work (20 - 50 °C) the cell was removed and placed in a thermostatted waterbath. Temperature control here was achieved using a mercury contact thermometer connected via an electronic relay to a 100 W heating element; this arrangement gave a temperature control of ±0.1 °C. Mercury-in-glass thermometers graduated to 0.1 °C were once again used for temperature measurement.

2.3 The Gas Saturator

The gas saturator, shown in Figure 3, produced a known concentration of permeant vapour. The design of the saturator was based on a description given by Weissberger[90]. An inert gas, in this work high purity nitrogen, was bubbled through the organic

Fig. 3 THE GAS SATURATOR

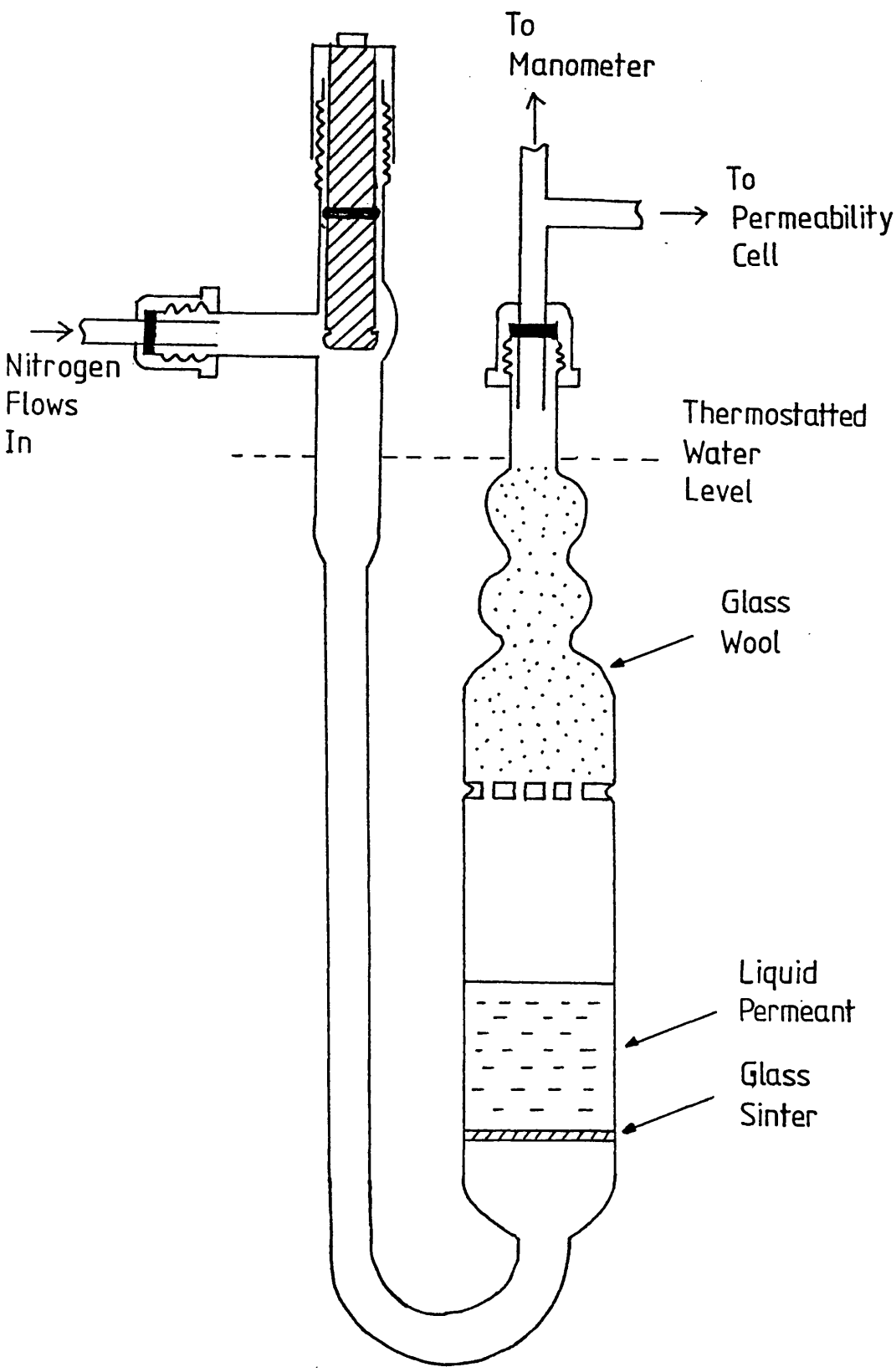

liquid at a sufficiently slow rate to ensure equilibrium saturation. Temperature control was achieved to ±0.05 °C by pumping water from a thermostatted reservoir through a water jacket surrounding the saturator. The water in the reservoir was maintained at a constant temperature with a contact mercury thermometer and electronic relay controlling a heating element. A mercury-in-glass thermometer, graduated to 0.1 °C, was used to measure the temperature of the water in the jacket.

If the saturator produces a completely saturated vapour stream and the gas and vapour are assumed to behave ideally, then the following measurements are needed to calculate the vapour partial pressure in the upstream side of the partition cell:- (i) the vapour pressure of the organic liquid, P_V, in the gas saturator (ii) the total saturator pressure, P_S, and (iii) the total pressure in the upstream chamber of the permeability cell, P_A. The Antoine equation can be used to compute the vapour pressure of the organic liquid in the gas saturator. The total saturator pressure is the sum of atmospheric pressure and the excess pressure above atmospheric, caused by restrictions in the gas flow due to the narrow bore of tubing and valves. Atmospheric pressure was measured to ±0.1 torr using a mercury barometer and the excess pressure above atmospheric measured to ±0.5 torr using a mercury manometer attached to the exit side of the saturator.

Since the upstream side of the partition cell was vented to the atmosphere, the chamber pressure was atmospheric. Therefore knowing the vapour pressure of the liquid, the total pressure in the saturator and the atmospheric pressure, and assuming that

the gas and vapour behave ideally, that equilibrium saturation is established and that Dalton's law applies, the partial pressure of vapour in the upstream chamber, p_C, could be calculated. From Dalton's law it follows that the ratio of the vapour pressure to the total pressure is equal to the ratio of the volume of vapour to the total volume of vapour and nitrogen leaving the saturator in unit time. Therefore,

$$p_C = \frac{p_V}{P_S} \times P_A$$

Provided the assumptions mentioned previously are valid, this method provided a satisfactory way of finding the partial pressure of permeant in the upstream chamber of the permeability cell. When calculating permeant partial pressure for the earlier experiments involving permeation through PET and PTFE films the saturator was assumed to produce a saturated vapour stream. For the later permeation experiments with FEP film the saturator efficiency was measured at the particular saturator temperature used and this efficiency value was included in the permeant partial pressure calculation. To measure the saturator efficiency vapour leaving the exit side of the saturator was trapped for a known time and weighed.

The vapour and nitrogen mixture was passed through a trap immersed in a Dewar containing a dry-ice/alcohol mixture. The nitrogen leaving the exit side of the trap was then bubbled through a Drechsel bottle containing water, before a flow rate measurement was taken using a bubble-flow meter. A Drechsel bottle was necessary to saturate the nitrogen with water vapour before its flow rate was measured. It was assumed that the

nitrogen was saturated with water vapour when calculating the vapour pressure of the permeant; with no Drechsel bottle in the set-up the bubble-flow meter would have saturated the nitrogen to an unknown degree, making correction of the flow rate measurement impossible. In the equations used to calculate the vapour partial pressure from trapping and weighing measurements, the following notation applies:-

W, weight of permeant,

t, time of trapping,

P_A, atmospheric pressure,

T, laboratory temperature,

p_w, partial pressure of water vapour at T,

(MW), molecular weight of permeant

R, the gas constant,

f, flow rate measured at T and P_A.

The volume of nitrogen at T and P_A flowing into the trap during a trapping run is given by,

$$\left(\frac{P_A - p_w}{P_A} \right) .f.t$$

The volume of vapour, at T and P_A, flowing into the trap during a trapping run is given by,

$$\frac{W}{(MW)} \cdot \frac{RT}{P_A}$$

Therefore the total volume of nitrogen and vapour is given by,

$$\left\{ \left(\frac{P_A - p_w}{P_A} \right) .f.t \right\} + \left(\frac{W}{(MW)} \cdot \frac{RT}{P_A} \right)$$

This gives a partial pressure of vapour in the upstream side of the permeability cell of

$$\frac{\left(\frac{W}{(MW)} \cdot \frac{RT}{P_A}\right) \cdot P_A}{\left[\left(\frac{P_A - P_w}{P_A}\right) .f.t\right] + \left(\frac{W}{(MW)} \cdot \frac{RT}{P_A}\right)} \qquad (2.1)$$

When producing permeant and calibration streams of dichloromethane in nitrogen the gas saturator was thermostatted between 13.7 °C and 13.9 °C. Vapour trapping runs were performed with the saturator thermostatted at 13.7 °C and a flow rate of inert gas through the saturator of about 30 $cm^3\ min^{-1}$. A series of four trapping runs gave a mean partial pressure of 257.7 torr with a probable error per trapping run of ±3 torr. If equation 2.1 is used to calculate the expected concentration of vapour in a saturated permeant stream, the mean partial pressure as determined from trapping runs was found to be 97.1% of the theoretically saturated value. When calculating permeability coefficients and the sensitivity constant for the flame ionization detector the partial pressure of dichloromethane was taken as 97.1% of the theoretically saturated value at the measured saturator temperature. The vapour pressure of dichloromethane at a given temperature was calculated using the equation[91].

$$\log_{10}(p_v/\text{torr}) = 7.141201 - \frac{1327.016}{(T/°C) + 252.676}$$

The error given in the reference is,

$$\frac{\sum |\text{Pressure(observed)} - \text{Pressure(calculated)}|}{\text{Data points}}$$

= 0.430 torr.

When producing a permeant stream of nitroethane in nitrogen the gas saturator was thermostatted at 13.9 °C for the high temperature (60 - 100 °C) measurements and 17.7 °C for the low temperature (20 - 50 °C) measurements. Trapping runs performed with the gas saturator thermostatted at 13.7 °C gave a mean partial pressure of 10.39 torr with a probable error of ±0.16 torr. This is 98.1% of the theoretical saturated value.

The vapour pressure of nitroethane at a given temperature was calculated using the equation[91].

$$\log_{10} (p_v/\text{torr}) = 7.58777 - \frac{1671.6}{(T/°C)+241.187}$$

The error given in the reference is,

$$\frac{\sum |\text{Pressure(observed)} - \text{Pressure(calculated)}|}{\text{Data points}}$$

= 0.501 torr

When calculating permeability coefficients with the gas saturator thermostatted at 13.9 °C, i.e. the high temperature measurements, the partial pressure of nitroethane was taken as 98.1% of the theoretical saturated value.

Since the flame ionization detector sensitivity constant for nitroethane was determined with the gas saturator thermostatted at 28.1 °C (which was necessary to produce peaks of sufficient size), trapping runs were performed at this temperature to determine the concentration of the vapour stream. A series of four runs gave a mean partial pressure of 23.08 torr with a probable error of ±0.35 torr. This is 97.3% of the theoretical saturated value.

When producing permeant streams of tetrachloroethylene the gas saturator was thermostatted at 13.7 °C for the low temperature measurements (20 - 50 °C) and 28.7 °C for the high temperature measurements (60 - 100 °C). Trapping runs with the gas saturator thermostatted at 13.7 °C gave a mean partial pressure of 9.40 torr with a probable error of ±0.12 torr. This was 98.3% of the theoretically saturated value. With the gas saturator thermostatted at 28.7 °C a mean partial pressure of 21.84 torr with a probable error of ±0.28 torr was obtained. This was 97.91% of the theoretically saturated value.

The vapour pressure of tetrachloroethylene at 28.7 °C needed for the calculation of the theoretical saturated vapour concentration was calculated using the equation[92]

$$\log_{10} (p_V/\text{torr}) = 7.05566 - \frac{144.819}{(T/°C) + 223.979}$$

The error given in the reference is,

$$\frac{\sum \left| \text{Pressure(observed)} - \text{Pressure(calculated)} \right|}{\text{Data points}}$$

= 0.314 torr

Because the above equation is only valid over the temperature range 28 - 107 °C the vapour pressure of tetrachloroethylene at 13.7 °C was calculated by interpolating between tabulated vapour pressure values given in reference 92.

2.4 Treatment of the Polymer Films Prior to Measuring Transport Parameters

When performing permeation runs with PET film using the Perkin-Elmer FID the polymer was heated in the permeability cell to the highest temperature at which a measurement was required; further permeation runs were then performed at descending temperature intervals. To reduce contamination of the electron capture detector, by low molecular weight species from the PET film, it was necessary when measuring transport parameters for the system PET/dichloromethane to maintain the polymer at 200 °C for at least 36 hours prior to performing an experiment.

To avoid changes in polymer morphology on measuring transport parameters at changing temperatures the PTFE and FEP films were annealed before a series of experimental runs. The annealing temperature was chosen to be at least as high as the highest temperature at which transport measurements were taken. FEP films used for the high temperature runs (60 - 100 °C) were annealed at either 100 °C or 200 °C for 24 hours. The annealing procedure consisted of mounting the films in the permeability cell and heating to the required temperature for 24 hours with nitrogen flowing through upstream and downstream chambers to maintain an inert atmosphere. After 24 hours the oven was turned off and the permeability cell left to cool to room temperature. Permeability runs were then performed at ascending

temperatures. Because the permeability cell was mounted in a water bath for the low temperature measurements (20 - 50 °C), it was not possible to anneal the FEP film in the cell. For these measurements the film was annealed in a glass vessel with nitrogen flushing through to maintain an inert atmosphere. Cooling rates for the oven, measured using a thermocouple and recorder, are shown in Fig. 4.

The PTFE films were mounted in the permeability cell and annealed at 200 °C for at least 12 hours with nitrogen flowing through both chambers of the cell. The polymer films were then cooled to ambient temperature and permeation runs performed at either ascending or descending temperature intervals.

2.5 Experimental Procedure for Measuring Permeation Rates Using the Pye 104 FID

The carrier gas flow rate was set to 10 cm^3 min^{-1} using the Brooks flow controller incorporated in the flow control unit, and measured with a bubble flow meter. The hydrogen and air supplies to the FID were set to 11 and 10 lb in^{-2} respectively, as shown on the pressure gauges incorporated in the flow control unit. The flame was then lit and the detector (which had been previously thermostatted to 250 °C) left for at least 2 hours before an experimental run was performed. To ensure that the permeability cell, which had a reasonably large thermal capacity, had reached thermal equilibrium it was also left thermostatted at the required temperature for at least 2 hours.

With the attenuator set to the required value and the chart recorder electronically 'backed-off' to the baseline, the equipment was ready for a permeation measurement. Changing the

Fig. 4 COOLING CURVES FOR THE ANNEALING OVEN

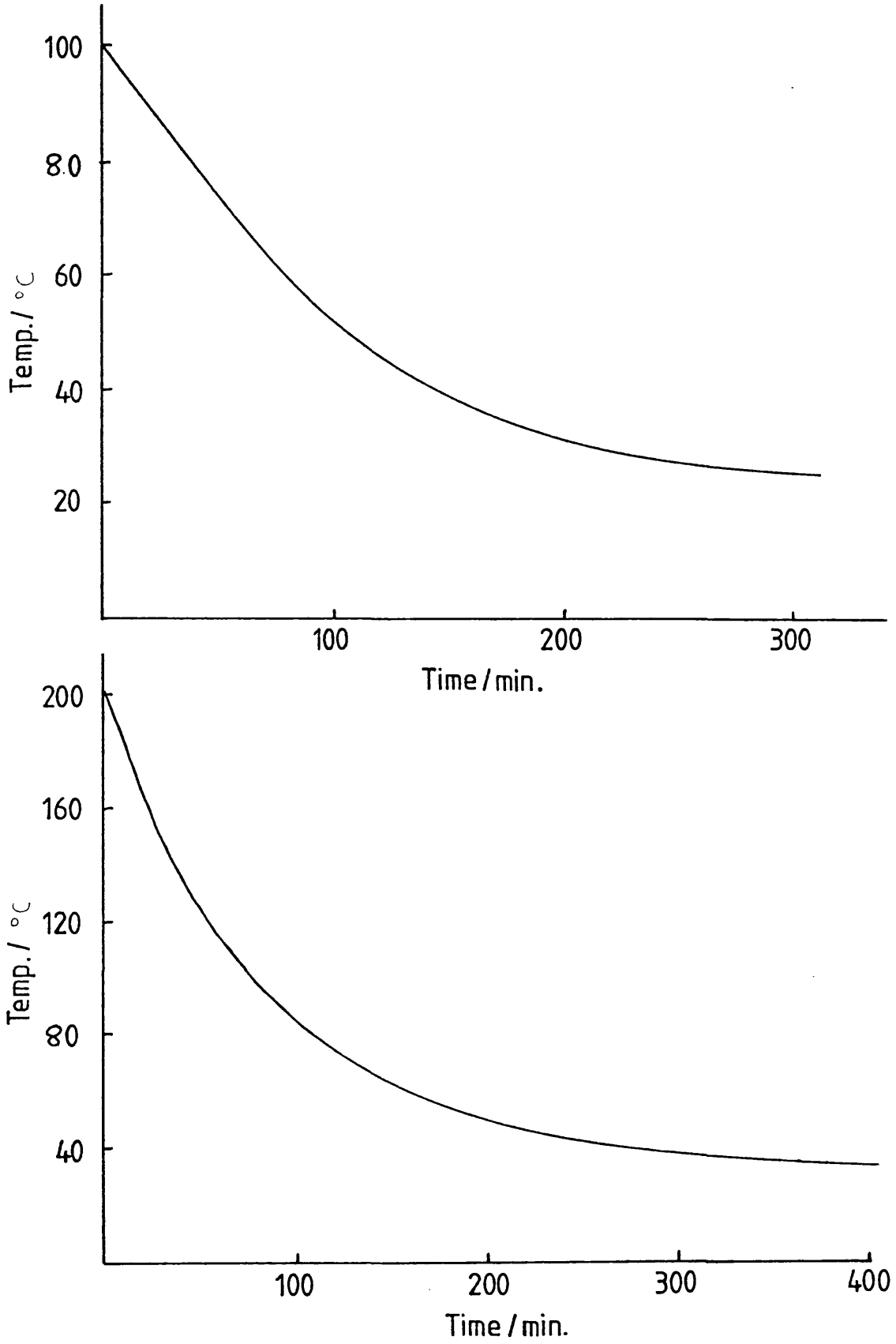

switching valve from flush to permeant began a permeation run, a typical recorder trace of which is shown in Fig. 5. Several distinct regions have been marked on the time axis of Fig. 5. If A is the time when the switching valve is changed from flush to permeant, AB represents the time taken for permeant to reach the upstream face of the polymer, and is dependent on the flow rate of the permeant stream and the 'dead' volume between the switching valve and the upstream chamber of the cell. BC represents the time taken for permeant to diffuse through the polymer film and is therefore a characteristic of the film thickness and the particular polymer/permeant system under investigation. The time-span marked CD in Fig. 5 is the time taken for the permeant to move from the downstream chamber of the cell to the flame ionization detector, and be registered as a signal on the recorder. The recorder signal continues to rise until the steady-state permeation rate is established, as shown by the trace levelling off to a plateau of signal height S_∞. This plateau height can be used to determine the permeant flux, F, through the film which is given by,

$$F = S_\infty \cdot K$$

The calibration constant, K, has units of $cm^3(STP)\ cm^{-1}\ s^{-1}$; therefore measurement of S_∞ in centimetres corrected to unit attenuator setting gives F units of $cm^3(STP)s^{-1}$.

A knowledge of the film area exposed to the permeant, A, the film thickness, L, and the partial pressure of the permeant, p_C, can then be used to calculate the permeability coefficient for the system, P, which is given by

$$P = \frac{S_\infty \cdot K \cdot L}{A \cdot p_C} \qquad (2.2)$$

Permeability coefficients in this work have been given in units of centibarrers, where

$$1cB = 10^{-12}\ cm^3(STP)\ cm/(cm^2\ cm\ Hg)$$

The gradient of the linear region, dS/dt in Fig. 5, can be used to determine the mutual diffusion coefficient for the polymer/permeant system. As explained in Section 1.10 of the Introduction the diffusion coefficient, D, can be approximated by equation[88] 1.21.

$$D = 0.176\ l^2(dS/dt)(1/S_\infty)$$

where dS/dt is the increase in the detector signal with time over the linear region of the trace. It was found in the present work that dS/dt increased slightly with increasing permeant flow rate. Measurements taken at different flow rates showed that dS/dt reached a maximum at a permeant flow rate of 40 $cm^3\ min^{-1}$. This effect has been noted previously by other workers[88] and is thought to be due to an increase in sharpness of the boundary between permeant and flush gas; this results in a more rapid change from flush to permeant in the upstream chamber of the permeability cell. For this reason a flow rate of 40 $cm^3\ min^{-1}$ was chosen for both permeant and flush streams.

2.6 The Flame Ionization Detector

The permeant vapour diffusing through the polymer film was entrained by a carrier gas stream of nitrogen, flowing at 10 $cm^3\ min^{-1}$, and carried to an independently thermostatted Pye model 104 single flame ionization detector. The detector signal was recorded as a trace on a Bryans chart recorder.

When steady-state permeation through a polymer film was established a trace of constant signal height was seen on the

Fig. 5 PERMEATION TRACE

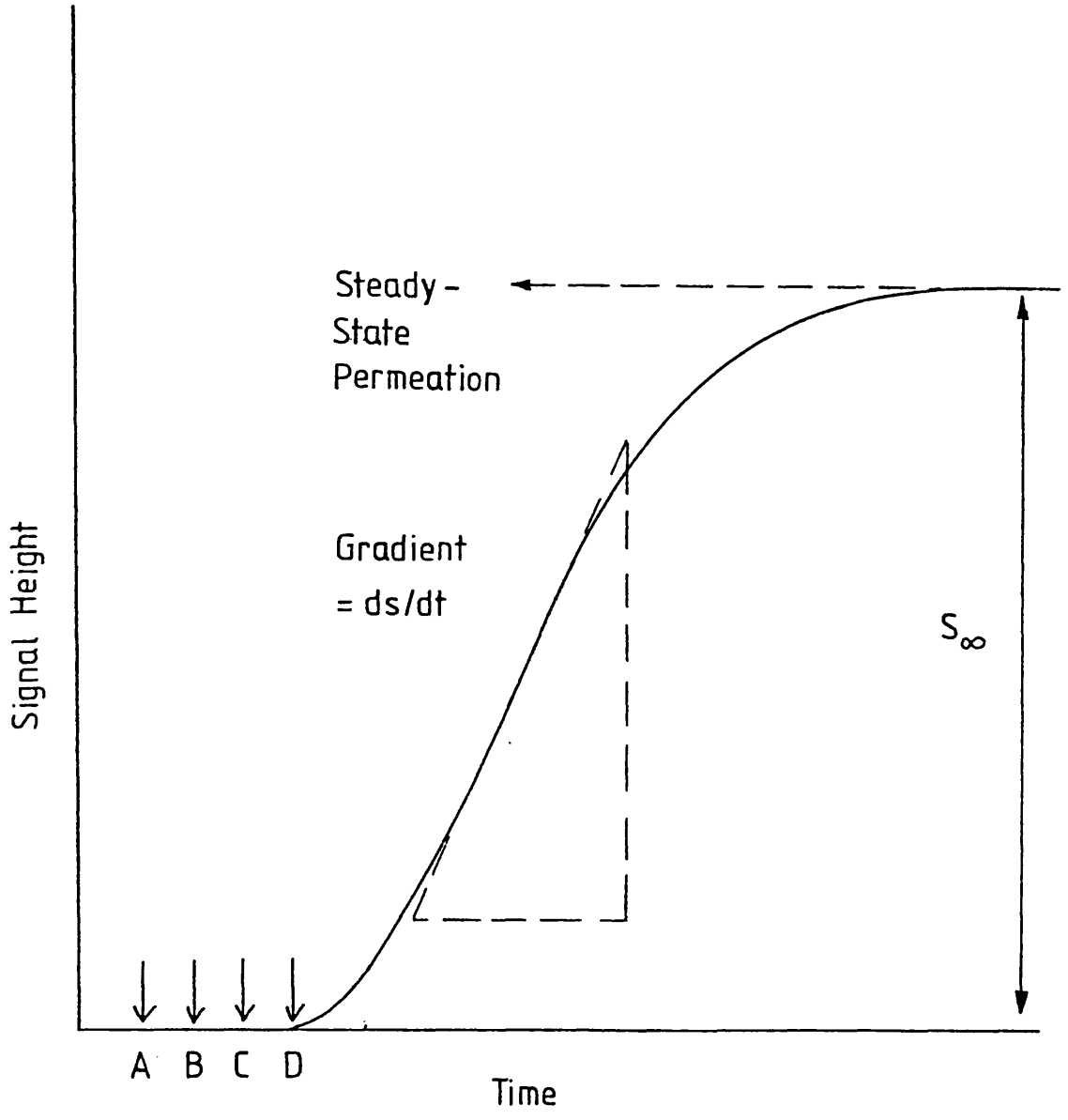

recorder. To calculate the flux through the film from this signal height it was necessary to calibrate the flame ionization detector. For dichloromethane the calibration was performed by passing a known volume of vapour through the detector and measuring, by a cut and weigh method, the area of the peak produced.

A Perkin-Elmer gas chromatographic sampling valve fitted with a loop of 1/8 inch o.d. stainless steel tubing was used to give a known volume of vapour. The loop volume was measured by weighing the mercury needed to fill the bore and using this value together with the density of the mercury to calculate the required volume. If the temperature and partial pressure of vapour in the loop are known then the peak area can be used to calculate a calibration constant in units of $cm^3(STP)\ s^{-1}\ cm(\text{signal height})^{-1}$, the peak area being corrected to unit chart speed and attenuation setting. In this work the temperature of the sampling loop was controlled to ±0.5 °C by enclosing it in a thermostatted cabinet. The partial pressure of vapour in the loop was determined using the gas saturator calculations described earlier.

The measurement of peak areas was used to determine the calibration constants for dichloromethane and nitroethane using the flame ionization detector. It was not possible to use the peak area method to determine the calibration constant for tetrachloroethylene because the peaks produced had inconveniently long tails, making area measurement difficult. To calibrate the detector for tetrachloroethylene a mixture of 12.5 ppm tetrachloroethylene in nitrogen was passed into the

detector through the carrier gas line, producing a signal of constant height on the recorder. The calibration constant for tetrachloroethylene could then be calculated from the flow rate and concentration of the calibration gas, and the signal height measured.

A sensitivity constant for methane was determined, as with dichloromethane and nitroethane, using the sample loop method. The methane was supplied from a cylinder containing a mixture of 2.05% methane in nitrogen.

2.7 The Electron Capture Detector

A Pye 104 series Ni^{63} electron capture detector was used to measure the permeation rate of dichloromethane through poly(ethylene terephthalate) (PET) film. The detector was operated in the pulse mode at 150 μs and a temperature of 250 °C. The high sensitivity of the electron capture detector meant that all tubing and valves had to be thoroughly cleaned before operation. High purity nitrogen was used as the carrier gas.

To calibrate the detector a diffusion dilution method was used as described by Desty et al[93]. This method provided the necessary low concentrations of vapour and being a continuous method it eliminated any adsorption errors. The calibration device shown in Fig. 6 consisted of a glass mixing chamber fitted with a piece of capillary tubing approximately 13 cm in length and with an internal diameter of 0.4 mm. Several different capillary sizes were tried before the required concentration of vapour was produced. The level of liquid in the capillary was measured to 0.1 mm using a cathetometer. The

Fig. 6 ELECTRON CAPTURE CALIBRATION DEVICE

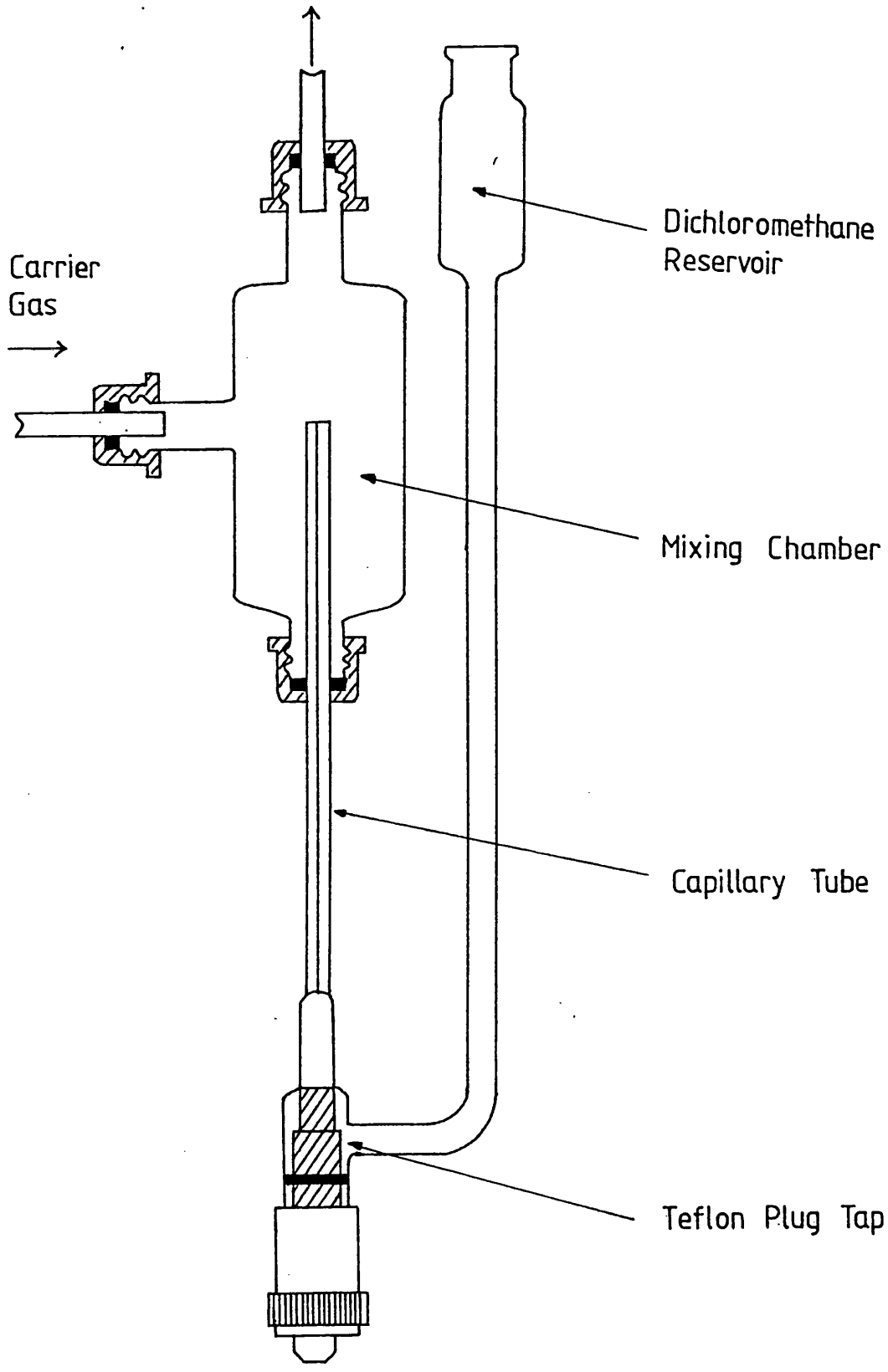

calibration method involved passing a stream of high purity nitrogen over the capillary tube which contained dichloromethane, and measuring the increase in the distance between the open end of the capillary and the liquid level with time. This gave a measure of the amount of liquid diffusing into the carrier gas stream. The rate of diffusion may be determined according to the following theory.

In an open capillary the rate of diffusion, S_r, is inversely proportional to the distance between the liquid meniscus and the open end of the capillary tube, l.

$$\text{i.e.} \quad S_r = \frac{K_e}{l} \tag{2.3}$$

where K_e is a constant under fixed experimental conditions. It is shown by Desty et al[93] that,

$$l^2 = \frac{2K_e t}{\rho A} + l_o^2 \tag{2.4}$$

where, ρ is the density of the liquid, l_o is the initial distance between the end of the capillary and the liquid meniscus, A is the cross-sectional area of the capillary bore and t is time.

The constant K_e was calculated from the gradient of a plot of l^2 against t and a knowledge of A and ρ. K_e was then substituted back into equation (2.3) and the rate of diffusion, S_r, found at a given time t. Therefore, knowing the flow rate of carrier gas through the mixing chamber the concentration of dichloromethane vapour in the carrier gas stream was calculated.

The electron capture detector responds to an electron capturing species by a reduction in a standing current established

with pure carrier gas. A detector which responds by a drop in current cannot be linear over a large range since the current cannot fall below zero. The detailed theory of operation of the electron capture detector has been studied by Wentworth et al[94], who find that in the conditions of their proposed mechanism the response of the detector is given by,

$$\frac{I_a - I_b}{I_b} = D_e.C \qquad (2.5)$$

where I_a is the standing current due to pure carrier gas, I_b is the current in the presence of a concentration, C, of electron capturing vapour and D_e is a constant which expresses the sensitivity of the detector to the vapour. Lovelock et al[95] have shown that the equation holds over at least two orders of magnitude.

In this work the constant D_e was calculated using the known concentration of the calibration vapour stream. D_e was then used, together with measured values of I_a and I_b, to calculate the concentration of dichloromethane vapour in the carrier gas stream flushing through the downstream chamber of the permeability cell. The rate of permeation through the PET film, F, was then calculated from a knowledge of the flow rate of the carrier gas, f_c, and the concentration of the dichloromethane vapour, C_D,

i.e. $F = f_c \,.\, C_D$

The experimental procedure for determining transport parameters using the Ni^{63} electron capture detector was similar to that described previously when using the flame ionization detector. The extreme sensitivity of the electron capture detector to impurities required a PET film sample to be mounted in the permeability cell and maintained at 200 °C, with nitrogen

flowing through both chambers for at least 36 hours before the standing current was sufficiently large to enable a run to be performed. This loss in standing current prior to heat treatment was presumably due to contamination of the detector by low molecular weight species being lost from the polymer.

2.8 Static Sorption Measurements

The uptake of permeant vapour by the FEP film was measured using a Sartorius electronic vacuum microbalance, model 4012. This is a quartz beam balance and was operated at ten times the basic sensitivity range enabling a weight change of up to 200 mg at a resolution of 0.01 mg to be measured. A schematic diagram of the balance and associated vacuum frame is shown in Figs. 7 and 8.

A sample of FEP film was suspended from the right hand side of the balance and a tare weight of silica glass hung from the left-hand side. This enabled a sample weight of about 1.8 g to be used while maintaining the measuring range of 200 mg. The sample was prepared from a strip of 0.001 inch thick FEP film wound into a spiral. The liquid permeant was kept under vacuum outside the balance housing and let into the chamber through a Hoke brass bellows valve.

To control accurately the temperature at which the absorption isotherms were determined, the hang-down tube around the sample was surrounded by a water jacket through which water from a thermostatted reservoir was circulated. The sample was maintained at a temperature of 29.89 ±0.01 °C (nominally 30 °C) as measured with a mercury-in-glass thermometer, T_W in Fig. 7, previously calibrated using a platinum resistance thermometer to

Fig. 7 SARTORIUS MICROBALANCE

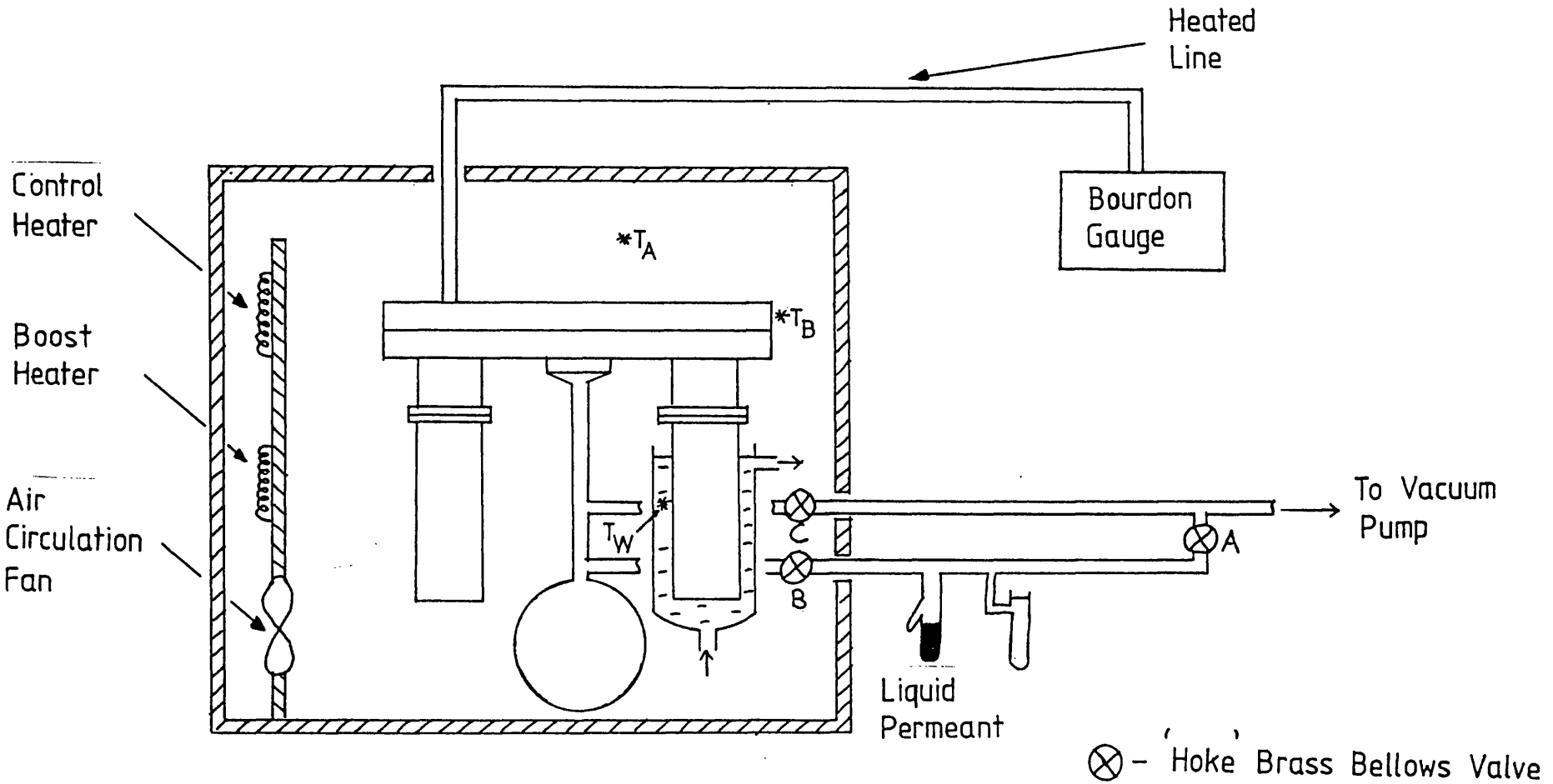

Fig. 8 MICROBALANCE VACUUM FRAME

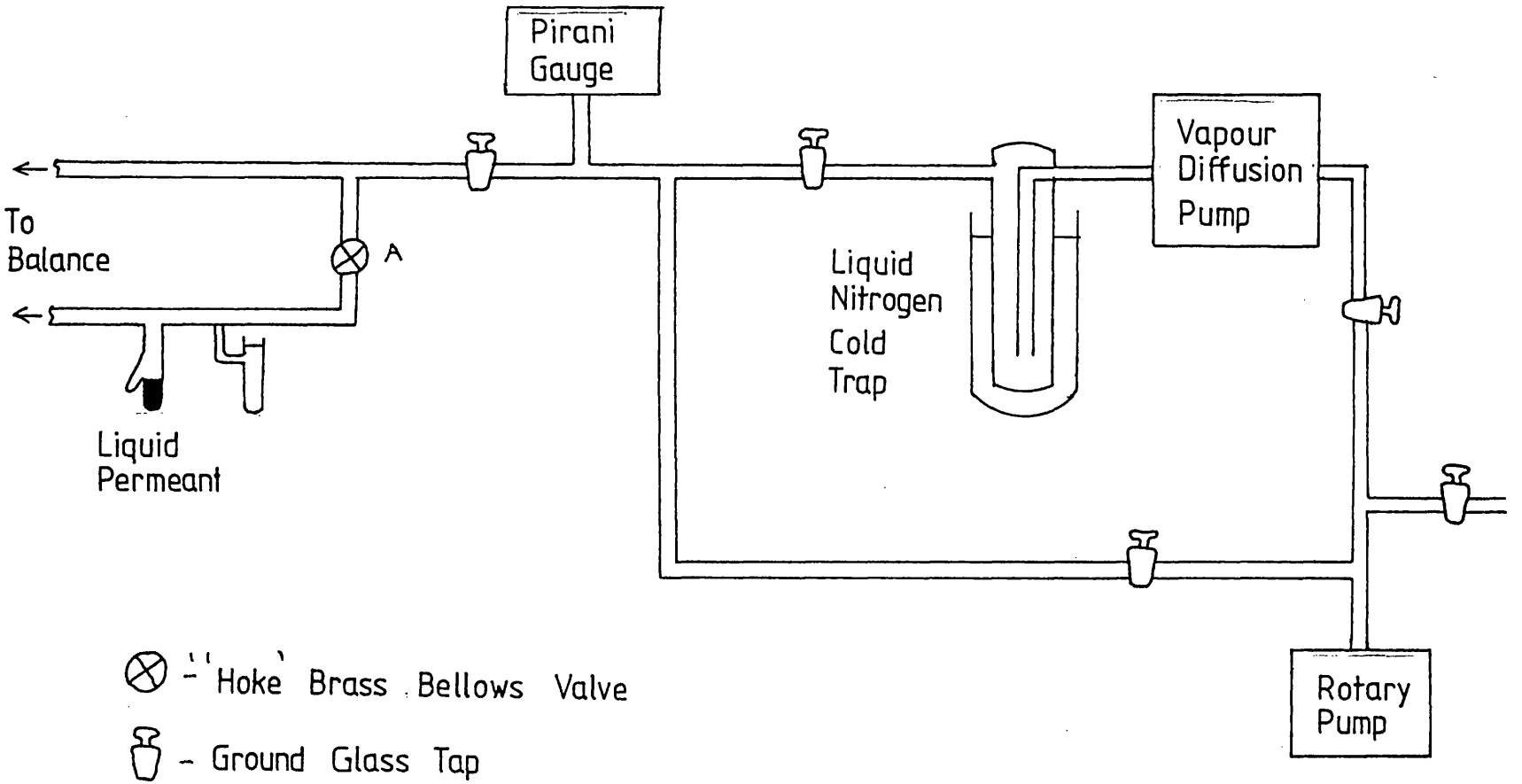

ensure accuracy. The whole balance mechanism was thermostatted using a mercury contact thermometer and heating element to control the temperature of the air circulated through the surrounding cabinet with a fan. The temperature of the balance block and surrounding air were monitored using mercury-in-glass thermometers, T_B and T_A in Fig. 7, and maintained at 30.0 °C and 30.1 °C respectively. This is slightly above the sample temperature to ensure that the pressure recorded is the pressure of the vapour in equilibrium with the sample.

The pressure of the system was measured on a Texas Instruments quartz spiral Bourdon gauge thermostatted at 48.5 °C and used with a 100 cm Hg gauge head. Since it was not included in the air thermostat it was connected to the balance chamber by a heated line maintained at a temperature above that of the balance chamber. The large 2-litre glass bulb included in the system minimised any pressure build-up due to leakage and out-gassing from balance seals during the recording of an isotherm. Also, because the internal volume is large it was ensured that the pressure drop on absorbing vapour was small and enabled experimental points to be recorded at essentially pre-determined partial pressures.

2.9 Experimental Procedure for Determining Sorption Isotherms

A sample of 0.001 inch thick FEP film (approximately 1.8 g) was prepared by cutting an approximately 2 cm wide strip of the film and winding it into a spiral, held together by a small piece (approximately 0.01 g) of electrical fuse wire. With the balance calibrated according to the manufacturer's instructions the sample was mounted on the right-hand side of the beam using

another small piece of fuse wire as a loop to attach it to the balance hang-down wire. The silica tare weights were then placed on the left-hand side of the beam, both copper hang-down tubes were securely fastened and pumping on the sample was commenced. This was begun with a rotary oil pump to reduce the pressure to approximately 0.1 torr, as registered on the Pirani gauge, and followed by an oil vapour diffusion pump. During this process valves A and B were closed to isolate the absorbate sample and valve C was open to allow pumping on the polymer sample.

When a suitable vacuum had been achieved, ie less than 10^{-4} torr on the Pirani gauge, the polymer sample was isolated by closing valve C. A check was then made on the leak and outgassing rate into the balance chamber, which if too high would have led to error in the pressure measurement. This consisted of isolating the balance chamber for an hour and then, with the vacuum pumps isolated, opening valve C to enable any pressure build-up to register on the Pirani gauge. If the leak and outgassing rate into the balance chamber was found to be less than 10^{-4} torr min^{-1} the polymer sample was pumped on again for 30 min. to re-establish the original vacuum. Before an absorption run was begun the absorbate was outgassed to remove any dissolved atmospheric gases. This was achieved by pumping on the absorbate, which was frozen by surrounding the glass limb with a Dewar of liquid nitrogen. The Dewar was then transferred to the second limb and the first limb warmed using a hot air blower. This caused the absorbate to distil over to the second limb where it was re-frozen and pumped on again. This cycle was

continued until no pressure increase was detected by the Pirani gauge on isolating the pumping system from the rest of the vacuum frame and opening valve A.

Having measured the leak and outgassing rate into the balance chamber, degassed the absorbate, tared the balance to zero and checked that the thermostat temperatures were correct, the vapour was then admitted to the polymer sample by opening valve B. The change in weight of the sample was followed on a chart recorder, with the system reaching equilibrium when the trace levelled off to a plateau. The time taken to reach equilibrium depended on the diffusion rate into the polymer sample, which was in turn a function of the molecular size of the penetrant and the film thickness. Because equilibrium times were found to be inconveniently long with the 0.002 inch thick FEP film used for the dynamic permeation measurements, a thinner film of 0.001 inch thickness was chosen for the static measurements. Once equilibrium had been established at the first pressure further doses of vapour were admitted into the balance chamber until measurements had been taken over the required pressure range. Corrections were made to the recorded pressure using the previously determined leak and outgassing rate into the balance chamber; this was necessary since errors in the pressure measurement became significant towards the end of a series of sorption runs.

2.10 Use of Differential Scanning Calorimetry (DSC) to Measure Changes in the Weight Percent Crystallinity of FEP Film on Annealing.

A Perkin-Elmer model 1B differential scanning calorimeter was used to measure relative amounts of crystallinity in the different FEP samples.

Conveniently-sized discs of 0.002 inch thick FEP film were cut out using a cork borer. Several discs, amounting to approximately 10 mg, were accurately weighed and placed in the aluminium sample holder provided with the instrument. With the reference holder in position a scan was performed at a speed of 32 K min^{-1} over the crystalline melting temperature of the polymer. A typical endotherm is shown in Fig. 9. Peak areas were measured by cutting out the peak and weighing it.

As mentioned in the Introduction DSC only provides a method for measuring differences in crystalline content between samples, rather than an absolute degree of crystallinity. Absolute measurements would require knowledge of the enthalpy of fusion of 100% crystalline polymer and this is not available.

2.11 Density Measurements to Detect Changes in the Volume Percent Crystallinity of FEP on Annealing.

A Sartorius model 4012 microbalance was used in a buoyancy method to determine the density of FEP film. Approximately 1.8 g was prepared as described for the static sorption measurements. The sample was then mounted on the right-hand side of the balance and a piece of silver wire (approximately 1.8 g) placed on the left-hand side. With a satisfactory vacuum ($<10^{-3}$ torr) established and the balance tared to zero, atmospheric air was leaked into the balance chamber and differences in upthrust between the FEP film and silver wire measured at increasing air pressures. The density of the FEP could then be determined from a knowledge of the densities of atmospheric air and silver, together with the gradient of a plot of balance reading against air pressure.

Fig. 9 DIFFERENTIAL SCANNING CALORIMETER ENDOTHERM

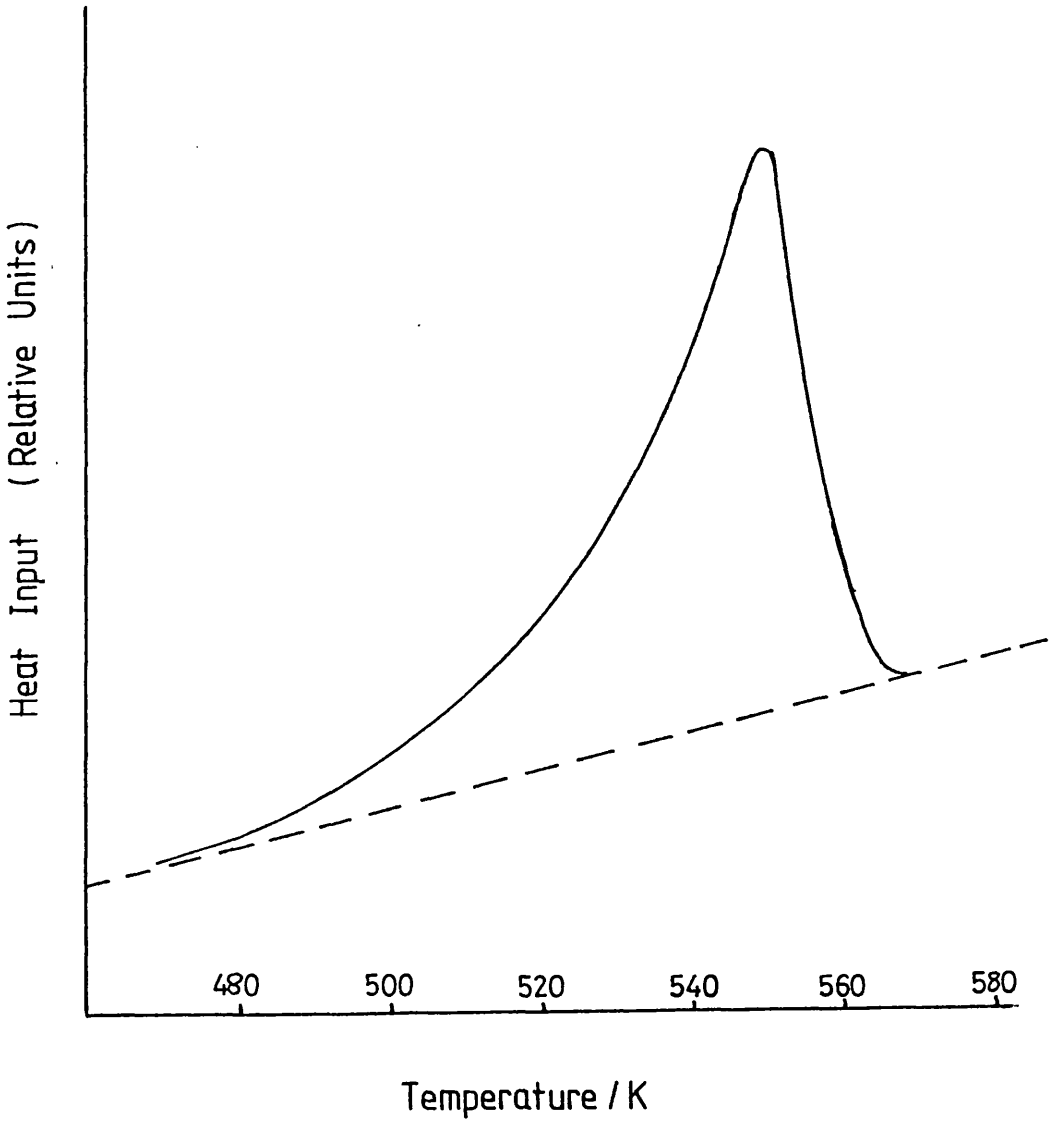

$$\text{Balance reading} = (M_1-M_2)-\left\{\frac{p}{P_A}\ D(V_1-V_2)\right\} \qquad (2.6)$$

where M_1 and V_1 are the mass and volume of FEP, M_2 and V_2 are the mass and volume of silver, p is the pressure of air in the balance, P_A is atmospheric pressure and D is the density of air at P_A. A plot of balance reading against pressure in the balance chamber yielded a linear graph of gradient $\frac{D}{P_A}(V_1-V_2)$ from which the difference in volume between the FEP and silver samples, (V_1-V_2) was found. The volume of silver, V_1, was calculated from its mass and density to give V_2 the volume of the FEP sample. The density of the FEP can then be calculated from its mass and volume.

2.12 Experimental Procedure for Density Determinations

After calibrating the balance the FEP film and silver wire were weighed and mounted on the appropriate balance hooks. The balance chamber was then pumped down to a pressure of less than 10^{-4} torr using the rotary and vapour diffusion pumps. Having tared the balance to zero (under vacuum), atmospheric air was leaked in, to the required pressure, and the balance left to stabilise for several minutes before weight and pressure readings were recorded. Nine separate balance readings were taken up to a pressure of about 450 torr. Linear regression analysis was used to determine the gradient of the balance reading against pressure plot.

The density of atmospheric air needed for the calculation was determined using the equation[96],

$$D_A = 1.2929\ (273.13/T)[(B-0.3783e)/760] \qquad (2.7)$$

where,

D_A = density of atmospheric air / g cm^{-3}

T = air temperature / K

B = barometric pressure / torr

e = vapour pressure of moisture / torr

2.13 Density Determinations Using the Liquid Displacement Method

A liquid displacement method was used to determine the density of 0.002 inch thick FEP film annealed at 100 °C for 24 hours, annealed at 200 °C for 24 hours and in the as-received state. A liquid was required for these determinations that was sufficiently involatile to use a density bottle, had a low uptake by FEP and had a low surface tension to avoid air bubbles being trapped on the polymer surface. The hydrocarbon xylene was found to fulfil these requirements. The procedure involved accurately determining the volume of a nominally 25 cm^3 density bottle which was thermostatted in a waterbath at 25 ±0.02 °C; this was achieved using distilled water. A weighed sample of FEP film (approximately 1.5 g) was then placed in the density bottle which was filled with xylene and thermostatted at 25 °C before weighing. A value for the density of the FEP film was then calculated from a knowledge of this weight, W_X, together with the weight of the FEP sample, W_F, the density of the xylene, D_X, at 25 °C and the weight, W_B, and volume, V_B, of the density bottle at 25 °C. The density of the FEP film, D_F, is given by

$$D_F = \frac{V_B - [(W_X - W_B - W_F)] \cdot D_X}{W_F} \qquad (2.8)$$

2.14 Infrared Absorption Spectrometry to Detect Changes in the Volume Percent Crystallinity of the FEP on Annealing

Miller and Willis[97], and also Moynihan[98], have used infrared absorption spectroscopy for measuring the crystallinity of poly(tetrafluoroethylene). Moynihan[98] used the ratios of the 778 cm^{-1} and 2367 cm^{-1} band intensities as a measure of the amorphous content of the polymer. Absorption by the amorphous fraction of the polymer produces a band at 778 cm^{-1}, and an overtone of the strong CF_2 absorption at 2367 cm^{-1} was used as an internal thickness standard.

The infrared absorption spectrum of FEP was accordingly determined and was also found to show bands at 778 cm^{-1} and 2367 cm^{-1}. The ratio of these band intensities was then used as a basis for measuring differences in crystallinity between the FEP samples. An absolute measure of crystallinity could not be made using this method since the absorbance of a 100% amorphous sample was not available.

Infrared absorption spectra were run on a Rank Hilger infragraph MK.3 H1200 infrared spectrometer. Absorbance measurements were taken for the bands at 2367 cm^{-1} and 778 cm^{-1}. The band at 2367 cm^{-1} was of measurable size, with no attenuation of the reference beam necessary, whereas the band at 778 cm^{-1} needed attenuation to reduce errors in measurement. An infrared absorption spectrum of FEP is shown in Fig. 10. Also shown are the baselines from which absorbance measurements were taken.

Fig. 10 INFRARED ABSORPTION SPECTRUM OF FEP FILM

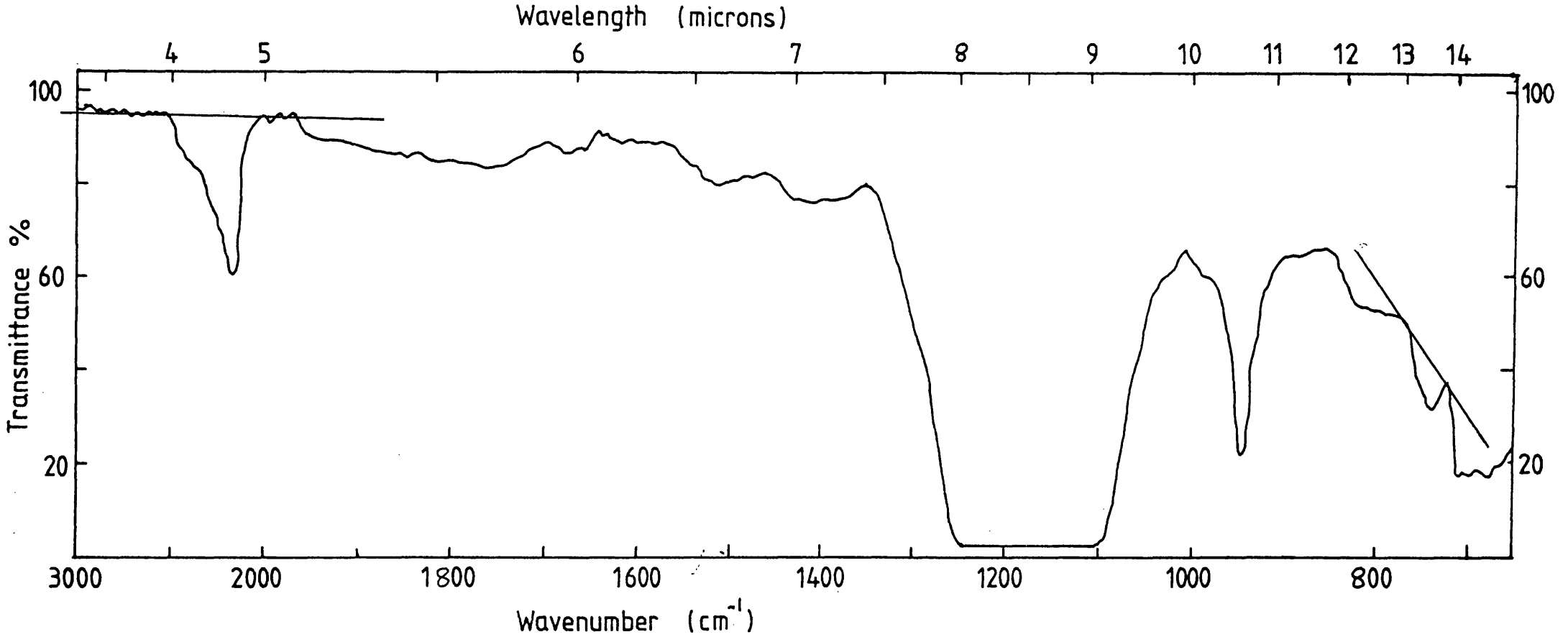

2.15 Materials

The PET film used in the study of the systems PET/dichloromethane and PET/nitroethane using the flame ionisation detector was Type S 'Melinex' polyester film of 12μm thickness supplied by Imperial Chemical Industries Ltd. The dichloromethane used for these measurements was a general purpose reagent 'A' grade supplied by Hopkins and Williams. The nitroethane, grade SLR, was supplied by Fisons.

The PET film used in the study of the system PET/dichloromethane using the electron capture detector was Type S 'Melinex' polyester film of 23μm thickness for the runs at 65, 70, 80 °C and 50μm thickness for the runs at 90, 100, 110 °C. High purity nitrogen supplied by Air Products was used as the carrier gas for all permeability measurements made using the dynamic system.

The PTFE film of 0.003 inch thickness was supplied by Fluorocarbon Co Ltd of Caxton Hill, Hertford, Herts.

The FEP film of 0.002 inch thickness used in the study of the systems FEP/methane (60 - 150 °C), FEP/nitroethane (60 - 100 °C), FEP/dichloromethane (60 - 100 °C) and FEP/tetrachloroethylene (60 - 100 °C) was obtained from the same suppliers.

The FEP film used for the remaining permeation measurements was of 0.002 inch thickness and was supplied by Klinger Ltd of Sidcup, Kent. Although the FEP film samples were obtained from two different suppliers they were known to originate from the same manufacturer which was Du Pont Ltd.

The dichloromethane used for the FEP and PTFE permeation measurements was grade AR supplied by Fisons. The nitroethane and tetrachloroethylene were general purpose reagents supplied by BDH. Gas mixtures of methane in nitrogen, 0.99% and 2.05% were supplied by Air Products. The 12.5 ppm tetrachloroethylene in nitrogen gas mixture used for calibration of the FID was supplied by Rank Hilger Special Products Group, Margate, Kent.

Low density PE film was supplied by Imperial Chemical Industries Ltd, specified as being of 45 - 50μm thickness and British Cellophane Ltd, specified as being of 50μm thickness.

The FEP film of 0.002 inch thickness used in the differential scanning calorimetry, infrared absorption spectroscopy and density determinations was supplied by Klinger Ltd of Sidcup, Kent.

Sorption isotherms were determined with 0.001 inch thickness FEP film from the same suppliers.

CHAPTER 3 RESULTS

Table 1 shows permeability and diffusion coefficients for the permeation of nitroethane through PET film of 12 μm thickness. Nitroethane was supplied to the upstream side of the permeation cell at a partial pressure of 4.5 ±0.05 torr. The results apply to a single PET film heated to 140 °C before measurements were taken at descending temperature intervals. Since the Perkin-Elmer flame ionisation detector was housed in the same oven as the permeability cell it was necessary to calibrate the detector at each measurement temperature. The partial pressure of permeant vapour was calculated assuming the gas saturator, which was thermostatted at 40 °C, produced a completely saturated vapour stream; saturator efficiency determinations were not made for these permeation measurements. Permeability coefficients were calculated using equation 2.2 and diffusion coefficients determined using equation 1.21.

Table 2 shows permeability and diffusion coefficients for the permeation of dichloromethane through PET film of 12 μm thickness. Dichloromethane was supplied to the upstream side of the permeation cell at a partial pressure of 545 ±5 torr. The results apply to a single PET film heated to 130 °C before measurements were taken at descending temperature intervals. The partial pressure of permeant vapour was calculated assuming the gas saturator, which was thermostatted at 24.2 °C, produced a completely saturated vapour stream. Permeability and diffusion coefficients were calculated as before.

TABLE 1 Transport of Nitroethane Through PET

T/°C	P/cB[a]	D x 10^{13}/cm^2 s^{-1}
50.0	6.37	-
70.0	17.5	3.20
90.0	48.2	8.50
110.0	161	45.0
125.0	382	103
140.0	893	252

[a] 1cB = 10^{-12} cm^3 (STP) cm/(cm^2 sec cm Hg)

TABLE 2 Transport of Dichloromethane Through PET

T/°C	P/cB	D x 10^{13}/cm^2 s^{-1}
60.0	10.4	7.00
65.0	13.5	7.00
76.0	17.9	11.6
95.0	48.4	38.0
110.0	145	102
130.0	382	255

Uncertainties of 9% and 15% are estimated for the permeability and diffusion coefficients, respectively. The main contribution towards the error in the permeability coefficient measurements was undoubtedly made by uncertainties in the permeant vapour concentration. Errors in the measurement of the gradient of the transient region of the permeation trace made the largest contribution towards uncertainties in the diffusion coefficients. Since repeat measurements were not made for these systems levels of precision could not be calculated. Table 3 shows permeability coefficient measurements for the permeation of dichloromethane through a single PET film using the electron capture detector. The measurements from 65 °C to 80 °C were recorded using a PET film of 23 μm thickness whereas the measurements taken between 90 °C and 110 °C apply to a PET film of 50 μm thickness. The dichloromethane was supplied to the upstream side of the permeability cell at a partial pressure of 290 ±1 torr. Measurements were taken at descending temperature intervals.

As with the FID measurements, the major source of error in the permeability coefficients was undoubtedly in the calculated value for the concentration of vapour in the permeant stream. An uncertainty of 10% is estimated for the results given in Table 3. Permeability and diffusion coefficients are shown in Table 4 for the transport of nitroethane through a 0.003 inch thickness PTFE film. The results were recorded using a PTFE film that had been annealed for 24 hours at 200 °C prior to measuring transport parameters. The permeant was supplied to the upstream side of the permeation cell at a partial pressure of 24.5 ±0.5 torr. A 100% saturator efficiency was assumed when calculating the concentration of permeant vapour.

TABLE 3 Permeability Coefficients for the Permeation of Dichloromethane through PET using the Electron Capture Detector

T/°C	P/cB
65.0	9.00
70.0	13.5
80.0	20.1
90.0	37.3
100.0	72.2
110.0	129

TABLE 4 Transport of Nitroethane through PTFE

T/°C	$P \times 10^{-2}$/cB	$D \times 10^{8}/cm^{2}s^{-1}$
69.1	11.0	1.81
79.2	13.5	2.91
89.6	16.3	4.48
109.7	23.8	8.89
119.6	27.7	11.5
129.9	34.2	15.4
140.1	39.8	19.3
160.2	55.8	22.8

A permeant flow rate of 10 cm^3 min^{-1} was used for these experimental runs. Later investigation into the effect of permeant flow rate on the gradient of the linear transient region of the trace, showed that increasing the flow rate of permeant produced a corresponding increase in the gradient. The gradient was found to increase to a limiting value at 35 cm^3 min^{-1} which was a factor of 1.4 times greater than at a permeant flow rate of 10 cm^3 min^{-1}. It is thought that this increase in gradient was produced by an increased sharpness of the boundary between permeant and flush gas passing through the downstream cell chamber. This effect has been noted by Pasternak[88] previously. Unfortunately the change in gradient was discovered after the PTFE/nitroethane runs had been completed, so the values for the diffusion coefficients in Table 4 have been corrected by a factor of 1.4 times the values calculated from the permeation trace. Permeability coefficients given in the same table are unaffected. A flow rate of 10 cm^3 min^{-1} was used for the earlier PET measurements but much smaller diffusion rates ensured that the reduced sharpness of the boundary between flush and permeant streams had no effect on the gradient of the linear region.

Table 5 shows permeability and diffusion coefficients for the permeation of dichloromethane through a PTFE film of 0.003 inch thickness. The film was annealed for 15 hours at 200 °C prior to measuring transport parameters. Permeant vapour was supplied at a partial pressure of 278 torr. When calculating permeant concentrations the saturator was assumed to produce a completely saturated vapour stream. Errors on these measurements are estimated to be the same as for the PET/permeant results.

TABLE 5 Transport of Dichloromethane through PTFE

T/°C	$P \times 10^{-2}$/cB	$D \times 10^{8}/cm^{2}s^{-1}$
81.0	11.0	4.21
100	15.7	8.53
120.0	22.0	17.7
140.7	32.3	30.5
151.7	37.8	36.1

TABLE 6 Transport of Methane through PTFE

Membrane 1		Membrane 2	
T/°C	$P \times 10^{-2}$/cB	T/°C	$P \times 10^{-2}$/cB
69.3	4.38	59.2	3.22
79.9	5.73	69.0	4.20
90.3	7.53	79.8	5.61
99.2	9.38	89.6	7.22
110.0	12.1	99.1	9.08
120.7	15.6	109.9	11.7
130.7	19.5	119.2	14.8
141.0	24.4	129.9	19.2
151.3	29.9	140.5	24.4
		150.6	29.9

Table 6 shows permeability coefficients for the permeation of methane through two separate PTFE films of 0.003 inch thickness. The methane was supplied from a cylinder as a 0.99% mixture of methane in nitrogen. Both films were annealed at 200 °C for 15 hours before taking measurements at descending temperature intervals. Diffusion coefficients were not calculated from the gradient of the linear region of the trace since the rapid attainment of steady-state permeation would have produced large errors in these values.

Table 7 shows permeability coefficients for the permeation of methane through FEP film of 0.002 inch thickness. The methane was supplied from a cylinder as a 0.99% mixture of methane in nitrogen. The film was annealed at 200 °C for 15 hours before permeation runs were performed at descending then ascending temperature intervals.

Tables 8 and 9 show permeability coefficients for the permeation of methane through low density PE film of 50 μm thickness supplied by British Cellophane Ltd. and 48 μm thickness supplied by Imperial Chemical Industries Ltd. The methane permeant was a mixture of 0.99% methane in nitrogen. The ascending temperature measurements were taken without annealing the film. Having completed the ascending temperature runs the film was cooled and measurements were taken at descending temperature intervals.

In Tables 10 - 13 permeability and diffusion coefficients are given for the permeation of tetrachloroethylene, nitroethane, dichloromethane and methane through FEP film of 0.002 inch thickness. For each polymer/permeant system investigated a different film was used

TABLE 7 Transport of Methane through FEP

T/°C	P x 10^{-2}/cB	T/°C	P x 10^{-2}/cB
59.0	2.67	69.3	3.79
69.2	3.88	89.9	9.01
79.8	5.97	110.0	19.26
89.7	9.07	130.2	38.2
99.8	13.4	150.2	67.9
110.0	18.9		
120.5	27.2		
130.6	38.6		
140.2	52.3		
150.9	69.0		

TABLE 8 Transport of Methane through Low Density PE Supplied by British Cellophane Ltd

Ascending Temperatures		Descending Temperatures	
T/°C	P x 10^{-2}/cB	T/°C	P x 10^{-2}/cB
49.4	10.9	49.8	14.8
54.3	14.4	54.8	18.6
59.4	18.7	59.4	22.2
64.0	23.3	64.6	28.8
69.4	30.9	80.3	55.4
80.2	51.8	90.7	83.1
90.7	83.1		

TABLE 9 Transport of Methane through Low Density PE Supplied by Imperial Chemical Industries Ltd

T/°C	$P \times 10^{-2}$/cB	T/°C	$P \times 10^{-2}$/cB
47.9	10.3	49.2	13.0
54.8	15.3	54.0	17.0
58.8	19.0	59.2	23.4
64.7	25.0	63.9	29.5
69.4	31.2	69.2	36.4
74.8	41.1	74.2	44.1
79.6	51.7	79.5	52.6
85.5	67.0	90.1	81.1
90.1	81.1		

TABLE 10 Transport of Tetrachloroethylene through FEP

T/°C	$P \times 10^{-3}$/cB	$D \times 10^{9}/cm^{2}s^{-1}$
20.0	0.283	0.105
30.5	0.410	0.287
40.6	0.627	0.651
51.3	0.910	1.51
60.6	1.30	3.31
65.2	1.49	4.47
69.7	1.70	6.15
75.0	2.03	9.04
79.3	2.40	11.9
84.5	2.90	16.6
89.8	3.52	24.2
95.1	4.28	33.7
100.9	5.35	43.0

TABLE 11 Transport of Nitroethane through FEP

T/°C	P x 10^{-3}/cB	D x 10^{8}/$cm^{2}s^{-1}$
20.1	0.257	0.0671
30.5	0.371	0.158
41.1	0.554	0.356
51.2	0.775	0.677
55.7	0.840	1.01
60.1	0.962	1.34
65.0	1.12	1.81
69.7	1.28	2.32
74.3	1.50	3.00
79.7	1.80	4.10
85.0	2.17	5.53
89.6	2.49	7.26
95.0	3.06	9.56
100.4	3.68	12.5

TABLE 12 Transport of Dichloromethane through FEP

T/°C	$P \times 10^{-3}$/cB	$D \times 10^{8}$/cm^{2}s^{-1}
20.0	0.181	0.151
29.9	0.272	0.340
40.4	0.413	0.663
51.1	0.576	1.37
59.4	0.721	2.24
65.0	0.862	3.19
69.7	1.00	4.25
74.3	1.18	5.27
79.7	1.40	7.02
84.9	1.68	9.52
89.6	1.96	12.0
95.0	2.32	15.2
100.3	2.75	17.6

TABLE 13 Transport of Methane through FEP

T/°C	P x 10^{-2}/cB
20.7	0.674
24.3	0.832
30.2	1.04
34.2	1.32
40.4	1.64
44.4	2.02
51.8	2.61
60.1	3.46
69.2	4.85
80.3	7.34
90.4	10.9
99.4	14.9

for the low temperature permeation measurements between 20 °C and 50 °C. All the films used were annealed at 100 °C for 24 hours before measuring the transport parameters at descending temperature intervals. The methane was supplied from a cylinder as a mixture of 2.05% methane in nitrogen. Tetrachloroethylene was supplied at a partial pressure of 22 torr for the high temperature measurements (60 - 100 °C) and 10 torr for the low temperature measurements (20 - 50 °C). Nitroethane was supplied at a partial pressure of 11 torr for the high temperature measurements and 10 torr for the low temperature measurements. Dichloromethane partial pressures of 264 torr and 255 torr were employed. Gas saturator efficiency determinations were performed at each of the temperatures used in the investigation of these systems. These efficiency measurements were included in the calculation of permeant partial pressures.

Table 14 shows permeation rates of nitroethane through an FEP film thermostatted at 99.8 °C with increasing partial pressure of permeant. The FEP film of 0.002 inch thickness was annealed at 100 °C for 24 hours before performing permeation runs at increasing partial pressures of permeant.

The precision of permeability and diffusion coefficients were determined for measurements made using the dynamic system incorporating the Pye 104 FID. Since the temperature control of the permeability cell was different for the air cabinet and water bath separate precision determinations were performed for these two set-ups. The standard deviations given in Table 15 were determined for the FEP/nitroethane system but are also considered a good estimate for

TABLE 14 Transport of Nitroethane through FEP at 99.8°C with an Increasing Partial Pressure of Permeant

Flux x 10^9/ $\frac{cm^3(STP).cm}{cm^2}$	Partial Pressure x 10^{-1}/torr
3.82	1.07
4.19	1.17
4.63	1.30
5.14	1.44
5.77	1.62
6.50	1.81
7.19	2.01
7.96	2.20
8.86	2.46

TABLE 15 Precision of Permeability and Diffusion Coefficient Measurements Using the Pye 104 FID

No. Determinations	Temp. Control of Cell	Permeant	Temp/°C	P/cB	$Dx10^8$/ $cm^2\ s^{-1}$	Standard Deviations P/cB	Standard Deviations $Dx10^9$/ $cm^2\ s^{-1}$
5	Air Cabinet	Nitroethane	90	2400	7.60	50.4	7.2
5	Waterbath	"	25	311	0.095	6.71	0.082
5	Air Cabinet	Methane	90	875	-	13.1	-
5	Waterbath	"	25	85.0	-	1.42	-

the other permeant vapour systems. A series of six permeation runs were performed in both the air cabinet and water bath with the recorder signal being left to return to the baseline between runs. A similar series of measurements was recorded using the 2.05% methane in nitrogen gas mixture. The standard deviations for these measurements are shown in Table 15.

Tables 16, 17 and 18 show the uptake of dichloromethane by FEP film of 0.001 inch thickness at 29.89 °C in the as-received state, annealed at 100 °C for 24 hours and annealed at 200 °C for 24 hours, respectively.

The uptake of nitroethane by FEP film of 0.001 inch thickness is shown in Table 19. The FEP was annealed at 100 °C for 24 hours prior to performing sorption measurements at 29.89 °C.

Table 20 shows the sorption of tetrachloroethylene by FEP film at 29.89 °C. The polymer had been previously annealed at 100 °C for 24 hours.

The mean of three endotherm area measurements obtained using a Perkin-Elmer Model DSC-1B differential scanning calorimeter are reported in Table 21. Approximately 10 mg of FEP film of 0.002 inch thickness was used for each scan.

Table 22 shows absorbance ratios for peaks in the FEP infrared absorption spectrum at 778 cm^{-1} and 2367 cm^{-1}. The results reported are the mean of three absorbance ratios for each of the FEP film samples in the as-received state, annealed at 100 °C for 24 hours and annealed at 200 °C for 24 hours.

TABLE 16 Sorption at 30 °C of Dichloromethane by FEP Film in the As-Received State

Pressure/torr	[a]Relative Pressure	Concentration/mg g^{-1}
5.89	0.0113	0.0968
15.23	0.0293	0.2300
25.52	0.0491	0.3807
40.96	0.0788	0.5983
56.50	0.1087	0.8119
72.02	0.1386	1.0175
102.31	0.1969	1.4123
132.42	0.2548	1.8263

[a]Relative pressure = pressure/saturated vapour pressure of dichloromethane at 29.89 °C

TABLE 17 Sorption at 30 °C of Dichloromethane by FEP Film Annealed at 100 °C for 24 Hours

Pressure/torr	Relative Pressure	Concentration/mg g^{-1}
5.39	0.0104	0.0839
14.91	0.0287	0.2291
25.85	0.0497	0.3896
41.11	0.0791	0.6036
56.36	0.1085	0.8134
71.78	0.1381	1.0227
87.67	0.1687	1.2322
103.24	0.1987	1.4355
121.04	0.2329	1.6599
135.14	0.2601	1.8436

TABLE 18 Sorption at 30 °C of Dichloromethane by FEP Film Annealed at 200 °C for 24 Hours

Pressure/torr	Relative Pressure	Concentration/mg g^{-1}
5.53	0.0106	0.0695
10.56	0.0203	0.1325
15.49	0.0298	0.1934
20.73	0.0399	0.2571
30.87	0.0594	0.3780
40.54	0.0780	0.4899
51.22	0.0986	0.6116
61.84	0.1190	0.7307
72.12	0.1388	0.8440
82.28	0.1583	0.9552
93.06	0.1791	1.0730

TABLE 19 Sorption at 30 °C of Nitroethane by FEP Film Annealed at 100 °C for 24 Hours

Pressure/torr	Relative Pressure	Concentration/mg g^{-1}
1.39	0.0525	0.0611
3.09	0.117	0.1332
4.25	0.161	0.1849
5.38	0.203	0.2361
6.17	0.233	0.2713

TABLE 20 Sorption at 30 °C of Tetrachloroethylene by FEP Film Annealed at 100 °C for 24 Hours

Pressure/torr	Relative Pressure	Concentration/mg g^{-1}
1.39	0.0576	0.710
2.75	0.114	1.40
3.60	0.149	1.79
4.54	0.188	2.27
5.57	0.231	3.08

TABLE 21 Differential Scanning Calorimeter Measurements

FEP Film	Endotherm Area/$cm^2 g^{-1}$	Standard Deviation /$cm^2 g^{-1}$
As-received	1.43	0.208
Annealed at 100 °C	1.54	0.182
Annealed at 200 °C	1.89	0.025

(Three measurements made on each film)

TABLE 22 Infrared Absorption Measurements

FEP Film	(778 cm^{-1}/2367 cm^{-1})	Standard Deviation
As-received	0.795	0.066
Annealed at 100 °C	0.718	0.074
Annealed at 200 °C	0.615	0.062

(Three measurements made on each film)

FEP film densities determined using the liquid displacement method described in the Experimental Section are shown in Table 23. The reported densities are the mean of the number of measurements indicated in the table.

Using the buoyancy method to determine densities gave values of 2.259 g cm^{-3} for the as-received polymer, 2.431 g cm^{-3} for the polymer annealed at 100 °C and 2.437 g cm^{-1} for the polymer annealed at 200 °C. Linear regression analysis was used to determine the gradient of the balance reading against air pressure plot needed for the density calculations.

TABLE 23 Density Measurement by Liquid Displacement

FEP Film	Density/g cm^{-3}	No Determinations	Standard Deviation/$cm^2 g^{-1}$
As-received	2.169	5	0.018
Annealed at 100°C	2.158	4	0.018
Annealed at 200°C	2.191	5	0.015

TABLE 24 Transport Parameters for the Permeation of Different Gases and Vapours Through PET

Permeant	T/°C	P/cB	Ep/kJmol^{-1}	Source
Nitroethane	70	18.5	72.6	This work
Dichloromethane	70	16.1	72.7	" "
Helium	25	132	25.5	ref. 43
Oxygen	25	3.5	44.3	" "
Nitrogen	25	0.65	58.9	" "
Carbon dioxide	25	17	51.0	" "
Methane	25	0.32	61.4	" "
Methyl bromide	60	8.0	-	ref. 101
Benzene	40	257.9	-	ref. 100
Carbon tetrachloride	40	24.9	-	" "
Hexane	40	45.7	-	" "

CHAPTER 4 DISCUSSION

4.1 Transport of Dichloromethane and Nitroethane Through PET Film

A survey of the literature[1] showed that PET might have the necessary permeability and solubility characteristics required in the early stages of this project. These characteristics were,

(i) low oxygen permeability,

(ii) high solubility in organic nitro-compounds,

and

(iii) low solubility in organic chloro-compounds.

It was therefore decided to investigate the selective permeability of the semi-crystalline PET film to organic nitro- and chloro-compounds.

The first polymer/permeant systems investigated using the dynamic technique were PET/dichloromethane and PET/nitroethane. Both these permeant streams were conveniently produced using the gas saturator described in the Experimental Section.

Fig. 11 shows Arrhenius plots of the diffusion coefficients for nitroethane and dichloromethane through PET. The diffusion coefficients were calculated using equation 1.21 given by Pasternak et al[88]. In deriving this equation it is assumed that the diffusion coefficient is not a function of concentration, that the surface concentration is proportional to the pressure of the permeant and that swelling of the membrane is negligible. Since the permeants used in this work were not simple gases it is likely that the diffusion coefficients were a function of concentration and that for measurements taken below the glass

Fig. 11 ARRHENIUS PLOTS OF DIFFUSION COEFFICIENTS FOR THE SYSTEMS PET/DICHLOROMETHANE AND PET/NITROETHANE

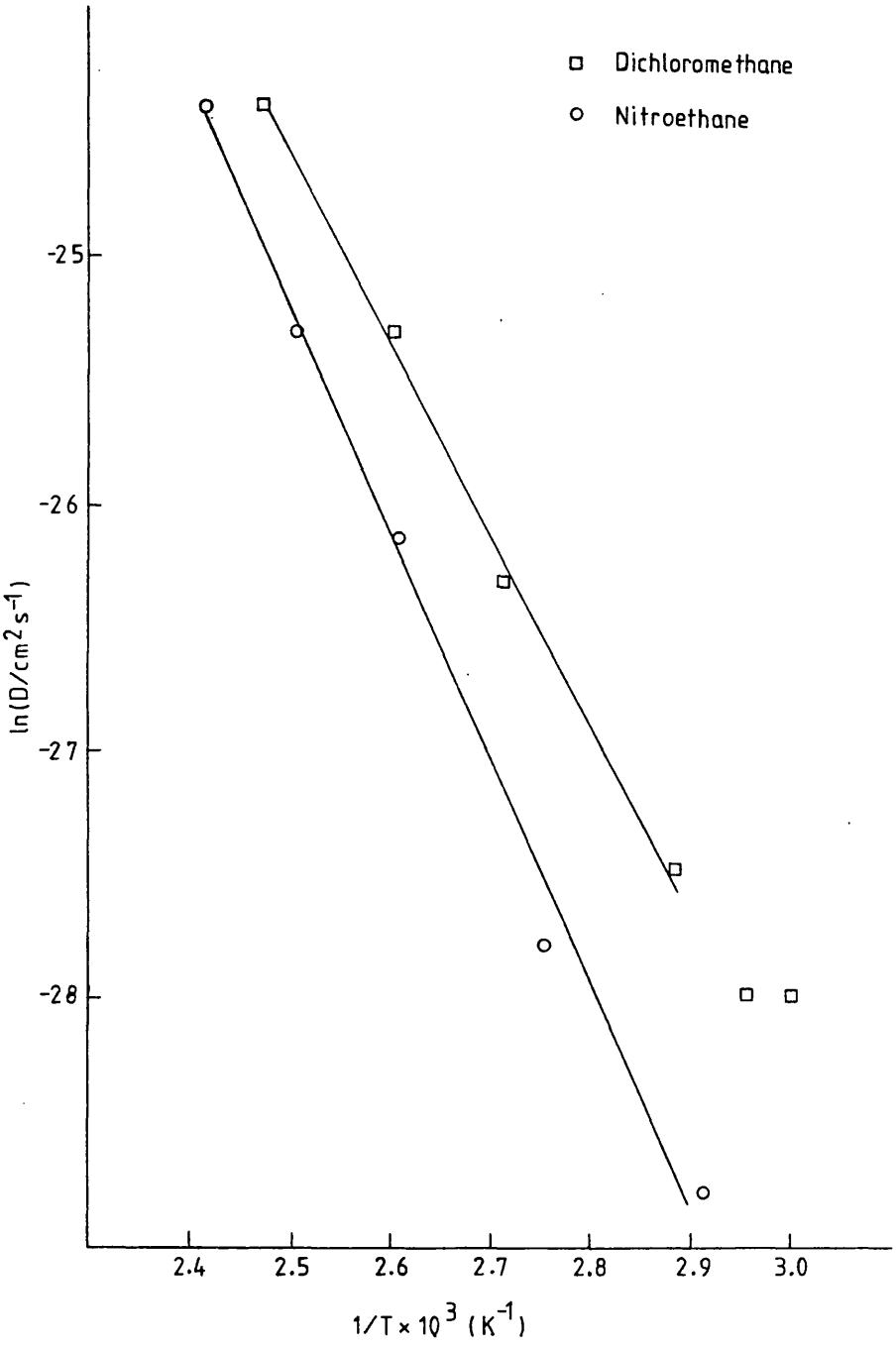

transition temperature, T_g, polymer relaxation effects produced an additional time dependence. The likely dependence of the diffusion coefficients on concentration of permeant and time, limit the accuracy of the values calculated using equation 1.21 for the PET/permeant systems investigated.

A linear Arrhenius plot is seen in Fig. 11 for the diffusion of nitroethane through PET. The Arrhenius plot for dichloromethane is linear in the higher temperature region but measurements made at the lower temperatures are greater than this linear relation would suggest. It is likely that the non-linearity of the plot in the lower temperature region is a result of a reduced activation energy for diffusion below T_g. Although crystallinity levels of the PET film used in this work were not measured, annealing the polymer at 200 °C undoubtedly gave crystallinity levels in excess of 50% giving an expected T_g of about 80 °C.

Michaels et al[43] on measuring diffusion coefficients for the permeants, helium, oxygen, argon, nitrogen, carbon dioxide and methane through crystalline PET found a transition region in the Arrhenius plot which began at about 80 °C and extended to about 95 °C. A linear relationship was apparent on either side of the transition region with a reduced slope and therefore reduced activation energy for diffusion at the lower temperatures.

Fig. 11 shows that diffusion rates of dichloromethane through PET are greater than nitroethane over the temperature range covered in this work. This is expected considering the larger size of the nitroethane molecule and therefore the greater energy needed to move the molecule against the cohesive

forces of the polymer. The van der Waals volumes for nitroethane and dichloromethane are given as 67.6 $Å^3$ [99] and 57.6 $Å^3$ [99] respectively.

Fig. 12 shows Arrhenius plots of the permeability coefficients for nitroethane and dichloromethane through crystalline PET. Both plots show changes in gradient in the region of T_g. The transition region is located at about 86 °C for nitroethane permeation and about 84 °C for dichloromethane permeation.

Another feature to notice in Fig. 12 is the higher permeation rates of nitroethane despite the higher diffusion coefficients of the smaller dichloromethane molecule. Since the permeability coefficient is a function of both the diffusion coefficient and the solubility, this indicates that the solubility of nitroethane is greater than dichloromethane. This is consistent with the solubility of a gas being related to its tendency to condense of which the boiling point, critical temperature and Lennard-Jones force constant are each measures. Table 24 gives a comparison of permeability coefficients obtained from the literature for gases and vapours through semi-crystalline PET film with values obtained for dichloromethane and nitroethane from this work. Also included, where available, are activation energies for permeation through the rubbery polymer.

PET was originally chosen for investigation because it was believed the polymer would have greater permeability towards organic nitro-compounds than organic chloro-compounds. The ratio of nitroethane permeability to dichloromethane

Fig. 12 ARRHENIUS PLOTS OF PERMEABILITY COEFFICIENTS FOR THE SYSTEMS PET/DICHLOROMETHANE AND PET/NITROETHANE

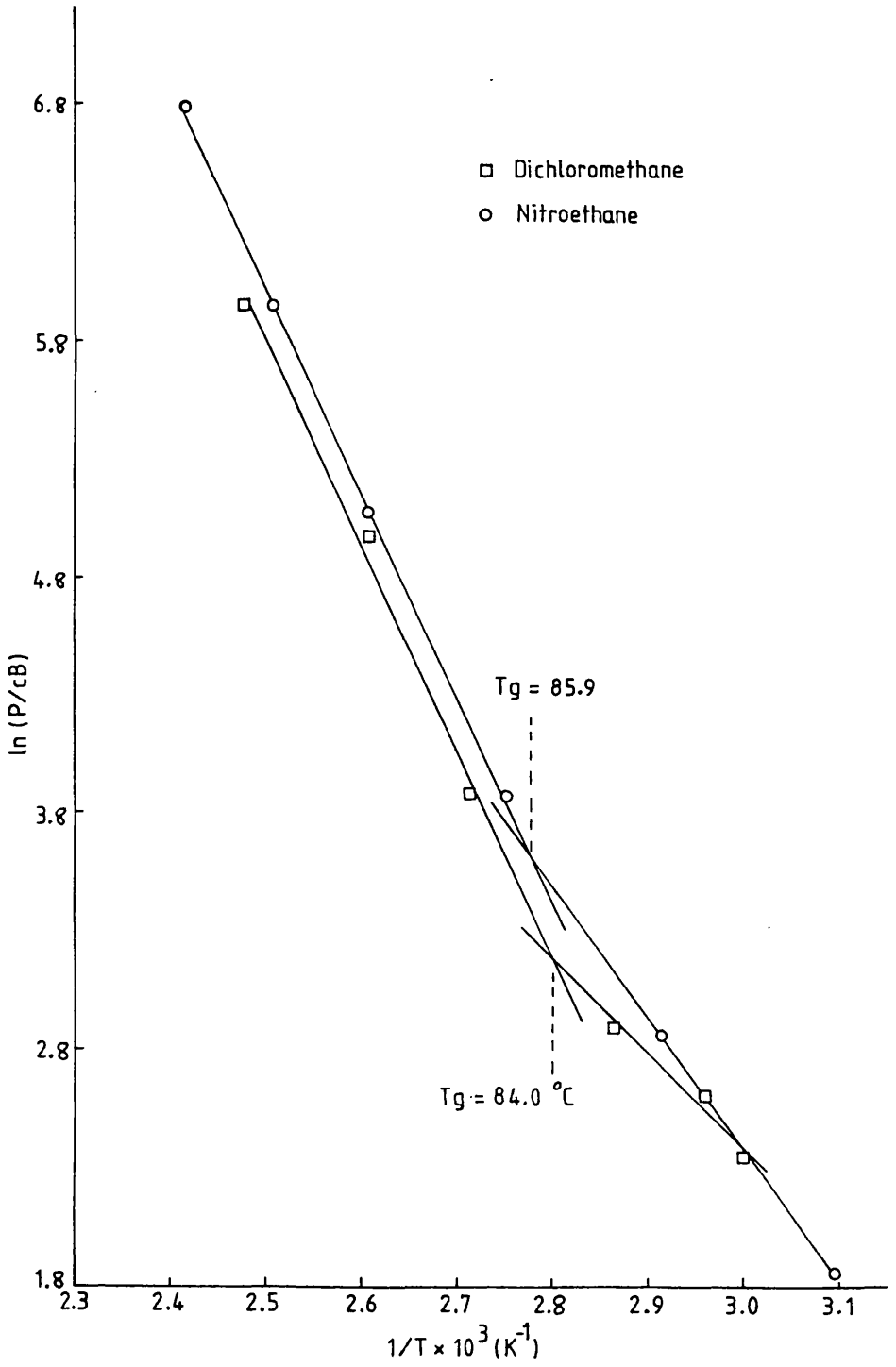

permeability at 70 °C is 17.5 cB/13.5 cB = 1.30. As explained previously the selectivity shown towards nitroethane is a result of its greater solubility in the polymer which is in turn related to its condensibility, this being greater for nitroethane. The solubility levels are also related to the degree of interaction between the polymer and permeant. The relative contributions to the solubility made by this effect cannot be determined from the results for the two permeants.

Since the flame ionization detector was working to its limits of sensitivity for the PET/permeant systems investigated it was decided at this stage of the work to incorporate a more sensitive electron capture detector in the flow system. Fig. 13 shows an Arrhenius plot of permeability coefficients for the system PET/dichloromethane obtained using the electron capture detector. A comparison with the results obtained using the flame ionization detector shows that they agree well above T_g.

It was recognized during this work that the electron capture detector suffered from several disadvantages.

(i) Leakage of low molecular weight species from the film reduced the standing current available for detecting permeant species, thus increasing measurement error.

(ii) Since the detector responded to a drop in current, if too high a concentration of electron capturing vapour was present all the available standing current was used up and the detector became saturated. The need to

Fig. 13 ARRHENIUS PLOTS OF PERMEABILITY COEFFICIENTS FOR THE SYSTEM PET/DICHLOROMETHANE USING THE ELECTRON CAPTURE DETECTOR

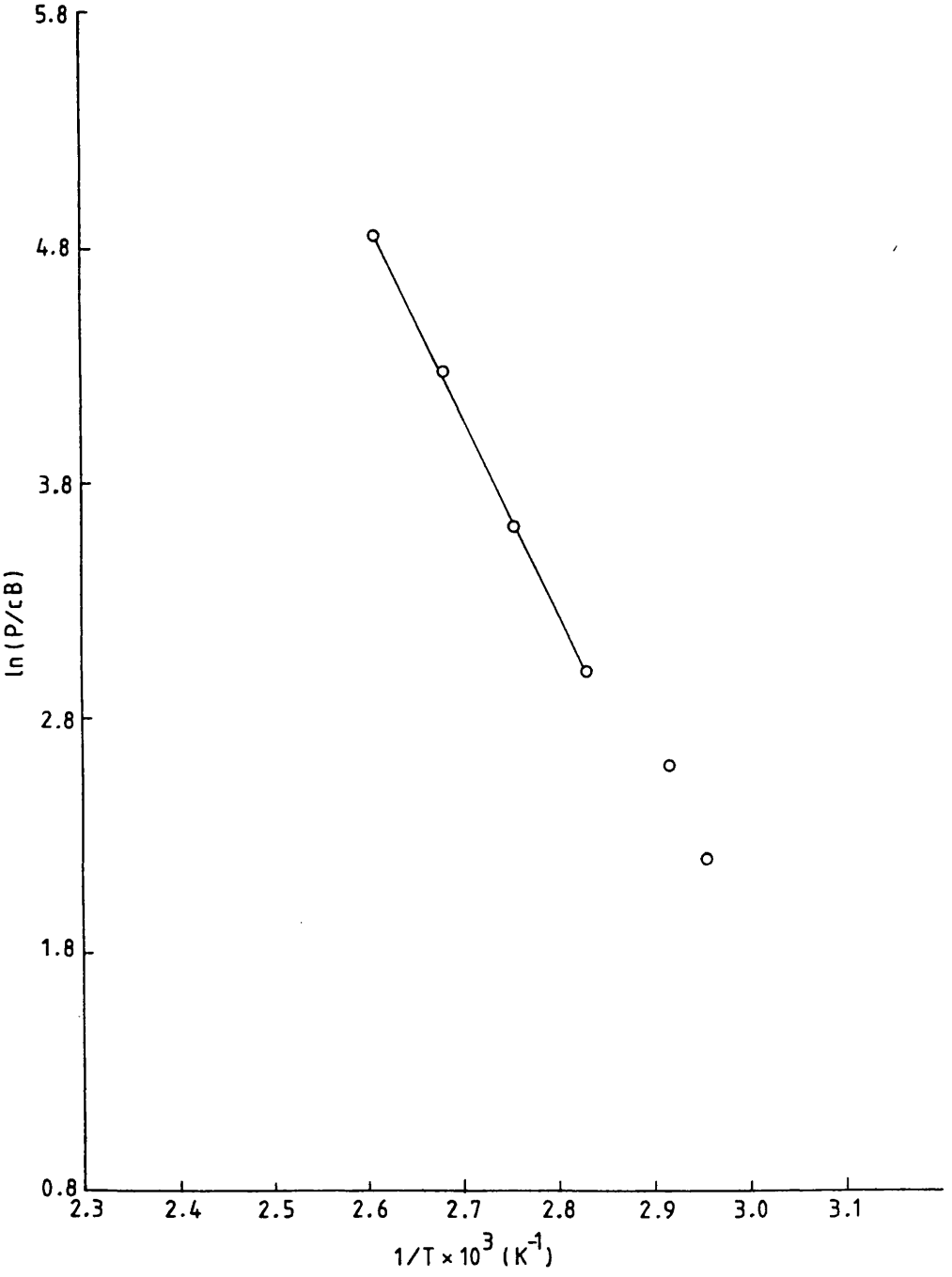

investigate more permeable films meant that saturation levels would have been obtained at relatively low temperatures.

(iii) The production of accurately known low concentrations of vapour was not easy and since different permeants would have had different response factors and permeability levels, different calibration methods would have had to have been devised for other vapours.

For the above reasons work was not continued with the electron capture detector. The detection system used for the remaining measurements was a Pye 104 series single flame ionization detector.

At this stage of the project the permeability requirements of the polymer film changed and the fluorocarbon polymers poly(tetrafluoroethylene) (PTFE) and poly(tetrafluoroethylene-co-hexafluoropropylene) (FEP) were thought to be more suitable for investigation.

Fig. 14 shows an Arrhenius plot of permeability coefficients for the system PTFE/methane. The graph is linear over the temperature range investigated and there is fairly good agreement between measurements taken using two separate PTFE films. The activation energy for permeation calculated from the mean of the slopes of the Arrhenius plots is 28.6 kJ mol^{-1}. Also shown in Fig. 14 is an Arrhenius plot of permeability coefficients for the system FEP/methane. Having annealed the film at 200 °C, measurements taken at both ascending and descending temperatures are seen to be in good agreement. The activation energy for permeation calculated from the Arrhenius plot is 42.7 kJ mol^{-1}.

Fig. 14 ARRHENIUS PLOTS OF PERMEABILITY COEFFICIENTS FOR THE SYSTEMS FEP/METHANE AND PTFE/METHANE

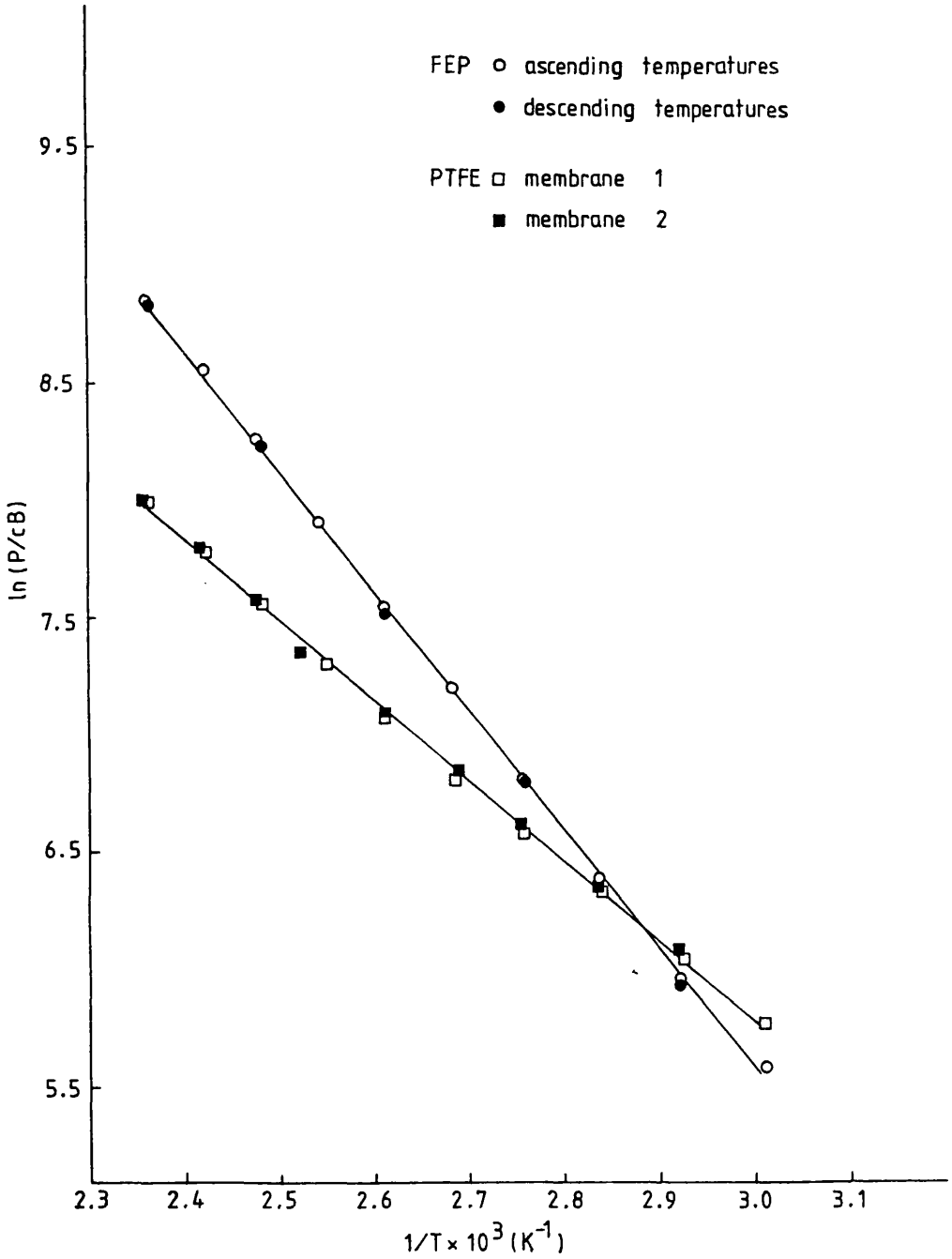

Comparisons are shown in Table 25 between results obtained in this work and by other workers for the two systems PTFE/methane and FEP/methane. In this work the approach to steady-state permeation levels was too rapid to enable diffusion coefficients to be calculated from the slope of the transient region. From Table 25 it can be seen that activation energies for permeation show differences from literature values. Small differences might be expected considering that gas transport behaviour is sensitive to the detailed nature of the polymer structure which varies from membrane to membrane. The differences shown, though, especially for PTFE are not small and for this reason it was decided to investigate the well characterised system low density polyethylene/methane and compare transport parameters obtained for this system with values from the literature.

It is clear from both this work and literature values (see Table 25) that activation energies for the permeation and diffusion of methane are greater for FEP than PTFE. Since complete fluorination of polyolefins leads to considerable stiffening of the carbon backbone this is an unexpected result which Pastenak et al[102] explain by suggesting that diffusion progresses partly through micropores in the PTFE. They maintain that this explanation is reasonable since PTFE of sufficiently high molecular weight to be usable virtually does not flow in the melt above its crystalline melting point of 327 °C because of its high viscosity. Fabrication requires compacting PTFE powder under high pressure near room temperature and then sintering at temperatures around 380 °C. The final product

TABLE 25 Transport Parameters for the Permeation of Methane Through PTFE and FEP, and Nitroethane and Dichloromethane through PTFE

Permeant	Polymer	P/cB at 90°C	E_p/kJmol^{-1}	P_ox10^{-6}/cB	Dx10^7/cm^{2}s^{-1} at 90°C	E_d/kJmol^{-1}	D_o/cm^{2}s^{-1}	Source
Methane	PTFE	788	28.6	9.35	-	-	-	This work
"	"	513	33.7	36.4	2.2	34.6	0.0213	ref. 27
"	FEP	992	42.7	1,200	-	-	-	This work
"	"	1330	35.0	145	4.9	41.3	0.43	ref. 27
"	"	1096	34.8	110	8.3	45.6	2.92	ref 102
Nitroethane	PTFE	1703	21.8	2.19	0.43	-	-	This work
Dichloromethane	"	1313	21.9	1.79	0.59	-	-	" "

usually obtained by machining very likely contains micropores.

Permeation and diffusion rates were also determined for the systems PTFE/nitroethane and PTFE/dichloromethane. Figs. 15 and 16 show Arrhenius plots of permeability and diffusion coefficients for these systems. Arrhenius plots of the diffusion coefficients for both permeants are linear over the low temperature region but show curvature at higher temperatures. The curvature almost certainly results from the rapid approach to steady-state permeation at the higher temperatures leading to errors in the diffusion coefficients calculated from the slope of the linear transient region. Fig. 16 shows that the smaller dichloromethane molecule diffuses more rapidly than nitroethane over the temperature range covered in this work. Values given in Table 25 for the diffusion coefficients at 90 °C for nitroethane and dichloromethane are 4.3×10^{-8} cm^2 s^{-1} and 5.0×10^{-8} cm^2 s^{-1} respectively.

Arrhenius plots of the permeability coefficients are shown in Fig. 15. The plots for dichloromethane and nitroethane are both linear. Permeability coefficients for nitroethane permeation are larger than dichloromethane despite the greater diffusivity of the smaller dichloromethane molecule. As explained previously when considering the permeability of PET this reflects the greater solubility of nitroethane which is related to its condensibility.

Fig. 17 shows an Arrhenius plot of permeability coefficients for the system low density PE/methane over the temperature range 50 - 80 °C; the low density PE film was supplied by British Cellophane Ltd. Measurements were taken first at ascending

Fig. 15 ARRHENIUS PLOTS OF PERMEABILITY COEFFICIENTS FOR THE SYSTEMS PTFE/DICHLOROMETHANE AND PTFE/NITROETHANE

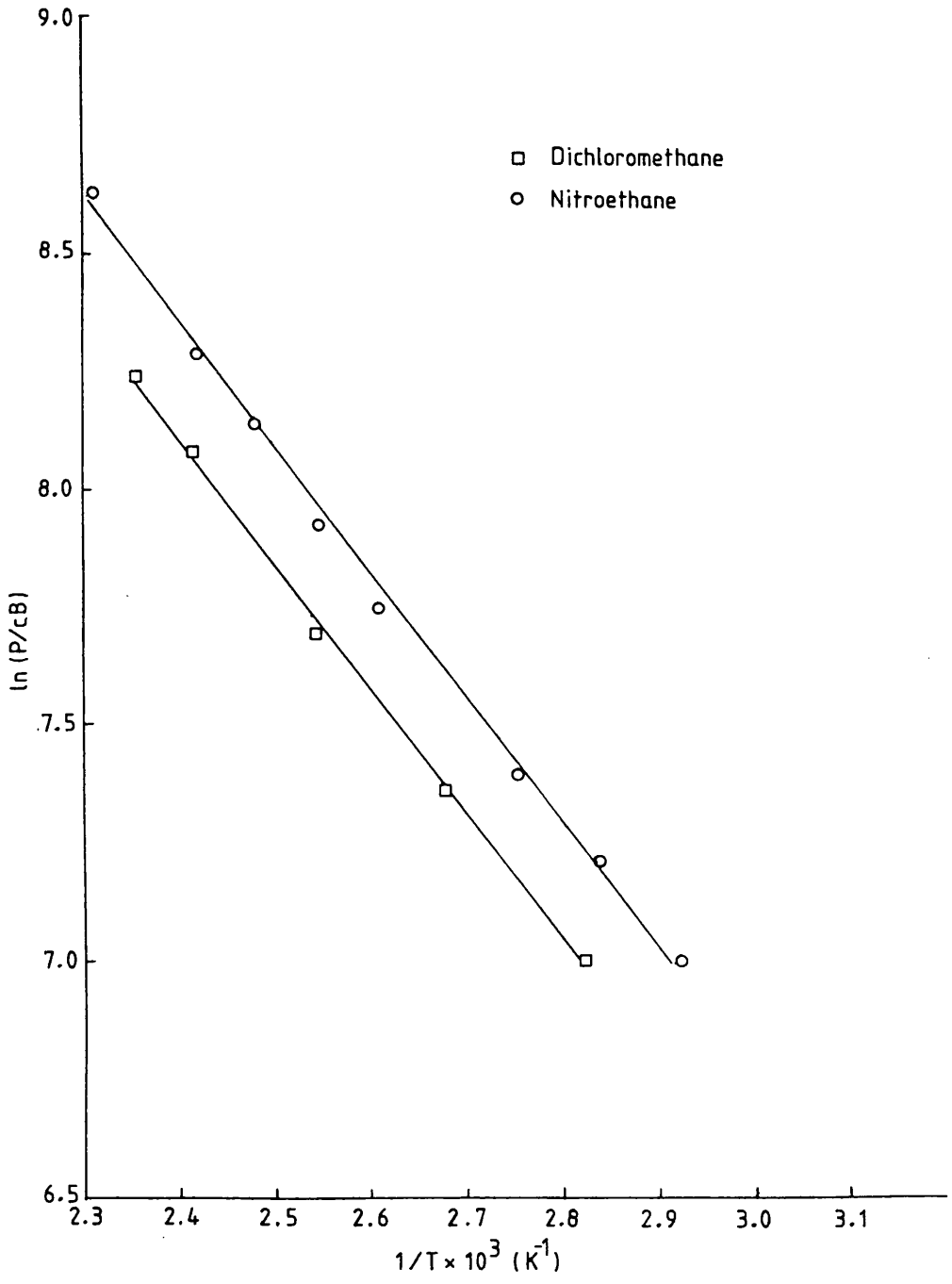

Fig. 16 ARRHENIUS PLOTS OF DIFFUSION COEFFICIENTS FOR THE SYSTEMS PTFE/DICHLOROMETHANE AND PTFE/NITROETHANE

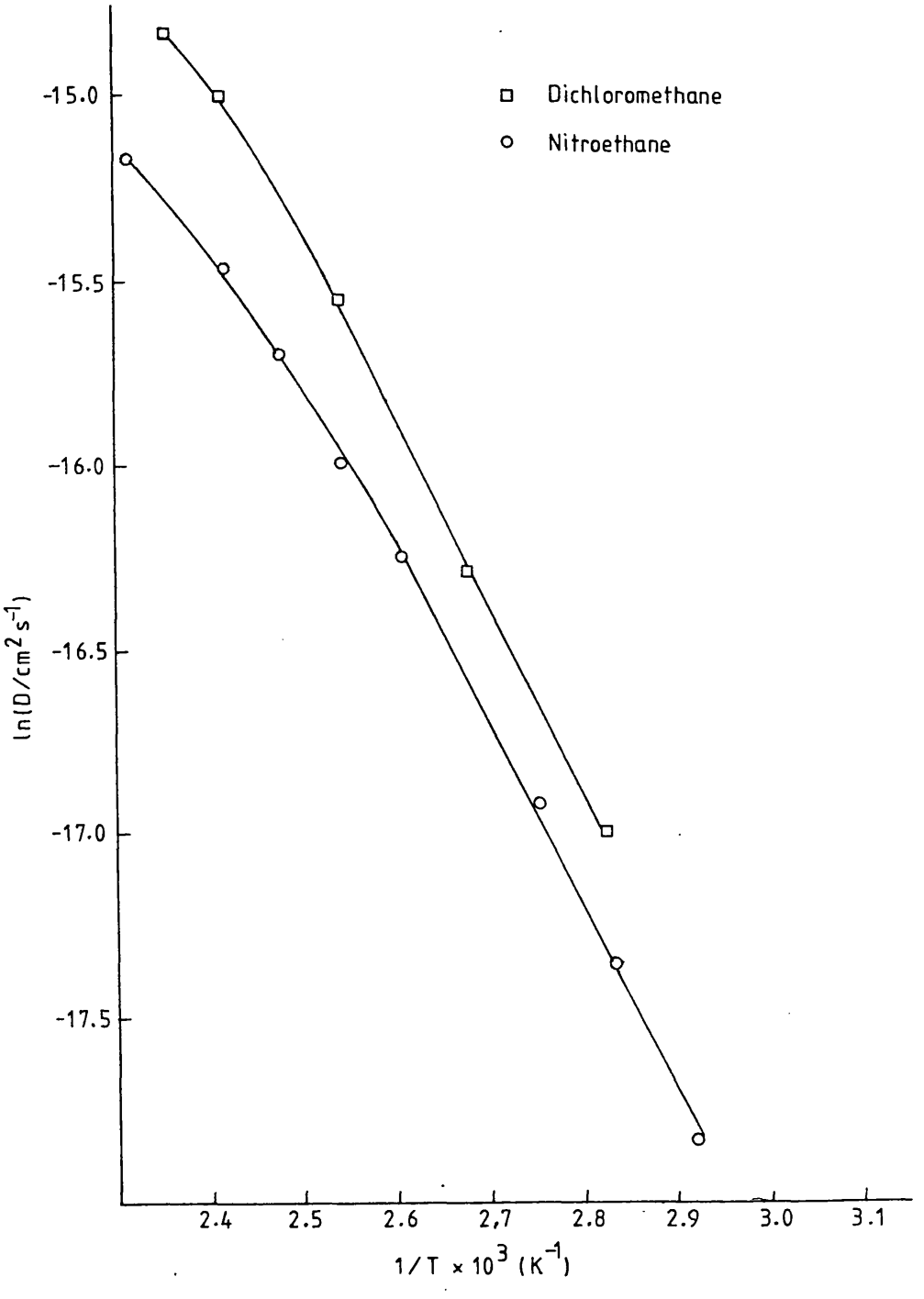

Fig. 17 ARRHENIUS PLOTS OF PERMEABILITY COEFFICIENTS FOR THE SYSTEM LOW DENSITY PE SUPPLIED BY BCL/METHANE

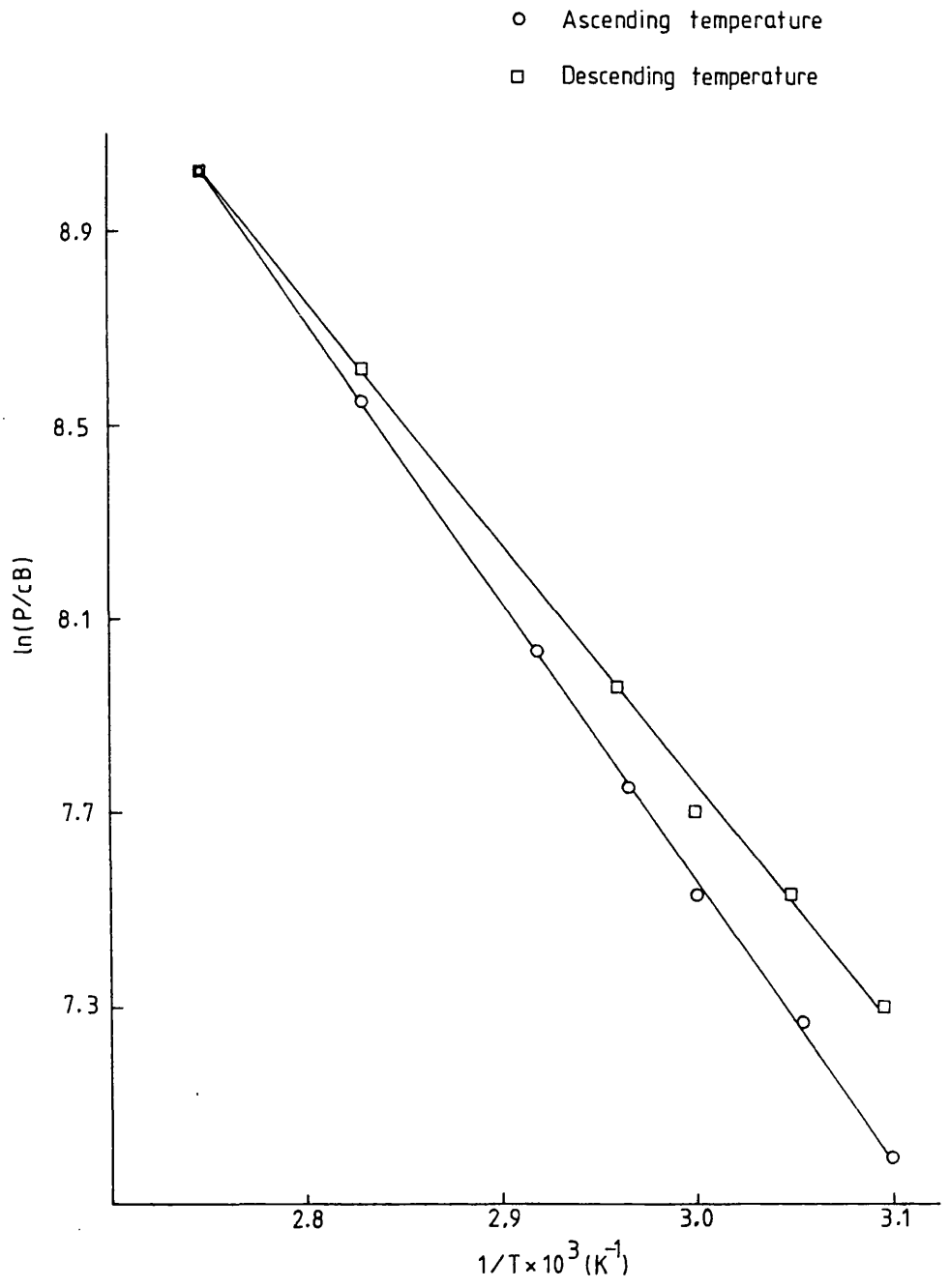

temperatures with the film then cooled and measurements taken at descending temperatures.

An Arrhenius plot is shown in Fig 18 for permeability coefficients measured for methane permeation through low density PE film supplied by Imperial Chemical Industries Ltd. over the temperature range 48 - 90 °C. Measurements were taken first at increasing temperatures then at decreasing temperatures. Both PE films show markedly different Arrhenius plot gradients for measurements taken at ascending and descending temperatures. The activation energies for permeation calculated from the ascending temperature Arrhenius plots is 47.8 kJ mol^{-1} for the film supplied by BCL and 47.2 kJ mol^{-1} for the film supplied by ICI. The activation energies for permeation calculated from the descending temperature Arrhenius plots is 41.3 kJ mol^{-1} for the BCL film and 42.1 kJ mol^{-1} for the ICI film. Michaels et al[35] found an activation energy for permeation of 47.2 kJ mol^{-1} for the system low density PE/methane over the temperature range 5 - 55 °C. Kanitz and Huang[103], and Tschamler and Rudorfer[104] have obtained values of 47.2 kJ mol^{-1} and 48.1 kJ mol^{-1} respectively for measurements taken over a similar temperature range. These results are summarised in Table 26.

The activation energies for permeation measured at ascending temperatures show good agreement with values obtained in the literature (see Table 26), whereas values obtained at descending temperatures are significantly lower. It might have been expected that taking permeability measurements at a temperature as high as 90 °C would have had an annealing effect on the polymer increasing its crystallinity. If a simple model of

Fig 18 ARRHENIUS PLOTS OF PERMEABILITY COEFFICIENTS FOR THE SYSTEM LOW DENSITY PE SUPPLIED BY ICI/METHANE

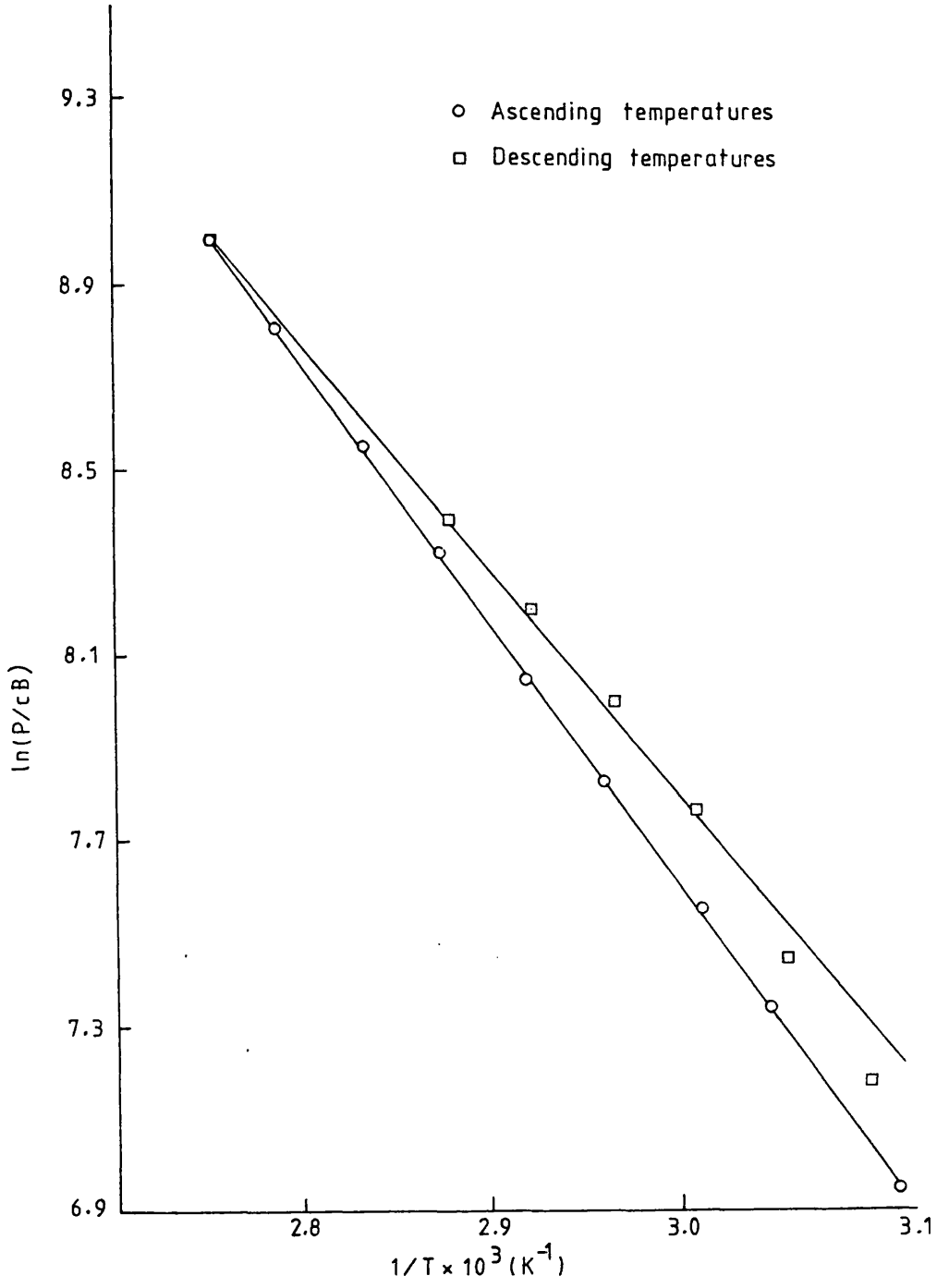

TABLE 26 Activation Energies for the Permeation of Methane through Low Density PE

Source	E_p/KJmol^{-1}	Temp Range/°C
This work, ICI PE	47.2	48-90
This work, BCL PE	47.8	50-90
Ref. 35	47.2	5 -55
Ref. 103	47.2	15-50
Ref. 104	48.1	-

impenetrable crystallites reducing diffusion rates and solubilities were considered this would have lead to reduced permeability coefficients on heating and then cooling the polymer. Since the reverse is true other changes in the morphology of the polymer must be taking place.

Michaels and Parker[77] suggested that two impedance factors are operating to reduce the diffusion constants in semicrystalline polyethylene below the values anticipated in the completely amorphous polymer. They proposed the expression: $D = D_a/\tau\beta$ where D_a is the diffusion constant in completely amorphous polyethylene, and τ is a geometric impedance factor accounting for the reduction in diffusion constant due to the necessity of molecules to bypass crystallites and move through amorphous regions of non-uniform cross-sectional area. β is a chain immobilization factor which takes into account the reduction in amorphous chain segment mobility due to the proximity of crystallites. Michaels et al[35] found that annealing a sample of linear PE despite the attendant increase in crystallinity was accompanied by a marked reduction in τ. The reduction was greatest for samples annealed at higher temperatures (130 °C) and cooled rapidly. They therefore concluded that any attempt to predict the gas permeability of PE on a basis of level of crystallinity alone, without regard to the prior history of the sample would lead to serious errors. Michaels et al[35] found that permeability coefficients for helium, argon and ethane permeating through samples of linear polyethylene of different thermal histories obeyed the Arrhenius relationship over the temperature range 0 - 55 °C. It was also

clear that the activation energy for permeation was virtually independent of thermal history. Differences were found though in actual permeability levels, with the rapidly cooled sample after annealing at 130 °C exhibiting significantly higher permeability to all gases than the slowly cooled polymer, despite the fact that the amorphous volume fraction of this form was about 25% less than the latter. This Michaels[35] concluded established that gas permeability of linear PE was not uniquely determined by levels of crystallinity but upon the path by which such crystallinity is developed.

It seems likely that in this work the increased permeability levels and apparent decrease in activation energy of permeation, for measurements taken at descending temperatures, was produced by a progressive change in the nature of the crystalline fraction on cooling between measurement temperatures. Any reduction in permeability produced by an increase in crystallinity, due to the annealing effect is therefore offset by changes in the nature of the crystallinity. This is probably shown by a reduction in the parameter τ described by Michaels and Parker[77] as being a geometric impedance factor.

The good agreement between activation energies for permeation obtained at ascending temperatures with values from the literature gave confidence in permeability measurements made using the dynamic system. Unfortunately comparison could not be made for diffusion rates and activation energies for diffusion since the approach to steady-state permeation was too rapid to give reliable values.

4.2 Further Investigation of FEP Film

The helical twist of the C-C chain of PTFE results in a nearly perfect cylinder with an outer sheath of fluorine atoms, giving outstanding chemical resistance and weak intermolecular attraction. The high chain stiffness of PTFE is usually attributed to the high bond energy of the C-F bond and the mutual repulsion of fluorine atoms, both factors which tend to resist bending of the chain backbone.

Commercially available FEP has a low % of hexafluoropropylene (15 - 20 mol %) so that the polymer can be considered as PTFE with an occasional F atom replaced by a perfluoromethyl group (CF_3). It is thought that the CF_3 groups enter the lattice as small, localized point defects and the regularity of the lattice is preserved except in the intermediate area of the defect[105-108].

The original patent on novel perfluorocarbon polymers by Bro and Sandt[109] describes how the weight % of hexafluoropropylene may be obtained from the ratio of the I.R. absorption at 980 and 2350 cm^{-1}; weight % hexafluoropropylene = I.R. absorbance ratio x 4.5. However, Akatsuka et al[110] investigated analytical methods for determining the composition of the copolymers by F - NMR, Curie-point pyrolysis gas chromatography and infrared spectroscopy. Their NMR method showed that the coefficient of the ratio is 3 rather than 4.5. The content of the CF_3 in the commercial FEP determined by NMR was 11.2 ±0.5 mol% (i.e. 5.6 CF_3 groups per 100 main chain carbon atoms).

Having checked the validity of permeability results using the PE/methane system it was decided to continue working with

FEP film. This polymer was thought to be more suitable than PTFE for further investigation since the latter was known to contain micropores introduced during its manufacture.

Fig. 19 shows an Arrhenius plot of permeability coefficients for the system FEP/tetrachloroethylene over the temperature range 20 - 100 °C. It is clear that the graph is composed of two distinct linear regions with a change in gradient, estimated from the graph, at 75.8 °C. This change in gradient and therefore reduction in E_p below about 76 °C, is produced by a change in the nature of the polymer from a rubbery to a glassy state. The glass transition temperature is given in the literature as about 80 °C[111]. E_p was determined above T_g from the slope of the Arrhenius plot and found to be 40.6 kJ mol^{-1}. E_p was determined below T_g from permeability measurements taken in the temperature range 20 - 50 °C (see Fig. 19) and found to be 29.8 kJ mol^{-1}.

An Arrhenius plot of diffusion coefficients is shown in Fig. 20. A change in gradient is seen at 77.2 °C indicating the change in the polymer from a rubbery to a glassy state. The change in gradient is less pronounced than was shown for the Arrhenius plot of permeability coefficients. E_d is calculated as 40.6 kJ mol^{-1} above T_g. A value for E_d below T_g was calculated from diffusion coefficients measured between 20 and 50 °C. The Arrhenius plot of these measurements is shown in Fig. 24.

Illustrated in Figs. 21 and 22 are plots of lnP against 1/T and lnD against 1/T respectively, for the system FEP/nitroethane over the temperature range 60 - 100 °C. As with tetrachloro-

Fig 19. ARRHENIUS PLOT OF PERMEABILITY COEFFICIENTS FOR THE SYSTEM FEP/TETRACHLOROETHYLENE

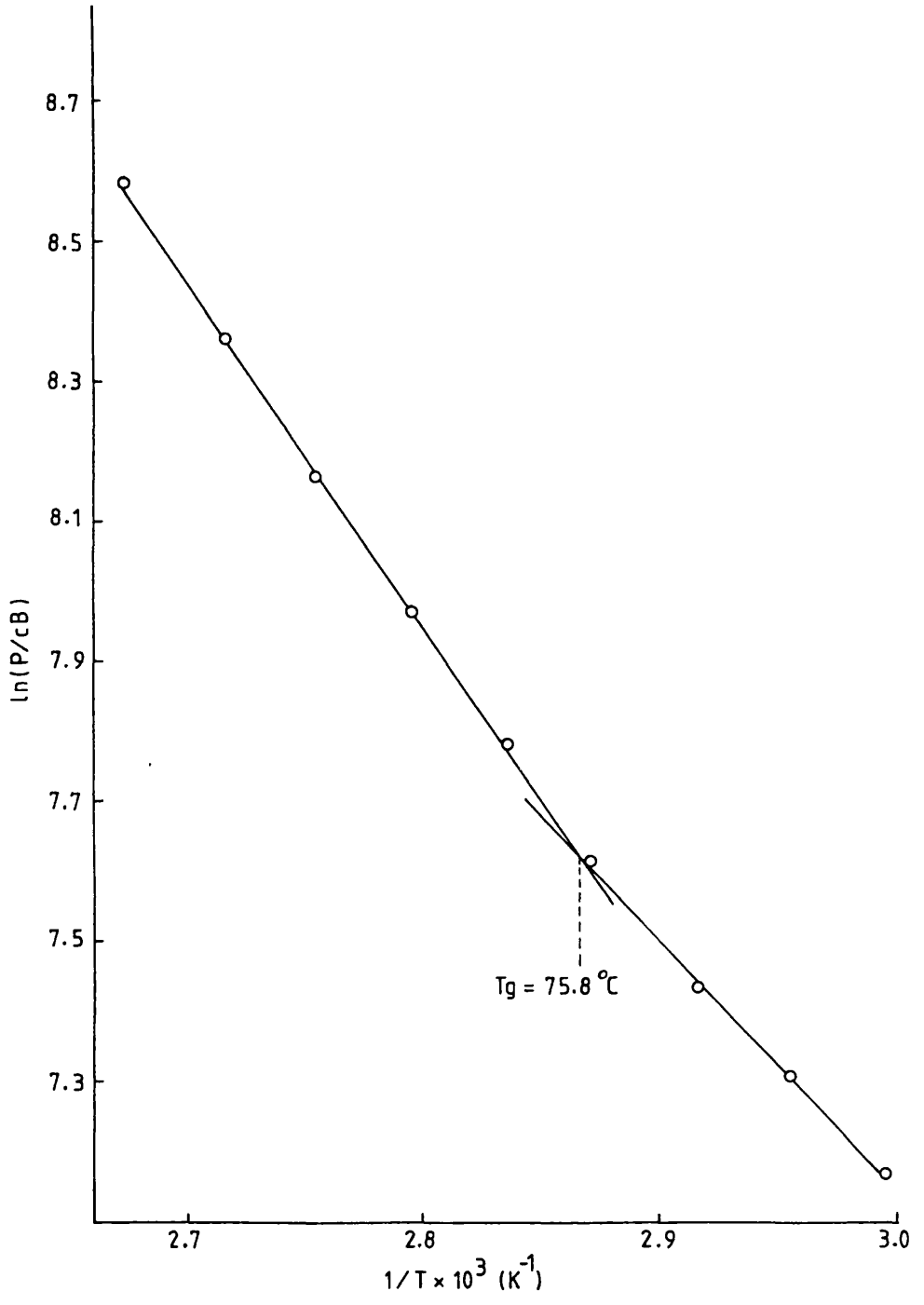

Fig. 20 ARRHENIUS PLOT OF DIFFUSION COEFFICIENTS FOR THE SYSTEM FEP/TETRACHLOROETHYLENE

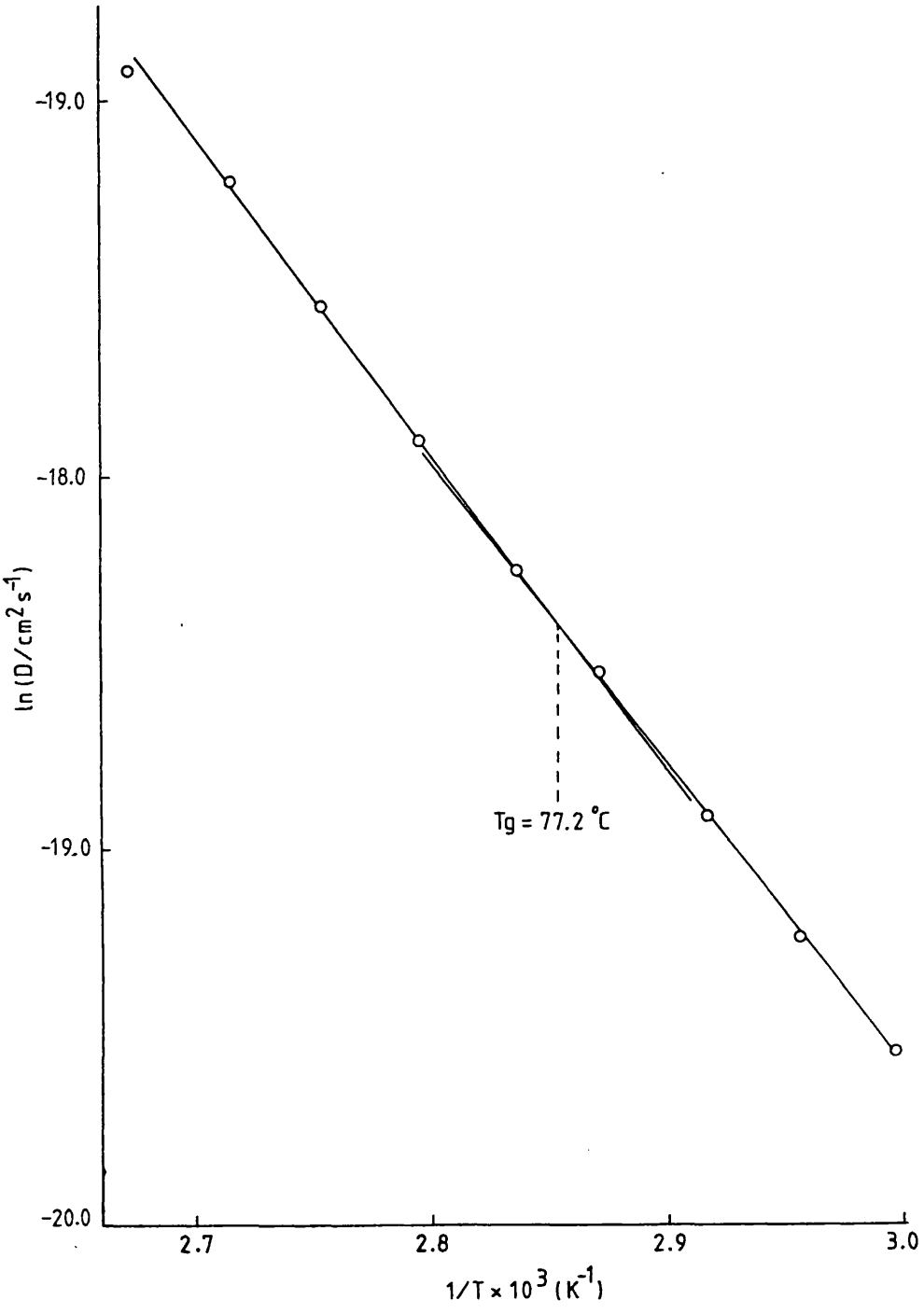

Fig. 21 ARRHENIUS PLOT OF PERMEABILITY COEFFICIENTS FOR THE SYSTEM FEP/NITROETHANE

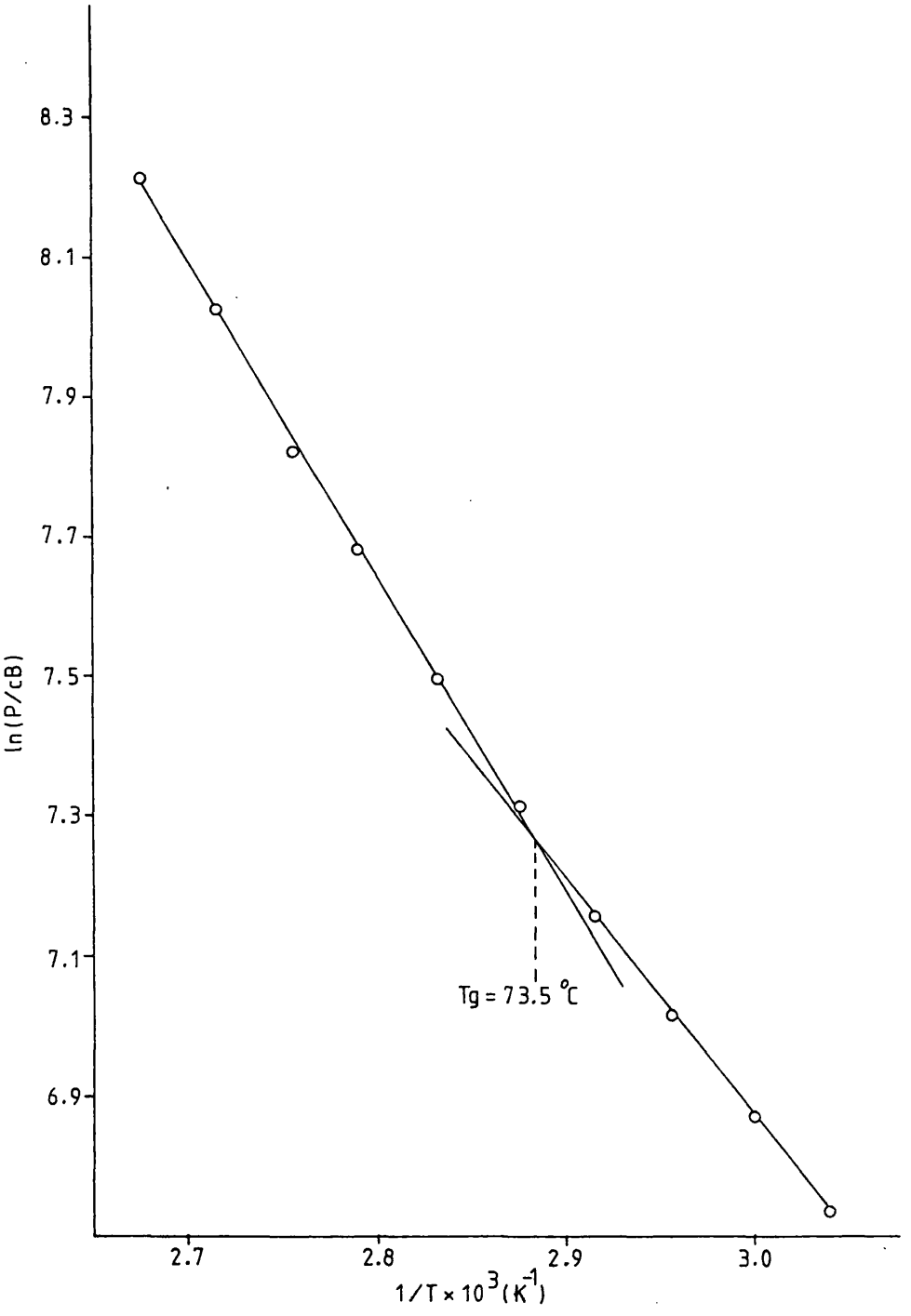

Fig. 22 ARRHENIUS PLOT OF DIFFUSION COEFFICIENTS FOR THE SYSTEM FEP/NITROETHANE

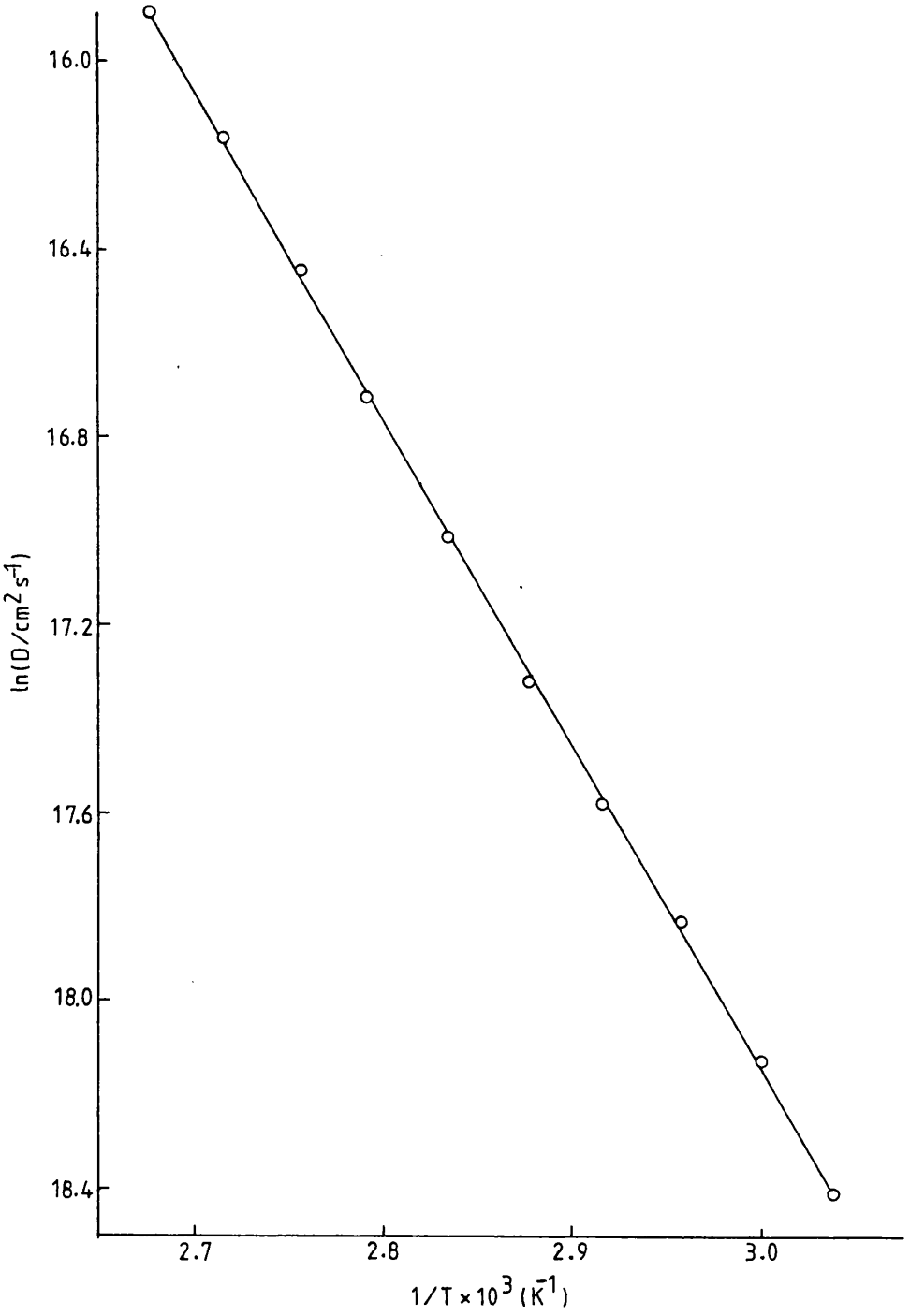

Fig. 23 ARRHENIUS PLOTS OF PERMEABILITY COEFFICIENTS FOR THE PERMEANTS INDICATED THROUGH FEP FILM

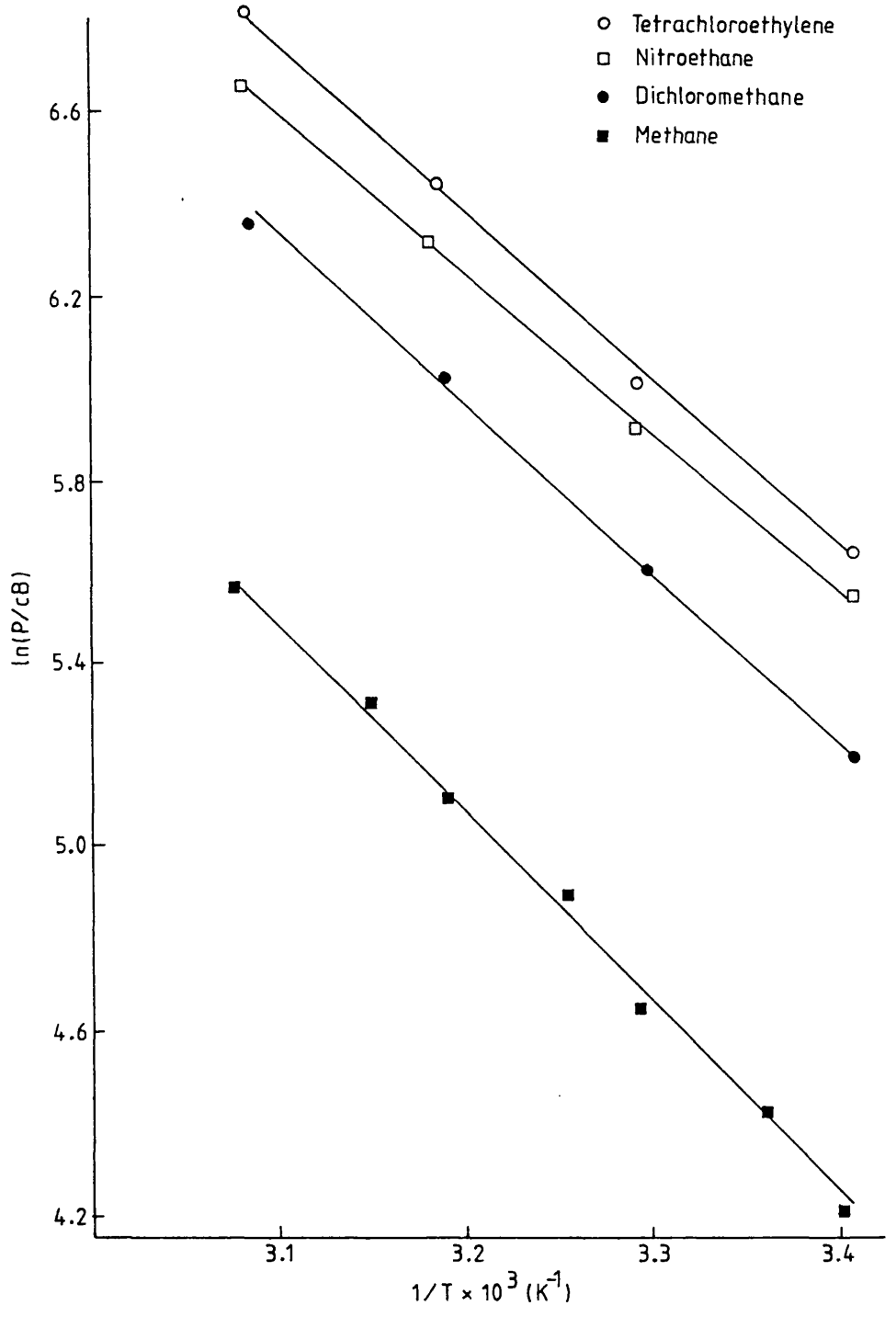

Fig. 24 ARRHENIUS PLOTS OF DIFFUSION COEFFICIENTS FOR THE PERMEANTS INDICATED THROUGH FEP FILM

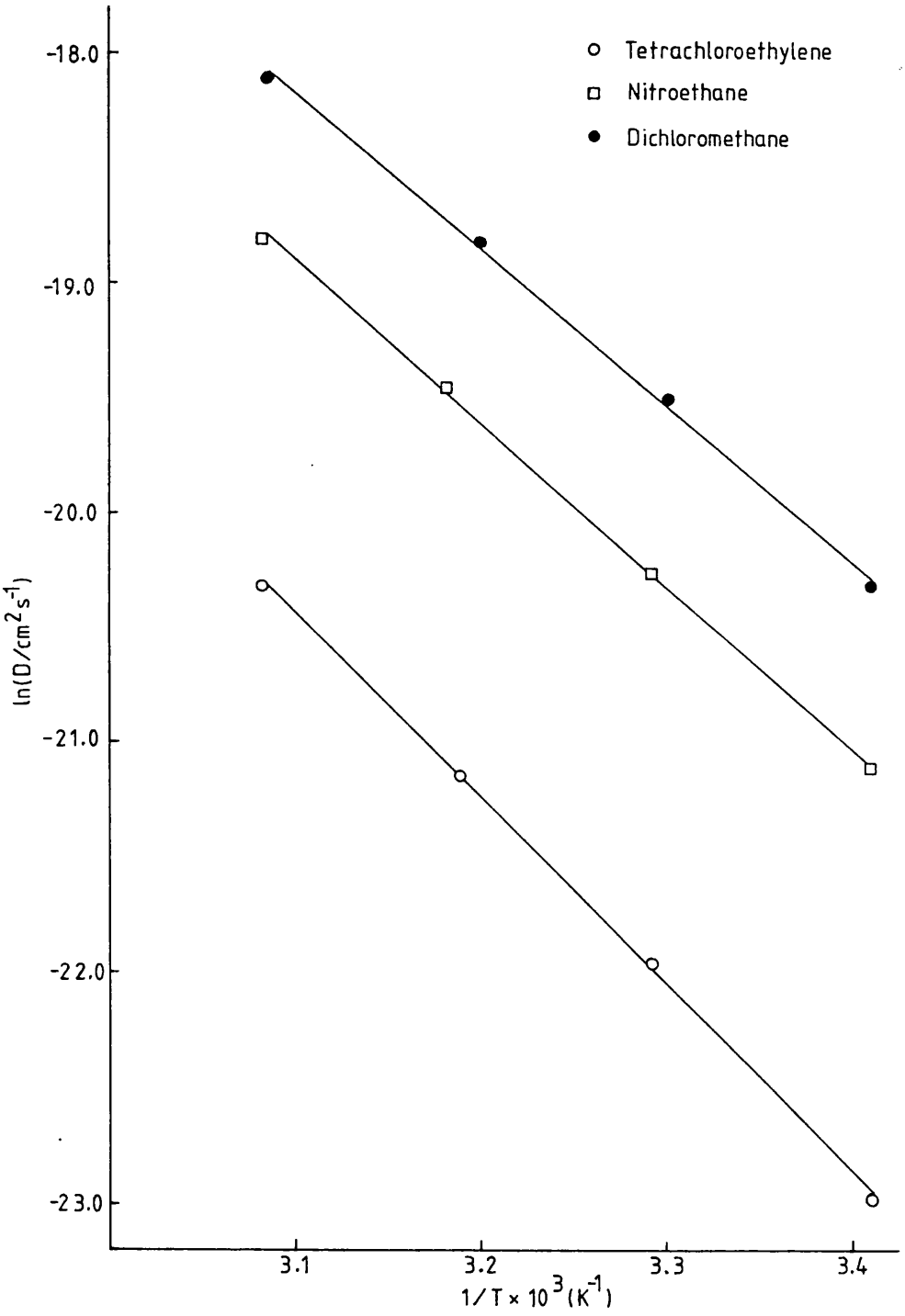

ethylene permeation two distinct linear regions are seen in the permeability plot with a change in gradient estimated from the graph at 73.5 °C. The activation energy for permeation above T_g calculated from the gradient of the graph in this region is 37.8 kJ mol^{-1}. A value for E_p below T_g of 28.3 kJ mol^{-1} was calculated from permeability coefficients measured between 20 and 50 °C. Arrhenius plots for permeability and diffusion coefficients over this temperature range are shown in Figs. 23 and 24. A plot of lnD against 1/T showed no change in gradient at T_g and gave an activation energy for diffusion calculated from the gradient over the temperature range 60 - 100 °C of 57.5 kJ mol^{-1}.

Figs. 25 and 26 show Arrhenius plots of permeability and diffusion coefficients respectively for the system FEP/ dichloromethane. The permeability plot shows a change in gradient at 76.7 °C which is less pronounced than similar plots for tetrachloroethylene and nitroethane. The activation energy for permeation above T_g is 35.7 kJ mol^{-1}. The value below T_g calculated from the gradient of the graph shown in Fig. 25 over the temperature range 20 - 50 °C is 29.6 kJ mol^{-1}. The Arrhenius plot of diffusion coefficients is linear over the temperature range investigated and shows no change in gradient. E_d calculated from the gradient is 54.6 kJ mol^{-1}. Diffusion measurements in the temperature range 20 - 50 °C gave an activation energy for diffusion of 55.3 kJ mol^{-1}.

4.3 Effect of Tg on Activation Energies for Permeation and Diffusion in FEP

Arrhenius plots of the permeability coefficients obtained for the three permeants tetrachloroethylene, nitroethane and

Fig. 25 ARRHENIUS PLOT OF PERMEABILITY COEFFICIENTS FOR THE SYSTEM FEP/DICHLOROMETHANE

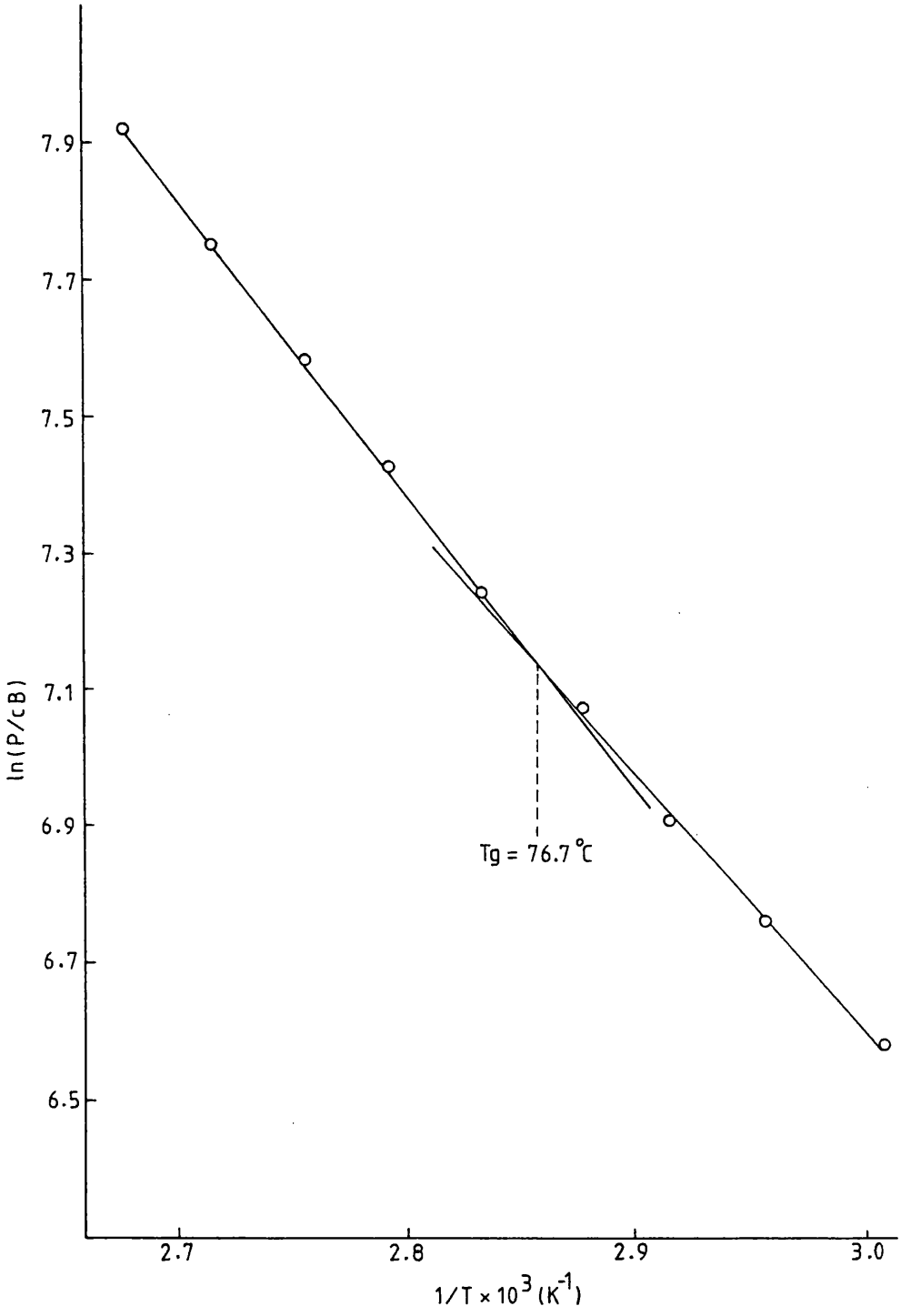

Fig. 26 ARRHENIUS PLOT OF DIFFUSION COEFFICIENTS FOR THE SYSTEM FEP/DICHLOROMETHANE

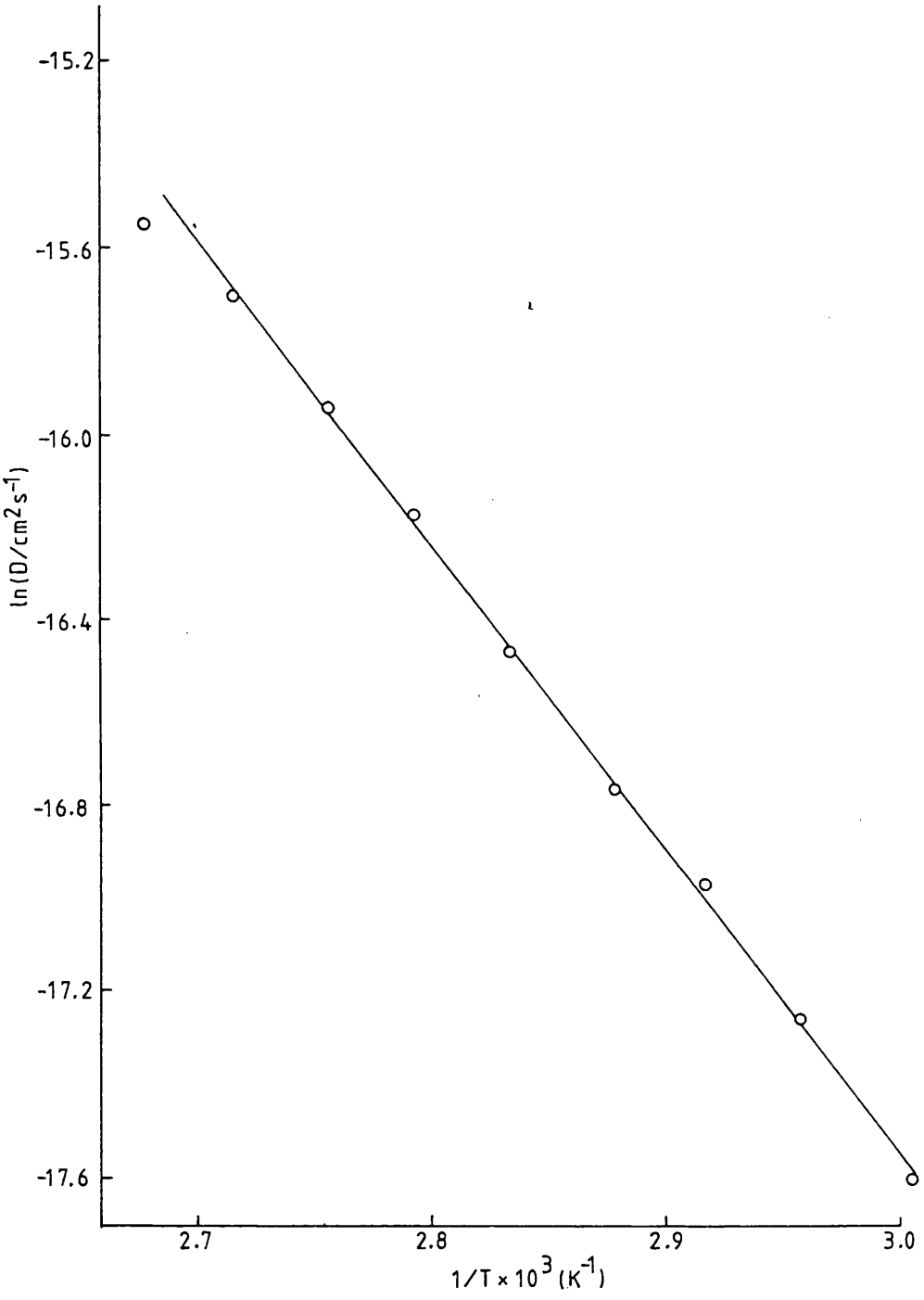

dichloromethane all show changes in gradient at T_g. The change in gradient is less pronounced for dichloromethane which showed a difference in activation energies above and below T_g of 3.2 kJ mol^{-1} compared with 8.5 kJ mol^{-1} for nitroethane and 10.9 kJ mol^{-1} for tetrachloroethylene. No change in gradient was observed in the Arrhenius plot for methane permeation over the temperature range 60 - 100 °C, shown in Fig. 27, although a lower E_p was found using the results obtained over the temperature range 20 - 50 °C. These results are shown in Table 27. Arrhenius plots of the diffusion coefficients only showed a change in gradient for tetrachloroethylene diffusion. An increase in activation energy for diffusion of 0.8 kJ mol^{-1} was observed for measurements above T_g.

Pasternak et al[102] have measured permeation and diffusion rates of several hydrocarbons and permeant gases through FEP over the temperature range 25 - 95 °C. Although insufficient low temperature measurements were made to locate T_g both permeation and diffusion coefficients measured at 95 °C were seen to lie significantly above the straight line Arrhenius plot. The authors suspected a phase transition. Duncan et al[119] obtained linear Arrhenius plots of diffusion and permeability coefficients for methylchloride and benzene permeation through FEP over the temperature range 47 - 150 °C. No change in gradient was seen at T_g for either permeant. Considering the less pronounced change in gradient found in this work for the permeability plot of the smaller dichloromethane molecule, it is unlikely that a T_g effect would be seen for the smaller methylchloride molecule. Since no T_g effect was

TABLE 27 A Comparison of Permeability Parameters for the Permeation of the Different Permeants through FEP

Permeant	E_p/ kJmol^{-1}	P/cB at 25°C	P/cB at 90°C	$P_o \times 10^{-8}$/cB	Temp. Range/°C	Annealing Temp/°C	Source
Tetrachloro -	40.6	-	3469	24.0	80-100	100	This work
ethylene	29.8	323	-	0.538	20- 50	"	" "
Nitroethane	37.8	-	2393	6.55	80-100	"	" "
	28.2	306	-	0.267	20- 50	"	" "
Dichloromethane	35.7	-	1949	2.66	80-100	"	" "
	29.6	212	-	0.326	20- 50		" "
Methane	42.7	-	865	12.0	60-151	200	" "
"	38.7	-	974	3.59	60-100	100	" "
"	34.5	80.0	-	0.886	20- 50	"	" "
"	35.0	-	1330	1.45	40-130	200	Ref 27
"	34.7	-	1096	1.10	25- 85	95	Ref 102
Propane	43.8	-	421	8.40	40-130	200	Ref 27
Methylchloride	34.8	-	1239	1.26	48-120	"	Ref 119
Benzene	49.5	-	1246	162	48-120	"	" "

Fig. 27 ARRHENIUS PLOT OF PERMEABILITY COEFFICIENTS FOR THE SYSTEM FEP/METHANE

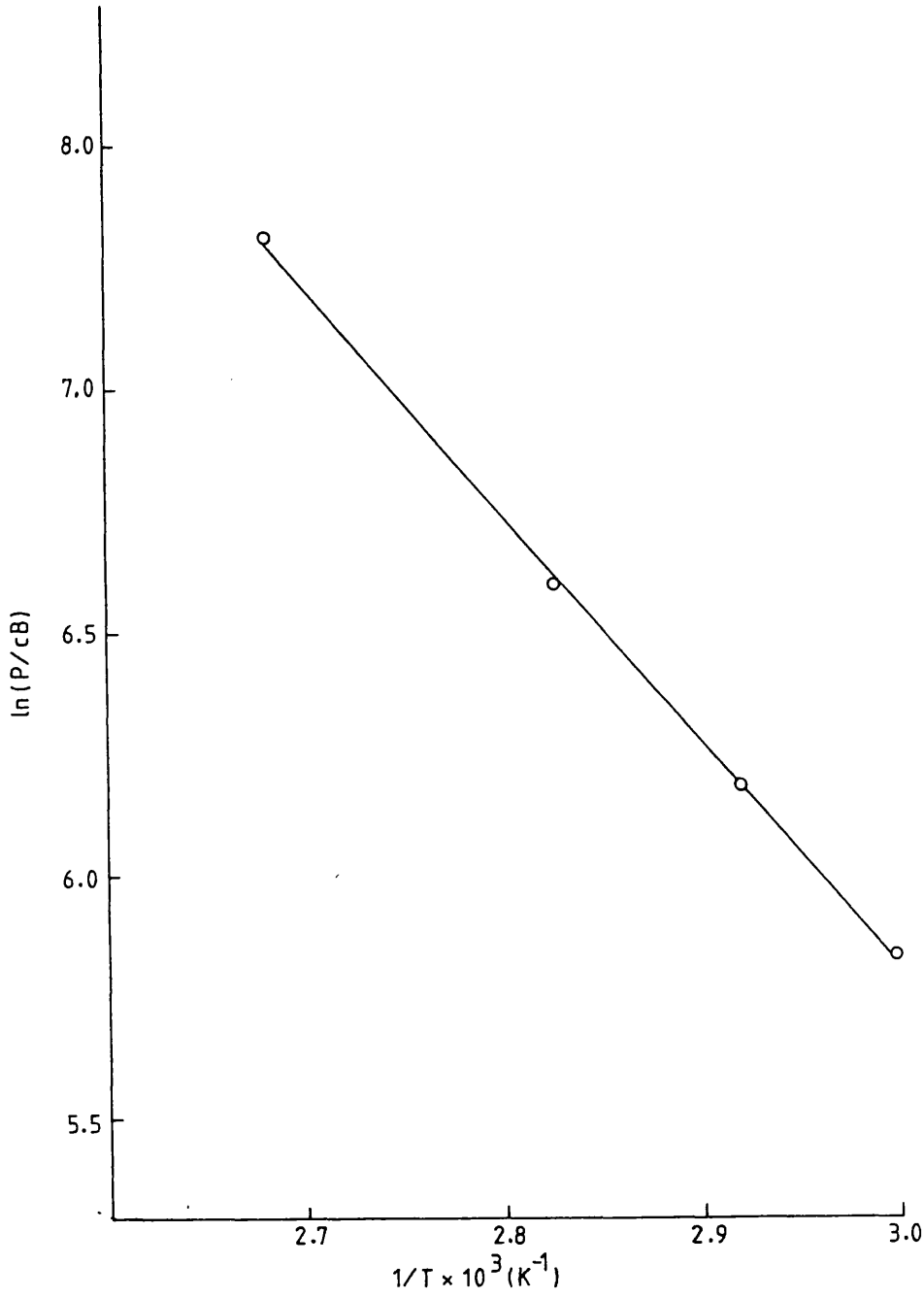

seen in this work for either dichloromethane or nitroethane diffusion no change in gradient would be expected in the Arrhenius plot of diffusion coefficients for methylchloride transport. Duncan et al[119] once again found no T_g effect for the larger benzene molecule in the Arrhenius plots of diffusion or permeability coefficients. Considering the van der Waals volumes of benzene, 80.2 A^3 nitroethane, 67.6 A^3 and tetrachloroethylene, 94.0 A^3 a T_g effect might have been expected in the Arrhenius plot of permeability coefficients for benzene permeation.

The change of gas permeability at T_g has been observed by Meares[41],[42] with poly(vinyl acetate). However, the changes of slope of the Arrhenius plots at T_g were observed with some but not all gases. The results of Stannett and Williams[44] with poly(ethyl methacrylate) showed no change in gradient of the Arrhenius plots for all gases studied. Kumins and Roteman[30] also report no effect of T_g for a vinyl chloride-vinyl acetate copolymer except for the permeation of carbon dioxide. It has been suggested by several authors[45],[30],[112] that whether or not a change in gradient is observed in the Arrhenius plots of permeability and diffusion coefficients depends on the relative sizes of the free volume elements in the polymer and the size of the penetrant molecule.

Yasuda and Hirotsu[46] have analysed results from the literature for many polymer/penetrant systems and suggest that the value of the diffusion coefficient at T_g can be used to predict whether a glass transition effect will be seen. These authors further suggest that a change in gradient of the

Arrhenius plot of gas permeabilities is seen only if the diffusion coefficient at T_g is smaller than 5×10^{-8} cm^2 s^{-1}. If T_g for FEP is taken as 78 °C[111] the values obtained in this work for the diffusion coefficients at 78 °C are; dichloromethane, 6.5×10^{-8} cm^2 s^{-1}; nitroethane, 3.7×10^{-8} cm^2 s^{-1}; tetrachloroethylene 1.1×10^{-8} cm^2 s^{-1}. The values for tetrachloroethylene and nitroethane are clearly lower than 5×10^{-8} cm^2 s^{-1} and indeed pronounced changes in gradient of the Arrhenius plots of permeabilities are seen at T_g. A change in gradient is still seen for dichloromethane at T_g where D only is slightly higher than 5×10^{-8} cm^2 s^{-1}. Although no change in gradient was apparent in the Arrhenius plot of permeability coefficients over the temperature range 60 - 100 °C for methane transport, the gradient over this temperature range is larger than over the range 20 - 50 °C suggesting a glass transition effect. A value for the diffusion coefficient at 78 °C of 3.14×10^{-7} cm^2 s^{-1} can be calculated from E_d and D_o values given by Yi-Yan et at[27]. This value is well above 5×10^{-8} cm^2 s^{-1} and therefore no glass transition effect would have been expected. Since different ovens were used to anneal the FEP samples used for the high and low temperature ranges, it is possible that the different heating and cooling characteristics of the ovens produced differences in E_p values between the samples.

If T_g for PET is taken as 87.5 °C[43] then the diffusion coefficients obtained in this work for dichloromethane and nitroethane transport at 87.5 °C are 2.7×10^{-12} cm^2 s^{-1} and 9.9×10^{-13} cm^2 s^{-1} respectively. A glass transition effect would

therefore be expected and is clearly seen in the Arrhenius plot of permeability coefficients shown in Fig. 12.

4.4 Diffusion Parameters

It is well known that diffusion in high polymers is an activated process and can be represented by the Arrhenius equation 1.7.

To explain the diffusion process Barrer[2] postulated that a diffusion 'jump' requires an activated region or 'zone' comprising the neighbourhood of the diffusing molecule. The size of the zone determines both E_d and the activation entropy $\Delta S_{\ddagger}$ or log D_o.

Diffusion data for the polymer/permeant systems FEP/dichloromethane, FEP/nitroethane and FEP/tetrachloroethylene are listed in Table 28. Also shown in the table are diffusion parameters obtained by Duncan et al[119] for the transport of propane, methylchloride and benzene through FEP. Values given in Table 28 for the diffusion coefficients of the permeants used in this work at 25 °C and 90 °C clearly show a decrease in diffusion rates with increasing molecular size. This is to be expected considering the larger zone of activation and therefore activation energy required for the permeant to move through the polymer structure.

E_d values obtained for the permeants used in this work are listed in Table 28. As expected, considering the larger zone of activation for the larger molecules, E_d values above and below T_g increase in the order dichloromethane, nitroethane and

TABLE 28 A Comparison of Diffusion Parameters for the Permeation of the Different Permeants through FEP

Permeant	E_d/ kJmol^{-1}	Dx10^8/cm^{2}s^{-1} at 25°C	Dx10^8/cm^{2}s^{-1} at 90°C	D_o/cm^{2}s^{-1}	Temp. Range/°C	Annealing Temp/°C	Lennard Jones Diameter/A	Van der Waals Volume/A^3	Source
Tetrachloro-	67.6	-	2.45	95.6	80-100	100	-	94.0	This work
ethylene	67.2	0.0173	-	100.5	20-50	"	-	"	" "
Nitroethane	57.5	-	7.13	13.3	60-100	"	-	67.6	" "
	59.1	0.099	-	22.4	20-50	"	-	"	" "
Dichloro-	54.6	-	7.41	5.29	60-100	"	-	57.6	" "
methane	55.3	0.230	-	11.25	20-50	"	-	"	" "
Propane	59.4	-	4.91	17.20	40-130	200	5.118	62.4	Ref 27
Methyl- chloride	50.1	-	20.0	3.941	48-120	"	4.182	42.0	Ref 119
Benzene	69.1	-	3.53	307.5	48-120	"	5.348	80.2	" "

tetrachloroethylene. A comparison with the E_d values given by Yi-Yan et al[27] for propane, methylchloride and benzene permeation show that the values for benzene and propane are larger than expected considering the van der Waals volumes of the permeants. This is probably explained by the annealing temperatures of 200 °C used by Yi-Yan et al[27] rather than 100 °C used in this work. Increasing the annealing temperature can be expected to increase the crystallinity of the polymer and therefore the activation energy required for diffusion.

According to the model proposed by Brandt and Anysas[28] E_d has two components; one depends on the cohesive energy of the polymer and is proportional to the molecular diameter of the permeant, the other depends on the chain flexibility and is proportional to the square of the diameter. Michaels and Bixler[35] estimate that for PE the contribution of the flexing energy to the activation energy is small and accordingly find a linear relationship between the activation energies and the molecular diameters. In contrast, the cohesive energy of the PE is smaller than FEP, but the FEP chain is stiffer. Therefore, the energy associated with chain flexing should be significant in FEP and the activation energies of diffusion should increase more than linearly with the molecular diameter of the permeants. Duncan et al[119] have found a linear relationship between E_d and the molecular diameter squared, as measured by the Lennard-Jones collision diameter of the penetrant. Fig. 28 shows a plot of E_d against the molecular diameter squared for the permeants used in this work and those used by Duncan et al[119]. Since the Lennard-Jones collision diameters were not available for all the

Fig. 28 PLOT OF ACTIVATION ENERGIES FOR DIFFUSION THROUGH FEP FILM AGAINST THE MOLECULAR DIAMETERS SQUARED

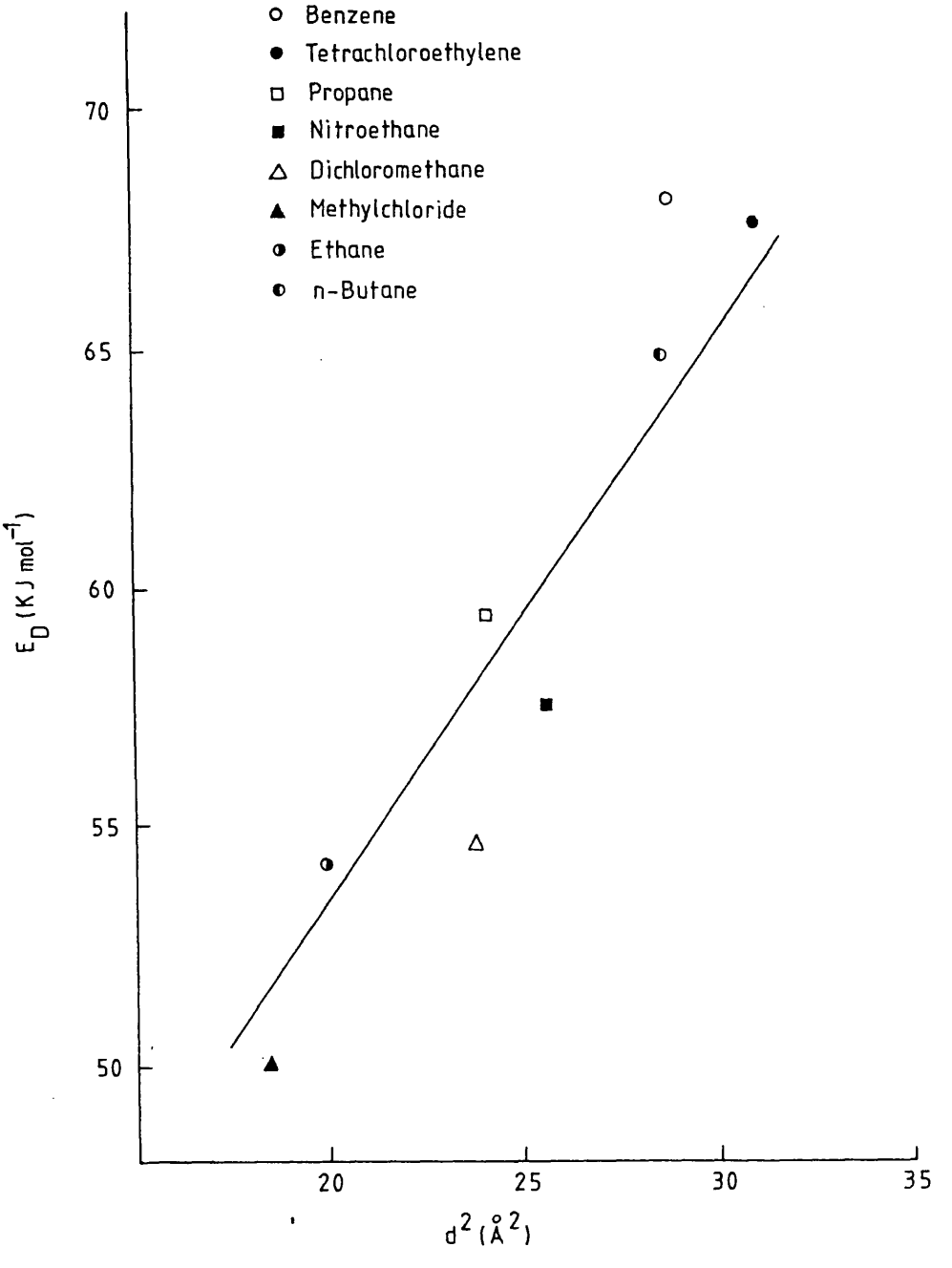

permeants used in this work the van der Waals volumes[99] were used to calculate the molecular diameters assuming the molecules to be spherical. The plot is apparently linear with the results obtained for the permeants used in this work correlating reasonably well with those obtained by Duncan et al[119].

As stated previously, Barrer[2] has postulated that the size of the activated region or 'zone' involved in the diffusion process determines both E_d and the activation entropy or log D_o. Lawson[113] similarly showed that several relatively simple models of the diffusion process lead to a linear relation between the energy and entropy of activation. Fig. 29 shows a plot of log D_o against E_d for the permeants used in this work and those used by Duncan et al[119]. The graph is linear with only benzene deviating significantly from the straight line. Possibly the planar configuration of the benzene molecule permits orientation - specific diffusional jumps that reduce E_d to a greater extent than log D_o.

4.5 Solubility Factors

Permeabilities and diffusivities are known to follow Arrhenius relations over moderate temperature ranges[34]. It follows therefore that the solution of gases and vapours also follows an Arrhenius relation, as shown in equation (1.9). The solubility factors can be calculated from diffusion and permeability data using the equations,

$$S_o = P_o/D_o$$

and $$\Delta H_s = E_p - E_d$$

Fig. 29 PLOT OF PRE-EXPONENTIAL FACTORS AGAINST THE ACTIVATION ENERGIES FOR DIFFUSION THROUGH FEP FILM

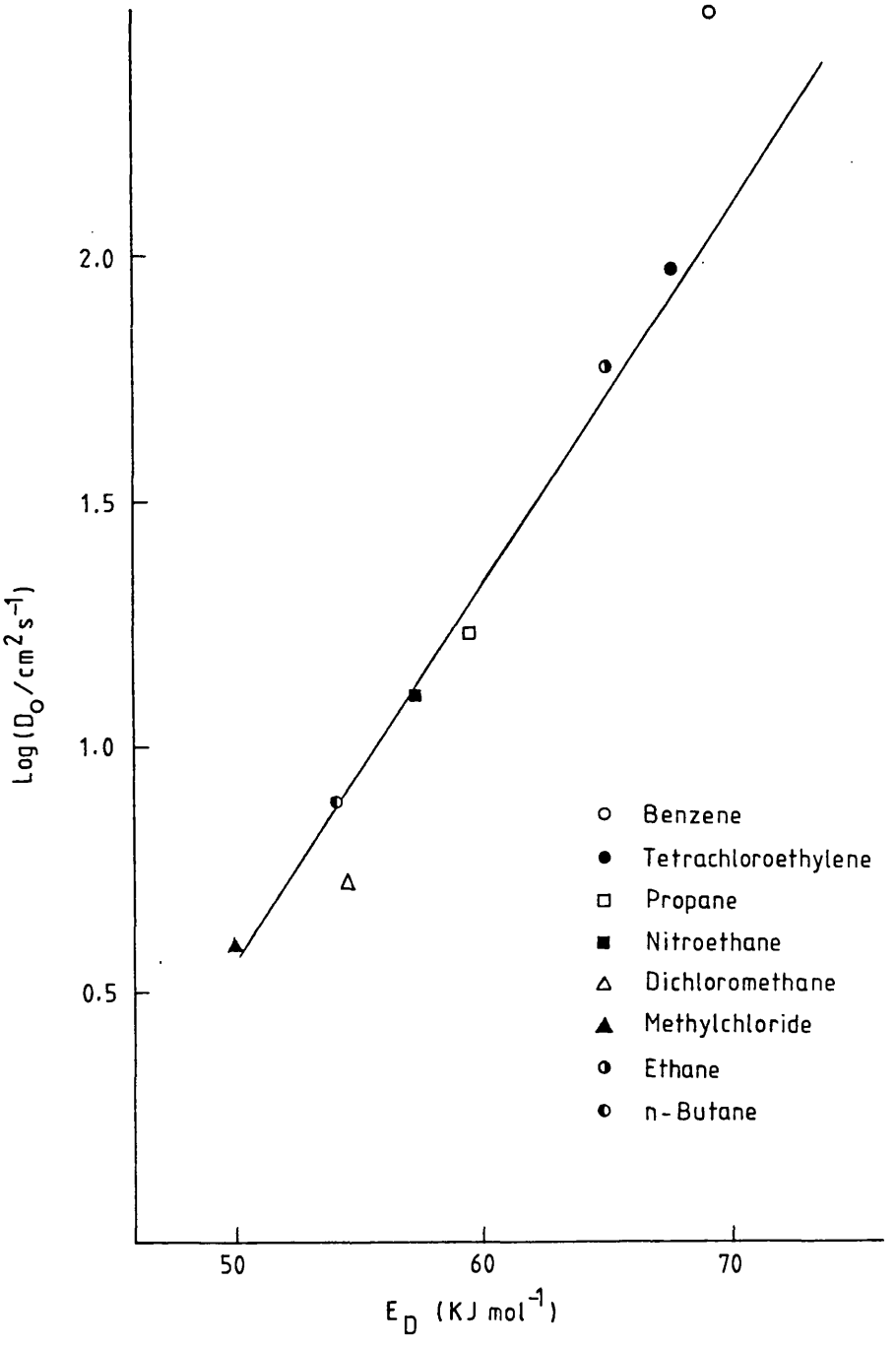

Table 29 shows solubility factors for the permeants used in this work. Also listed in the table are solubility factors obtained by Duncan et al[119] for propane, benzene and methylchloride. It is clear from Table 29 that the heat of solution becomes more negative with increasing boiling point of the permeant, T_b. Since the heat of solution of a gas or vapour depends to a large extent on the ease of condensibility of that gas or vapour, of which T_b and the Lennard-Jones force constant are measures, this reduction in the heat of solution with increasing T_b is expected.

The solubilities of gases in PE[35] natural rubber[114], and PET[43,61] have been found to be an exponential function of the Lennard-Jones force constant E/k or the boiling temperature T_b[115]. Fig. 30 shows a plot of the logarithm of the solubility of the permeants at 90 °C against T_b. Also included in the graph are results obtained by Yi-Yan et al[27] and Duncan et al[119] for the solution of benzene, propane, methylchloride, ethane and n-butane in FEP. Although the points show a wide scatter the graph is apparently linear with tetrachloroethylene, nitroethane and methylchloride deviating significantly from the straight line. Since the solubility is dependent on the heat of solution this quantity is apparently more negative than expected for tetrachloroethylene and less negative than expected for nitroethane and methylchloride. The heat of solution is itself composed of the heat of condensation of which E/k and T_b are a good measure, and the heat of mixing. The polar nature of the methylchloride and nitroethane molecules probably lead to a more positive heat of mixing thus

TABLE 29 A Comparison of Solubility Factors for the Permeation of the Different Permeants Through FEP

Permeant	ΔH_s/ kJmol^{-1}	$^aS_o \times 10^6$	$^aS \times 10$ at 25°C	$^aS \times 10^3$ at 90°C	Temp. Range/°C	Annealing Temp/°C	T_b/K	Source
Tetrachloro-	-26.2	2.514	-	17.7	80-100	100	394.3	This work
ethylene	-37.4	0.0535	2.01	-	20- 50	"	"	" "
Nitroethane	-19.7	4.92	-	3.35	80-100	"	388.2	" "
	-30.8	0.119	0.296	-	20- 50	"	"	" "
Dichloromethane	-18.9	5.03	-	2.63	80-100	"	313.2	" "
	-25.7	0.290	0.0953	-	20- 50	"	"	" "
Propane	-15.6	4.88	-	0.856	40-130	200	231	Ref 27
Methylchloride	-15.3	3.209	0.0154	0.510	48-120	"	249	Ref 119
Benzene	-19.6	5.265	0.143	3.47	48-120	"	353	" "

^aS in cm^3(STP)cm^{-3} torr^{-1}

Fig. 30 PLOT OF LOG_{10} OF THE SOLUBILITIES IN FEP AGAINST THE BOILING POINTS OF THE PERMEANTS SHOWN

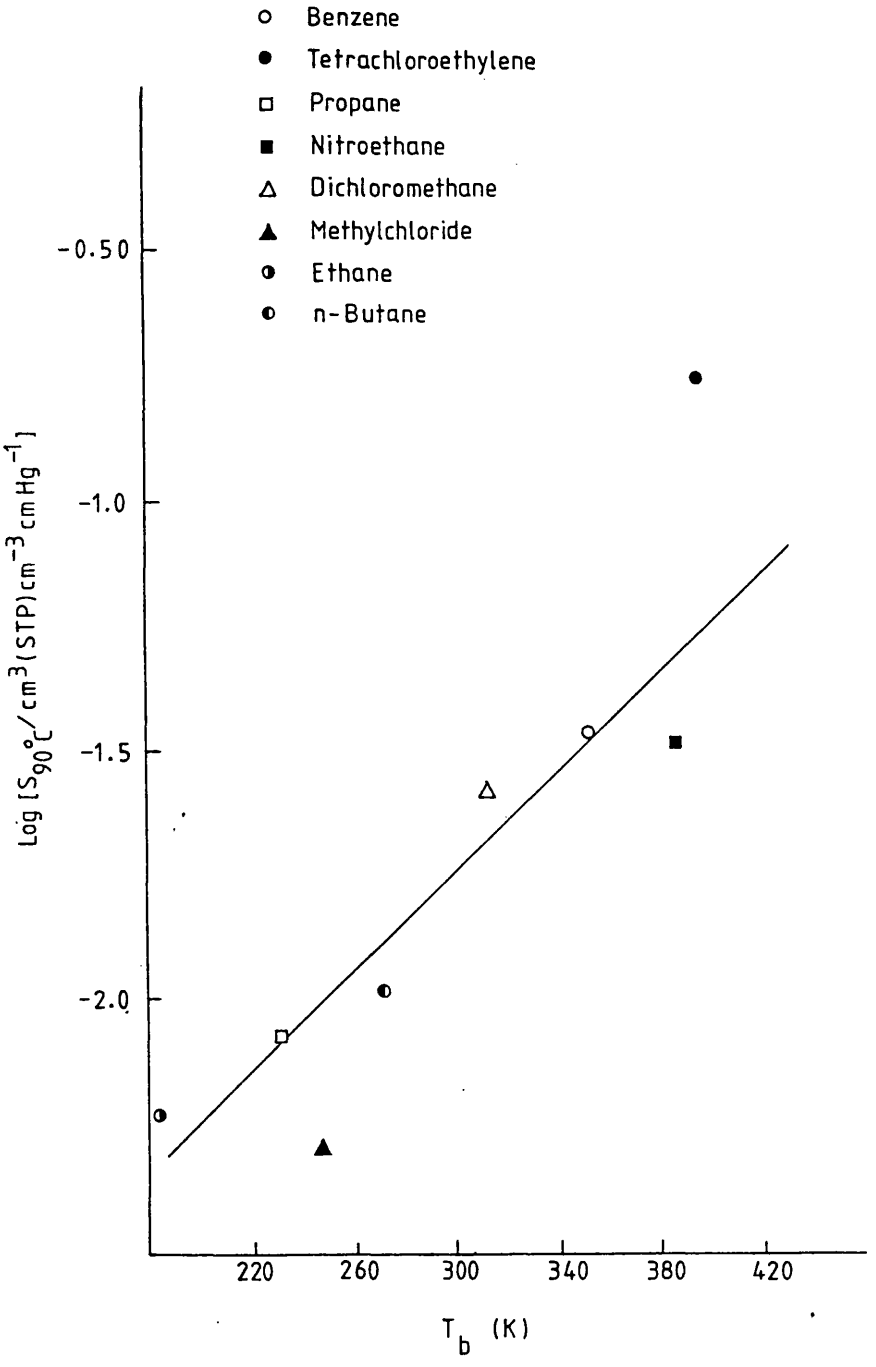

reducing the overall heat of solution and therefore the solubility. The non-polar tetrachloroethylene molecule apparently shows a larger interaction with the polymer and therefore a less positive heat of mixing. This results in a higher solubility than might be predicted from its T_b.

4.6 Permeability Parameters

Table 27 shows E_p values, pre-exponential factors and permeability coefficients at 25 °C and 90 °C for the transport of the permeants used in this work through FEP film. Also listed for comparison are the Arrhenius parameters obtained by Duncan et al[119] for methylchloride and benzene transport and values obtained by Yi-Yan et al[27]and Pasternak et al[102] for methane permeation. Since E_p is the sum of both E_d and ΔH_s, and P_o is a linear function of D_o and S_o there is no direct correlation between these parameters and molecular size. For the permeants used in this work, namely tetrachloroethylene, nitroethane, dichloromethane and methane permeability coefficients at 25 °C and 90 °C increase with increasing molecular size. This shows that the greater solubility of the larger permeant molecules more than compensates for the reduced diffusion levels.

Permeability coefficients for methane transport were measured for FEP film annealed at 200 °C over the temperature range 60 - 151 °C, and FEP film annealed at 100 °C over the temperature ranges 60 - 100 °C and 20 - 50 °C. Annealing at 200 °C gave an E_p of 42.7 kJ mol^{-1} compared to 38.7 kJ mol^{-1} for FEP annealed at 100 °C. Both these series of measurements were taken above T_g and a significantly increased

E_p is evident for the polymer annealed at the higher temperature. Permeability coefficients were found to decrease on annealing the polymer at the higher temperature. These changes in E_p and permeation levels are almost certainly produced by an increased crystalline content resulting from an increased annealing temperature.

Pasternak et al[102] found an E_p of 34.7 kJ mol^{-1} for FEP film annealed at 95 °C, whereas Yi-Yan et al[27] found an E_p of 35.0 kJ mol^{-1} for polymer annealed at 200 °C. In this work permeability coefficients determined below T_g for film annealed at 100 °C gave an E_p of 34.5 kJ mol^{-1} and therefore agrees well with the values determined by the other authors[27,102].

4.7 Measurement of Crystallinity

Because differences were found between the transport parameters determined for methane permeation through FEP film annealed at 100 °C and 200 °C attempts were made to measure changes in the crystalline content of the polymer using differential scanning calorimetry (DSC), density determinations and infra-red absorption spectrometry.

DSC can be used to measure the weight % crystallinity of a polymer sample only if a sample of known crystalline content is available. The crystalline fraction can be calculated using the equation,

Weight % crystallinity of a sample, a

$$= C_d \times \frac{[\text{endotherm area/g (sample a)}]}{[\text{endotherm area/g (sample b)}]} \qquad (4.1)$$

where C_d is the known weight % crystallinity of sample b.

Table 21 shows endotherm areas determined for FEP film samples in the as-received state, annealed at 100 °C for 24 hours, and annealed at 200 °C for 24 hours. In order to calculate the crystalline fraction of the annealed samples the crystalline fraction of FEP in the as-received state is required. This can be determined from a knowledge of the density of as-received FEP film, and the density of 100 % amorphous polymer and 100 % crystalline polymer. The manufacturers give a typical density value for FEP of 2.15 g cm^{-3} at 25 °C. Using values given by Reneker et al[116] for the amorphous density of 1.96 g cm^{-3} and the crystalline density of 2.31 g cm^{-3} the weight % crystallinity of the as-received FEP film can be determined from the equation,

$$C_d = \frac{\rho_c}{\rho} \times \frac{\rho - \rho_a}{\rho_c - \rho_a} \times 100 \qquad (4.2)$$

where, ρ_a and ρ_c are the amorphous and crystal densities

ρ is the known density

C_d is the weight % crystallinity

Substituting the values given above for ρ, ρ_a and ρ_c into equation 4.2 gives a weight % crystallinity of the polymer in the as-received state of 58.3 %. This value, and the endotherm areas listed in Table 20 can then be substituted in equation 4.1 to give a weight % crystallinity of 59.3 % for the FEP annealed at 100 °C and 65.6 % for the polymer annealed at 200 °C. These measurements clearly indicate that the weight % crystallinity increases on increasing the annealing temperature from 100 °C to 200 °C. They further support the idea that the

increase in E_p for the permeation of methane through the polymer annealed at the higher temperature is due to an increase in the crystallinity.

Densities of the FEP film samples were determined in this work using both a buoyancy method and liquid displacement. The buoyancy method, which is described in the experimental section, gave densities of 2.259 g cm^{-3} for the as-received polymer, 2.431 g cm^{-3} for the polymer annealed at 100 °C and 2.437 g cm^{-3} for the polymer annealed at 200 °C. These values are higher than expected, with the densities determined for the two annealed samples being higher than the value given by Reneker et al[116] of 2.31 g cm^{-3} for 100 % crystalline polymer. Since the technique involves measuring differences in buoyancy between a polymer sample and silver wire, in atmospheric air at different pressures, the apparently high density values are probably due to the inevitable uptake of atmospheric gases by the polymer. The densities of the two annealed samples are similar, i.e. 2.431 g cm^{-3} for polymer annealed at 100 °C and 2.437 g cm^{-3} for the film annealed at 200 °C. This suggests similar levels of crystallinity. Both the annealed sample densities are significantly higher than the value obtained for the as-received polymer of 2.259 g cm^{-3}.

The liquid displacement method for measuring densities of the FEP samples at 25 °C gave values of 2.169 g cm^{-3} for the as-received polymer, 2.158 g cm^{-3} for the sample annealed at 100 °C and 2.191 g cm^{-3} for the sample annealed at 200 °C. Huang and Kanitz[103] give a value of 2.148 g cm^{-3} for the density of FEP, and the data sheet supplied by the manufacturers gives a

typical density value for the polymer of 2.15 g cm^{-3}. Using values for the amorphous density of 1.96 g cm^{-3} [116] and the crystalline density of 2.31 g cm^{-3} as before using equation 4.2 gives weight % crystallinities of 60.6 for the as-received sample, 58.3 for the sample annealed at 100 °C and 77.8 for the sample annealed at 200 °C.

Although an increase in crystallinity is indicated on changing the annealing temperature from 100 °C to 200 °C, the as-received polymer is apparently more crystalline than the 100 °C annealed polymer. This does not agree with the results obtained using DSC and infra-red absorption spectroscopy. The discrepancy probably arises because of the low precision of the density measurements.

Infra-red absorption spectroscopy was used as a technique to detect changes in the volume % crystallinity of the FEP on annealing. Absorbance ratios of the amorphous and reference bands at 778 cm^{-1} and 2367 cm^{-1} are listed in Table 21. If it is assumed that the density of as-received FEP is 2.15 g cm^{-3} then the volume % crystallinity can be calculated as 54.3% using the equation (1.18).

This value for the volume % crystallinity of the as-received sample can now be used to calculate the crystalline fraction of the annealed samples which is given by the expression,

$$1 - \left[(1 - 0.543)\ \frac{\text{Absorbance ratio of annealed sample}}{0.795}\right]$$

where 0.795 is the absorbance ratio of the as-received FEP and (1 - 0.543) is the amorphous fraction of the as-received FEP. Substituting the experimentally determined absorbance ratios in the above equation gives volume % crystallinities of 58.7 % for the FEP annealed at 100 °C and 64.6 % for the film annealed at 200 °C, and weight % crystallinities of 62.6 and 68.3 respectively.

The results obtained using the techniques of infra-red absorption spectroscopy and DSC both indicate differences in the levels of crystallinity for the FEP annealed at 100 °C and 200 °C. Further evidence is presented in the next section on static sorption measurements which also supports the idea of crystallinity levels increasing at the higher annealing temperature.

Although diffusion rates do not necessarily decrease with increasing levels of crystallinity, it is likely that lower levels of amorphous material and therefore a smaller fraction accessible to the diffusing molecules will lead to lower diffusion rates and higher E_d values. This was observed for methane transport through the two samples of FEP with different amounts of crystallinity.

4.8 Static Sorption Measurements

Sorption isotherms are shown in Fig. 31 for the uptake of dichloromethane by FEP in the as-received state, annealed at 100 °C and annealed at 200 °C. The isotherm for the as-received polymer and the polymer annealed at 100 °C are almost superimposable showing a linear region up to a pressure of about 25 torr followed by a curved region up to about 70 torr with a linear region at higher pressures. The isotherm for the FEP

Fig. 31 SORPTION ISOTHERMS FOR THE UPTAKE OF DICHLOROMETHANE BY FEP FILM

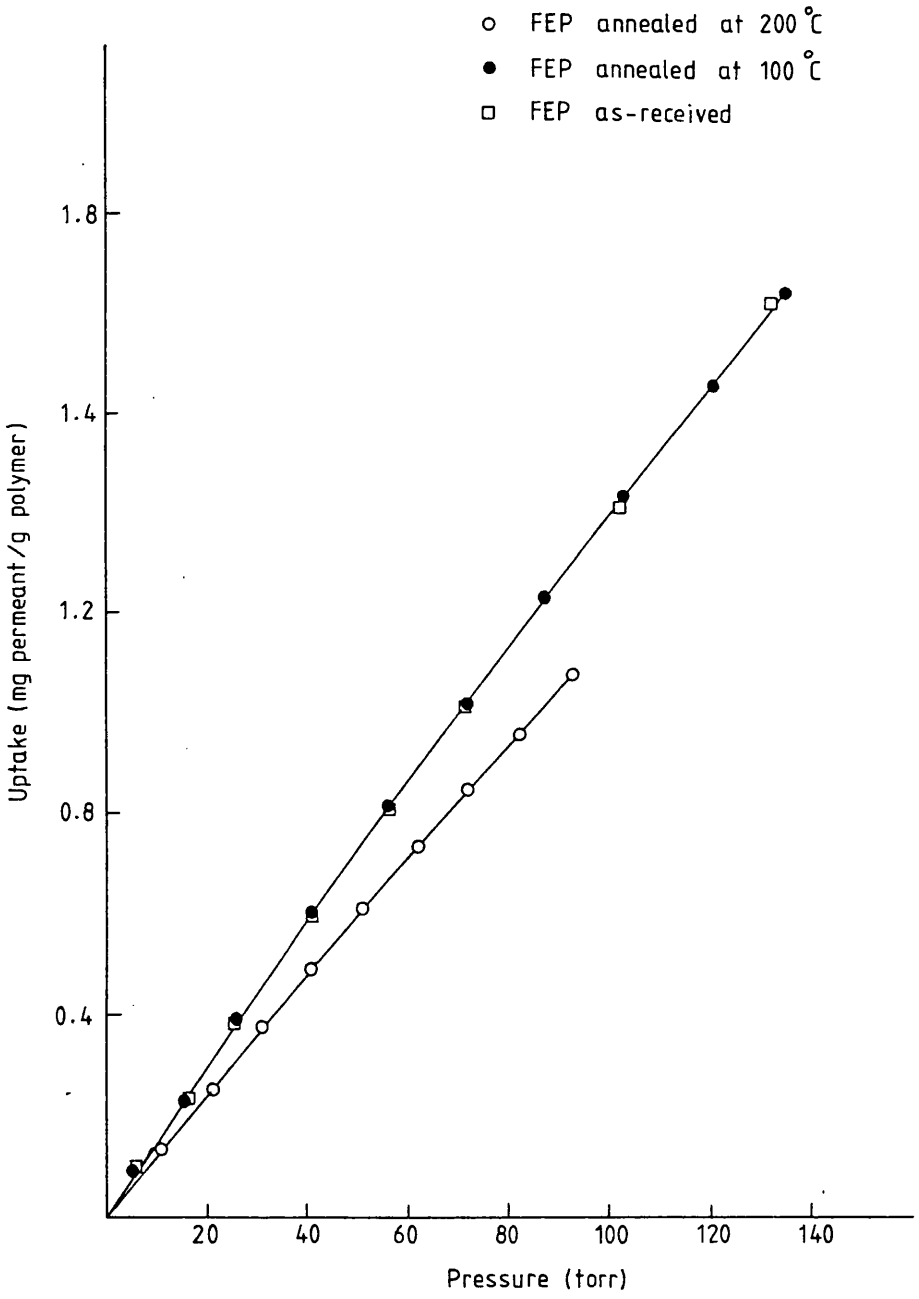

annealed at 200 °C shows the same three regions but with lower sorption levels. These non-linear isotherms are characteristic of a dual-mode type sorption where the uptake of gas or vapour can be explained by a combination of ordinary dissolution and Langmuir type adsorption in pre-existing microvoids. At high pressures the microvoids are saturated and linear Henry's Law sorption is followed.

If it is assumed that the gas or vapour only dissolves in the amorphous fraction of the polymer, then the Henry's Law constant calculated from the linear high pressure region can be used as a basis for estimating the crystalline fraction of the polymer. The Henry's Law constant for a polymer sample is given by αk_D where α is the amorphous fraction per unit weight of polymer and k_D is the Henry's Law constant for 100 % amorphous polymer. The weight % crystallinity of as-received FEP has previously been calculated as 58.3 % using Renekers[116] values for the crystalline and amorphous densities and a density of 2.15 g cm^{-3} given by the manufacturer for the as-received polymer. A value for k_D can now be calculated from the known amorphous fraction of the as-received polymer and the gradient of the linear region of the sorption isotherm. k_D can be used together with the gradients of the Henry's Law region of the sorption isotherms obtained using the annealed polymers, to give weight % crystallinities of 59.3 % for the FEP annealed at 100 °C and 66.6 % for the FEP annealed at 200 °C. These results show a significant increase in crystallinity on annealing at the higher temperature and therefore agree with the DSC and infra-red absorption measurements.

Michaels, Vieth and Barrie[61] working with PET provided the first quantitative description of the solubility of several gases in a glassy polymer. They found that non-linear isotherms could be explained in terms of a Langmuir part, and a Henry's Law part. The equation that fitted their data is given in section 1.8 of the Introduction (equation 1.14). As explained earlier, the Henry's Law dissolution constant can be obtained from the slope of the high pressure region of the isotherm. This can then be used to calculate the dissolved concentration, C_D, which in turn by subtraction from the total concentration gives the concentration in the microvoids, C_H. If the dual sorption equation applies to the system under investigation, a plot of p/C_H versus p is linear with a gradient of $1/C'_H$ and an intercept of $1/ C'_H b$

Sacher and Susko[57] found that Henry's Law plots for the sorption of water vapour by FEP did not intercept the origin and suspected a dual-mode process to be occurring. Fig. 32 shows plots of p/C_H versus p for the sorption of dichloromethane by FEP in the as-received state, annealed at 100 °C and annealed at 200 °C. Since the plots are not linear sorption cannot be explained by a simple dual-sorption model. Berens et al[117,118] found that whereas the dual sorption model explained satisfactorily the sorption of CO_2 by poly(vinylchloride) relaxation controlled swelling of the polymer was responsible for a significant portion of the total sorption of organic vapours. Since in this work the equilibrium sorption of dichloromethane by the FEP film took several hours, it is likely that relaxation

Fig. 32 PLOT OF P/C_H AGAINST PRESSURE FOR THE UPTAKE OF DICHLOROMETHANE BY FEP

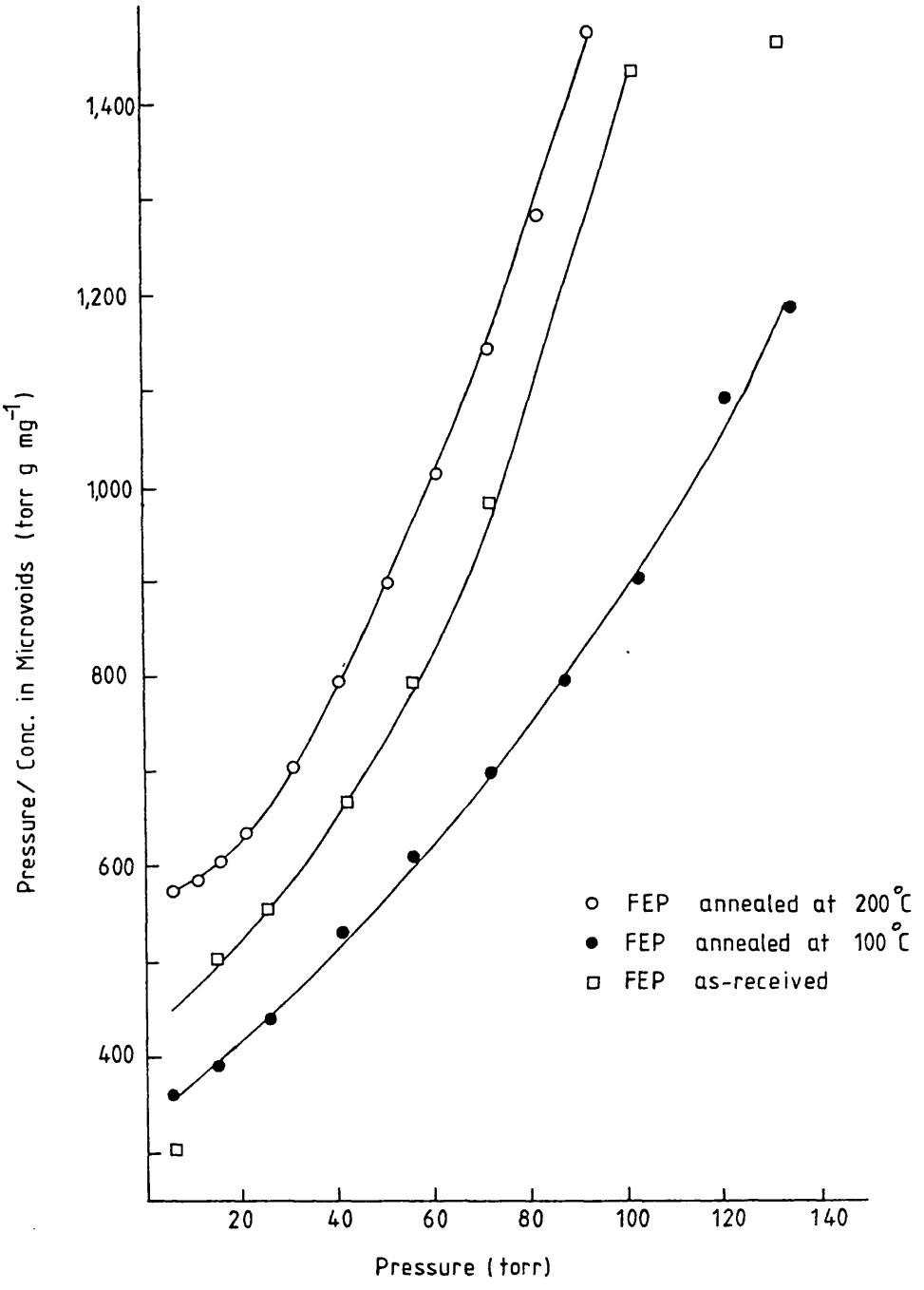

controlled swelling of the polymer made a contribution towards the total sorption of dichloromethane. This would explain why a plot of P/C'_H against p is not linear indicating that the simple dual-sorption model does not apply.

Fig. 33 shows the uptake of tetrachloroethylene at 30 °C by FEP film in the as-received state up to a relative pressure of 0.2. The plot is linear and therefore not characteristic of the downward curvature shown by the dual mode type sorption. Since the diffusion rate into the polymer of the larger tetrachloroethylene molecule was slower than dichloromethane, equilibrium sorption took longer to be achieved probably resulting in a larger proportion of the total uptake being due to relaxation controlled swelling of the polymer. This would be expected to make the simple dual-sorption model less applicable.

Fig. 34 shows the uptake of nitroethane at 30 °C by FEP film annealed at 100 °C up to a relative pressure of 0.23. The isotherm is linear showing no downward curvature characteristic of dual-mode sorption. As with tetrachloroethylene sorption relaxation controlled swelling of the polymer probably conceals any adsorption in microvoids.

Berens[58] has shown that the solubility of several gases and organic vapours is lower in heat-treated PVC samples than in samples recovered from the melt without additional heating. He[58] also found that the history-dependence of gas or vapour solubility was associated only with the "hole filling" term of the dual-mode model, with the Henry's Law term remaining the same. This suggests that no increase in the impenetrable crystalline fraction is occurring on heat treatment. Since PVC

Fig. 33 PLOT OF TETRACHLOROETHYLENE UPTAKE BY FEP AGAINST PRESSURE

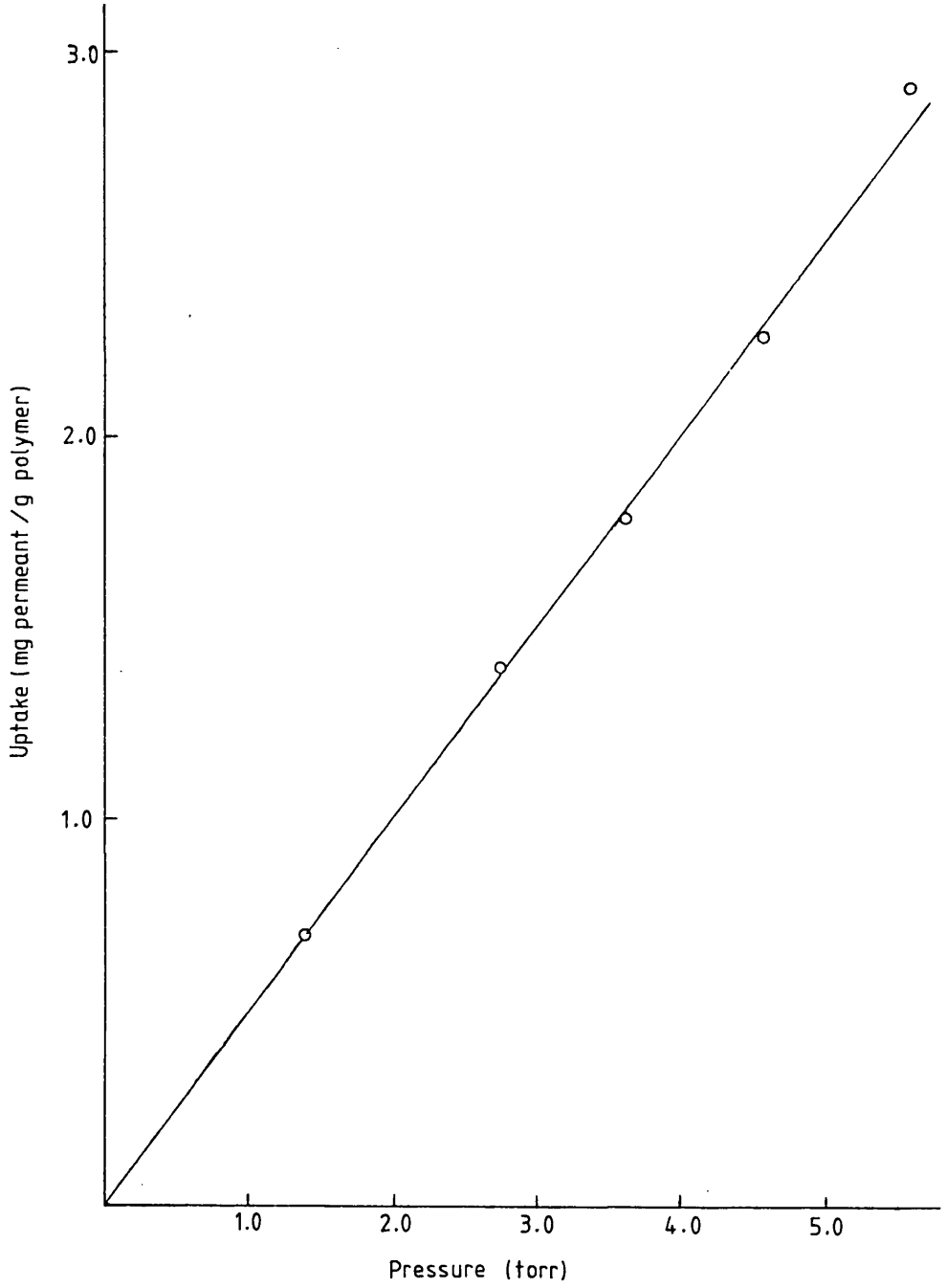

Fig. 34 PLOT OF NITROETHANE UPTAKE BY FEP AGAINST PRESSURE

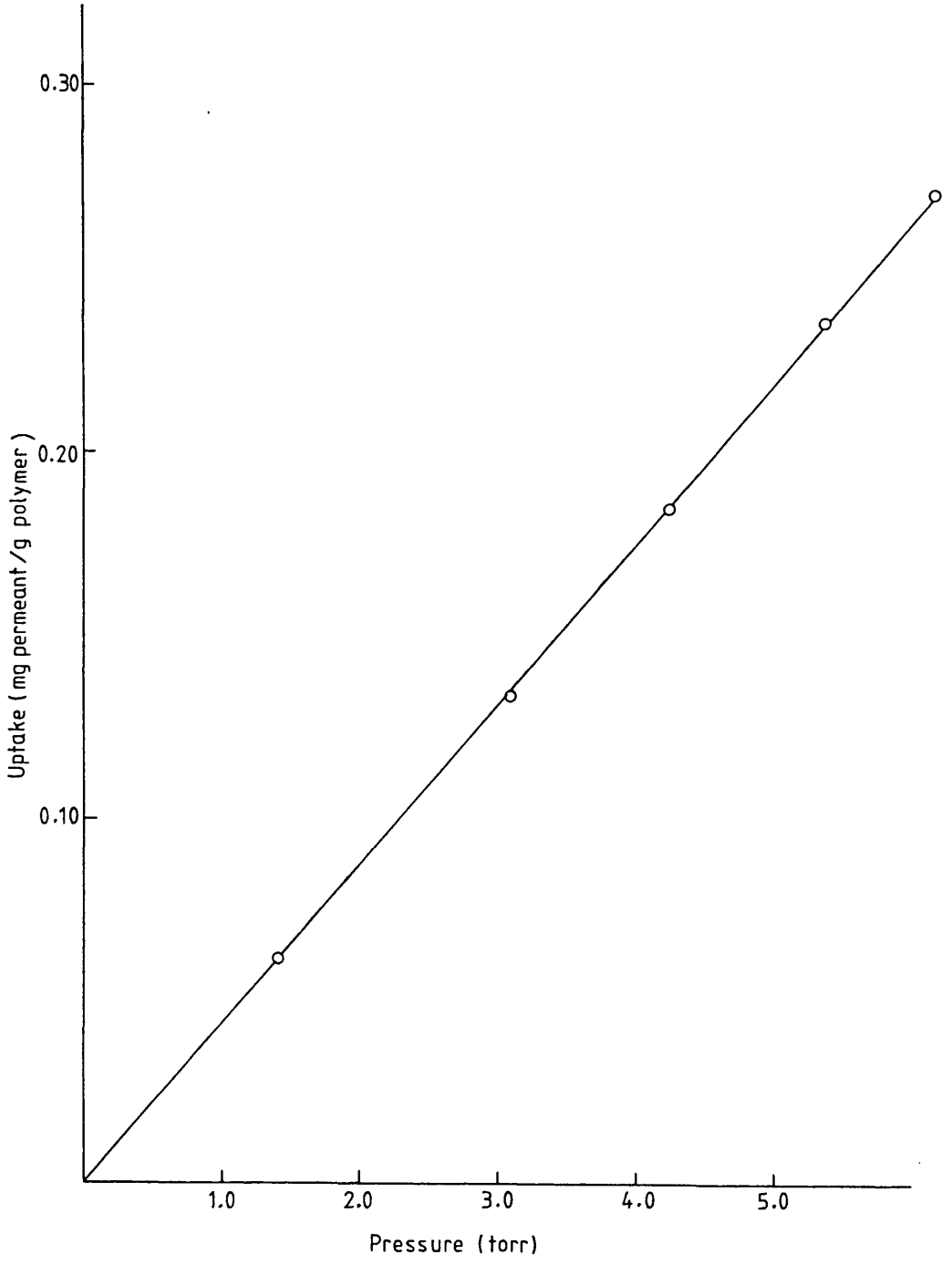

is an almost completely amorphous polymer, this seems reasonable. In this work a reduction in the Henry's Law term for dichloromethane sorption in heated-treated FEP was explained by an increased level of crystallinity in the annealed polymer. Unfortunately it was not possible to calculate Langmuirian parameters due to the non-linearity of the P/C_H versus p plot and therefore decide whether the overall reduction in solubility was due in any measure to a change in the size or number of microvoids in the structure.

Duncan et al[119] found that the permeabilities and diffusivities of benzene and methylchloride through FEP film were independent of the penetrant partial pressure, and the permeation process was well described by a Henry's Law sorption-Fickian diffusion model. However, measurements of diffusion and permeability coefficients with varying partial pressures were taken at 98 °C, and since the measurement temperature was above T_g for the polymer no dual-sorption effects would be expected.

4.9 Comparison of Solubilities Derived Using the Dynamic and Static Techniques

Table 30 shows solubility coefficients at 30 °C measured using the static sorption technique and calculated from permeability and diffusion parameters. Considering the inevitably large error in the solubility coefficients calculated from permeability and diffusion parameters which are themselves subject to error, the solubility coefficients obtained by the two methods are in reasonable agreement. It is interesting though that the values obtained from the dynamic measurements

TABLE 30 A Comparison of Solubilities in FEP at 30°C Obtained Using the Sartorius Microbalance and Calculated from the Transport Parameters Obtained Using the Dynamic Method

Permeant	Thermal Treatment	Dynamic Method Pressure/torr	Dynamic Method $^{a}S_{30°C} \times 10^{-1}$	Microbalance Method Pressure/torr	Microbalance Method $^{a}S_{30°C} \times 10^{-1}$
Dichloromethane	As-received	104.4	0.0786	-	-
"	100°C	104.4	0.0789	255	0.0778
"	200°C	104.4	0.0655	-	-
Nitroethane	100°C	5.32	0.281	10	0.241
Tetrachloroethylene	As-received	4.83	1.70	-	-
"	100°C	-	-	10	1.49

^{a}S in cm^3 (STP) cm^{-3} $torr^{-1}$

are consistently higher than the static sorption values. Michaels et al[61] used the time-lag and static sorption techniques to measure the solubility coefficients for oxygen at 25 °C and 35 °C, nitrogen at 25 °C and 40 °C, and carbon dioxide at 70 °C in crystalline PET. These measurements obtained using the two techniques were found to fall on the same correlation line whereas data points for carbon dioxide at 40 °C obtained by the time-lag method fell above the correlation line. Michaels et al[61] explained this apparently greater solubility by suggesting that the time-lag experiment included the effects of "hole-filling" which delayed the achievement of steady-state. The resulting apparent diffusion coefficient is lower than the actual one giving a higher value for the solubility coefficient. Since this effect was only seen for the larger carbon dioxide molecule Michaels et al[61] considered the diffusion medium to be homogeneous for nitrogen and oxygen.

In this work diffusion coefficients were determined from the slope of the transient response which would clearly be reduced if molecules were impeded due to microvoids being present in the structure. This would therefore reduce the measured diffusion coefficient which would in turn increase the apparent solubility coefficient. It seems likely that this explains the larger solubilities derived from the dynamic measurements. It is interesting that better agreement is seen between the two solubilities obtained for the smaller dichloromethane molecule, i.e. 0.00789 cm^3 (STP) cm^{-3} $torr^{-1}$ and 0.00778 cm^3 (STP) cm^{-3} $torr^{-1}$ compared with 0.0281 cm^3 (STP) cm^{-3} $torr^{-1}$ and 0.0241 cm^3 (STP) cm^{-3} $torr^{-1}$ for nitroethane, and

0.170 cm^3 (STP) cm^{-3} $torr^{-1}$ and 0.149 cm^3 (STP) cm^{-3} $torr^{-1}$ for tetrachloroethylene. This follows the same pattern as Michaels[61] results where the smaller nitrogen and oxygen molecules showed good correlation whereas differences were found for the larger carbon dioxide molecule.

Table 30 shows that the solubility of tetrachloroethylene at 30 °C is much higher than nitroethane despite the fact that their normal boiling points (T_b) of 394.3 K for tetrachloroethylene and 388.2 K for nitroethane are similar. Dichloromethane has a T_b of 313.2 K and therefore as expected, considering that solubility is a function of the condensibility of the vapour, shows a lower solubility than the other two permeants.

Starkweather[120] has measured the uptake of organic liquids by FEP. This work showed that the permeants could readily be divided into two categories, those which contain hydrogen and those which do not. The sorption of the hydrogen-containing compounds was always low, with less than a 1% increase in weight shown in most cases, and did not depend on the solubility parameter over a wide range. Compounds that did not contain hydrogen were found to be taken up much more readily with the weight gain being strongly dependent on the solubility parameter, δ, declining from the maximum amount near $\delta = 6$ $cal^{\frac{1}{2}}$ $cm^{-3/2}$ to less than 1% at $\delta = 10$ $cal^{\frac{1}{2}}$ $cm^{-3/2}$. Other workers[121,122] have found anomalously low miscibilities of fluorocarbons and hydrocarbons.

The much larger solubility of tetrachloroethylene in FEP than the hydrogen containing nitroethane is in line with the

results found by Starkweather[120]. Since the condensibilities of the vapours are similar the difference in solubilities must be accounted for by a greater interaction between FEP and tetrachloroethylene producing a more negative enthalpy of solution. Thus it would appear that FEP favours chloro-organic rather than nitro-organic molecules.

4.10 Future Work

In view of the differences found for the solubilities of nitroethane and tetrachloroethylene in FEP it would be interesting to examine the solubility of other compounds of similar condensibility. Using molecules of varying hydrogen content and dipole moment might yield relationships between these factors and the solubility, this would then give an indication of the expected degree of interaction between a given permeant and FEP.

It was also interesting to notice the closer agreement between solubilities determined for the smaller molecules using the static and dynamic methods. Since measurements were only made for dichloromethane, nitroethane and tetrachloroethylene it would be informative to study permeants with both a larger and smaller molecular size than the size range covered by the permeants used in this work.

Methylchloride and dichloromethane are both included in the graph of E_d against d^2 and are seen to fall below the line drawn through all the permeants. It would be interesting to include measurements for trichloromethane and carbon tetrachloride in this graph and determine whether this trend is

continued. Attempts to measure density of the FEP film using liquid displacement and buoyancy in air techniques were not very successful. A better method might be to use a density gradient column, where a direct comparison could be made between FEP sample densities and hence crystallinities.

CONCLUSIONS

(i) Permeability coefficients and activation energies for permeation for the transport of methane through low density PE measured using the dynamic system agreed well with literature values, provided measurements were made at ascending temperatures.

(ii) Arrhenius plots of permeability coefficients for the systems PET/nitroethane and PET/dichloromethane were linear both above and below T_g with a smaller gradient and hence activation energy for permeation in the lower temperature region. Arrhenius plots of diffusion coefficients for the two systems were linear above T_g with deviations from linearity being found below T_g.

Arrhenius plots of permeability coefficients for the transport of methane, dichloromethane, nitroethane and tetrachloroethylene through FEP were linear both above and below T_g with the plots for dichloromethane, nitroethane and tetrachloroethylene showing a break point at T_g. Arrhenius plots of diffusion coefficients only showed a break point for tetrachloroethylene permeation. It is concluded from these results that the degree of change in E_p and E_d at T_g is associated with the size of the permeant molecule, the larger the molecule the greater the change in activation energies.

(iii) For a given polymer film E_d increased and diffusion rates decreased with increasing size of the permeant molecule. This is expected considering the greater energy required to overcome cohesive forces in the polymer for the transport of larger permeant molecules through the film.

(iv) Levels of crystallinity in FEP film increased on annealing. Higher levels of crystallinity were found for polymer annealed at 200 °C than polymer annealed at 100 °C. Annealing at the higher temperature also produced a higher E_p for methane permeation.

(v) A comparison of solubilities for dichloromethane, nitroethane and tetrachloroethylene in FEP measured using a microbalance, and determined from the transport parameters showed reasonably good agreement. The solubilities determined from the dynamic technique were consistently higher than those determined using the static method. This effect was attributed to microvoids present in the FEP film reducing the apparent E_d and hence increasing the solubilities determined by the dynamic technique.

(vi) A plot of E_d against the molecular diameter squared gave a linear plot with the permeants used in this work correlating reasonably well with those investigated by Duncan et al[119].

REFERENCES

1. Polymer Handbook, 2nd edition, ed. J. Brandrup and E. H. Immergut, J. Wiley and Sons, New York, 1975.

2. R. M. Barrer; J. Phys. Chem., 61, 178, (1957).

3. R. M. Barrer; Trans. Faraday Soc., 35, 628,(1939).

4. R. M. Barrer and G. Skirrow; J. Polym. Sci., 3, 549, (1948).

5. A. Aitken and R. M. Barrer; Trans. Faraday Soc., 51, 116, (1955).

6. G. J. van Amerongen; J. Appl. Phys., 17, 972, (1946).

7. P. Meares; Trans. Faraday Soc., 54, 40, (1958).

8. A. S. Michaels and H. J. Bixler; J. Polym. Sci., 50, 393, (1961).

9. V. Stannett and M. Szwarc; J. Polym. Sci., 16, 89, (1955).

10. C. E. Rogers, J. A. Meyer, V. Stannett and M. Szwarc; Technical Association of the Pulp and Paper Industry, 39, 741, (1956).

11. G. J. van Amerongen; J. Polym. Sci., 5, 307, (1950).

12. R. J. Kokes and F. A. Long; J. Amer. Chem. Soc., 75, 6142, (1953).

13. A. C. Newns; Trans. Faraday Soc., 52, 1533, (1956).

14. G. King; Trans. Faraday Soc., 41, 325, (1945).

15. F. A. Long and L. J. Thompson; J. Polym. Sci., 15, 413, (1955).

16. I. C. Watt; J. Appl. Polym. Sci., 8, 1737, (1964).

17. L. Mandelkern and F. A. Long; J. Polym. Sci., 6, 457, (1951).

18. G. S. Park; Trans. Faraday Soc., 48, 11,(1951).

19. G. S. Park; J. Polym. Sci., 11, 97, (1953).

20. E Bagley and F. A. Long; 77, 2172, (1955).

21. A. C. Newns; Trans. Faraday Soc., 52, 1533, (1956).

22. F. A. Long and I. C. Watt; J. Polym. Sci., 21, 554, (1956).

23. R. M. Barrer; J. A. Barrie and J. Slater, J. Polym. Sci., 23, 315, (1957).

24. A. Kishimoto, H. Fujita, H. Odani, M. Kurata and M. Tamura; J. Phys. Chem., 64, 594, (1960).

25. A. Alfrey, E. F. Gurnee and W. G. Lloyd; J. Polym. Sci., Part-C, 12, 249, (1966).

26. R. Laine and J. O. Osburn; J. Appl. Polym. Sci., 15, 327, (1971).

27. N. Yi-Yan, R. M. Felder and W. J. Koros; J. Appl. Polym. Sci., 25, 1755, (1980).

28. W. W. Brandt and G. A. Anysas; J. Appl. Polym. Sci., 7, 1919, (1963).

29. D. R. Paul and A. T. DiBenedetto; J. Polym. Sci., Part-C, 10, 17, (1966).

30. C. A. Kumins and J. Roteman; J. Polym. Sci., 55, 683, (1961).

31. R. Ash, R. M. Barrer and D. G. Palmer; Polymer, 11, 421, (1970).

32. W. W. Brandt; J. Phys. Chem., 63, 1080, (1959).

33. R. M. Barrer; Trans. Faraday Soc., 39, 237, (1943).

34. V. Stannett; Diffusion in Polymers, Ed. J. Crank and G. S. Park, Chapter 2, 2nd ed., Wiley-Interscience, New York, (1971).

35. A. S. Michaels and H. J. Bixler; J. Polym. Sci., 50, 413, (1961).

36. S. Prager and F. A. Long; J. Amer. Chem. Soc., 73, 4072, (1951).

37. G. Blyholder and S. Prager; J. Phys. Chem., 64, 702, (1960).

38. R. J. Kokes and F. A. Long; J. Amer. Chem. Soc., 75, 6142, (1953).

39. I. Auerbach, W. R. Miller, W. C. Kuryla and S. D. Gehman; J. Polym. Sci., 28, 129, (1958).

40. C. A. Kumins, C. J. Rolle and J. Roteman; J. Phys., Chem., 61, 1290, (1957).

41. P. Meares; J. Amer. Chem. Soc., 76, 3415, (1954).

42. P. Meares; Trans. Faraday Soc., 53, 101, (1957).

43. A. S. Michaels, W. R. Vieth and J. A. Barrie; J. Appl. Phys., 34, 13, (1963).

44. V. Stannett and J. L. Williams; J. Polym. Sci., Part-C, 10, 45, (1966).

45. H. L. Frisch; J. Polym. Sci., Part-B, 3, 13, (1965)

46. H. Yasuda and T. Hirotsu; J. Appl. Polym. Sci., 21, 105, (1977).

47. C. E. Rogers, V. Stannett and M. Szwarc; in Technical Association of the Pulp and Paper Industry, No. 23, 78, (1962).

48. W. R. Vieth, H. H. Alcalay and A. J. Frabetti; J. Appl. Polym. Sci., 8, 2125, (1964).

49. C. M. Peterson; J. Appl. Polym. Sci., 12, 2649, (1968).

50. V. M. Patel, C. K. Patel, K. C. Patel and R. D. Patel; Makromol. Chem., 158, 65, (1972).

51. W. R. Vieth and J. A. Eilenberg; J. Appl. Polym. Sci., 16, 945, (1972).

52. K. Toi; J. Polym. Sci., Part A-2, 11, 1829, (1973).

53. R. L. Stallings, H. B. Hopfenberg and V. Stannett; J. Polym. Sci., Part-C, 41, 23, (1973).

54. S. Kubo and M. Dole; Macromolecules, 7, 190, (1974).

55. J. A. Barrie, M. J. L. Williams and K. Munday; Polym. Eng. and Sci., 20, No. 1, 20, (1980).

56. W. J. Koros, A. H. Chan and D. R. Paul; J. Membrane Sci., 2, 165, (1977).

57. E. Sacher and J. R. Susko; J. Appl. Polym. Sci., 24, 1997, (1979).

58. A. R. Berens; Polym. Eng. and Sci., 20, 95, (1980).

59. P. Masi, D. R. Paul and J. W. Barlow; J. Polym. Sci., Part-C, 20, 15,(1982).

60. R. M. Barrer, J. A. Barrie and J. Slater; J. Polym. Sci., 27, 177, (1958).

61. A. S. Michaels, W. R. Vieth and J. A. Barrie; J. Appl. Phys., 34, 1, (1963).

62. W. R. Vieth and K. J. Sladek; J. Colloid Sci., 20, 1014, (1965).

63. D. R. Paul; J. Polym. Sci., Part A-2, 7, 1811, (1969).

64. J. H. Petropoulos; J. Polym. Sci., Part A-2, 8, 1797, (1970).

65. J. H. Tshudy and C. von Frankenberg; J. Polym. Sci., Part A-2, 11, 2027, (1973).

66. R. C. Goodnight and I. Fatt; J. Phys. Chem., 65, 1709, (1961).

67. A. S. Michaels, H. J. Bixler and H. L. Fein; J. Appl. Phys., 35, 3165, (1964).

68. B. Olofson; J. Tex. Inst. Trans., 47, 464, (1956).

69. W. R. Vieth, A. S. Douglas and R. Bloch; J. Macromol. Sci. - Phys., B3, 737, (1969).

70. C. W. Bunn and T. C. Alcock; Trans. Faraday Soc., 41, 317, (1945).

71. C. W. Bunn and E. V. Garner; Proc. Roy. Soc. (London), A189, 39, (1947).

72. A. Keller; Polymer, 3, 393, (1962).

73. S. W. Lasoski and W. H. Cobbs; J. Polym. Sci., 36, 21, (1959).

74. T. M. Connelly and J. C. R. Turner; Chem. Eng. Sci., 34, 319, (1979).

75. C. H. Klute; J. Appl. Polym. Sci., 36, 21, (1959).

76. W. Vieth and W. F. Wuerth; J. Appl. Polym. Sci., 13, 685, (1969).

77. A. S. Michaels and R. B. Parker; J. Polym. Sci., 41, 53, (1959).

78. R. K. Eby; J. Appl. Phys., 35, 2720, (1964).

79. J. D. Hoffman and J. J. Weeks; J. Res. Nat. Bur. Stand., 66A, 13, (1962).

80. J. D. Hoffman, G. Williams and E. Passaglia; J. Polym. Sci., Part-C, 14, 173, (1966)

81. H. Daynes; Proc. Roy. Soc., A, 97, 286, (1920).

82. H. L. Frisch; J. Phys. Chem. 61, 93, (1957).

83. R. M. Barrer and R. R. Ferguson; Trans. Faraday Soc., 54, 989, (1958)

84. P. Meares; J. Polym. Sci., 27, 405, (1958).

85. P. Meares; J. Appl. Polym. Sci., 9, 917, (1965).

86. T. L. Caskey; Mod. Plast., 45, 148, (1967).

87. K. D. Ziegel, H. K. Frensdorff and D. E. Blair; J. Polym. Sci., Part-A2, 7, 809, (1969)

88. R. A. Pasternak, J. F. Schimscheimer and J. Heller; J. Polym., Sci., Part-A2, 8, 467, (1970).

89. D. G. Pye, H. H. Hoehn and M. Panar; J. Appl. Polym., Sci., 20, 287, (1976).

90. Technique of Organic Chemistry, Vol. 1. Physical Methods Pt. 1, 3rd edition, ed. A. Weissberger, Chap. IX, p. 447, Interscience Publishers Inc., New York, (1959).

91. Computer Aided Data Book of Vapour Pressure, S. Ohe, Data Book Publishing Company, Tokyo, Japan, (1976).

92. Physical Data, Chemical Engineering, Vol. 5e, ESDU International Ltd., (1976).

93. D. H. Desty C. J. Geach and A. Goldup; Gas Chromatography, ed. R. P. W. Scott, p.46, Butterworths, London, (1960).

94. W. E. Wentworth and E. Chen; J. Gas Chrom., 5, 170, (1967).

95. J. E. Lovelock and A. Zlatkis; Anal. Chem., 39, 1428, (1967).

96. CRC Handbook of Chemistry and Physics, 63rd Ed., ed. R. C. Weast and M. J. Astle, CRC Press Inc., (1982).

97. R. G. J. Miller and H. A. Willis; J. Polym. Sci., 19, 485, (1956).

98. R. E. Moynihan; J. Amer. Chem. Soc., 81, 1045, (1959).

99. A. Bondi; J. Phys. Chem., 68, 441, (1964).

100. Encyclopaedia of Polymer Science and Technology, Ed. H. F. Mark and N. G. Gaylord Vol. 11, p.54, J. Wiley and Sons, (1969).

101. R. Waack, N. H. Alex, H. L. Frisch, V. Stannett, M. Szwarc; Ind. Eng. Chem., 47, 2524, (1955).

102. R. A. Pasternak, G. L. Burns and J. Heller; Macromolecules, 4, 471, (1971).

103. P. J. F. Kanitz and R. Y. M. Huang; J. Appl. Polym. Sci., 14, 2739, (1970).

104. H. Tschamler and D. Rudorfer; Mitt. Chem. Forschungsinst. Wirt. Oesterr. Oesterr. Kunstoffinst., 27(1), 25, (1973).

105. R. K. Eby and F. C. Wilson; J. Appl. Phys., 33, 2951, (1962).

106. R. K. Eby; J. Appl. Phys., 34, 2442, (1963).

107. R. K. Eby; J. Res. Natl. Bur. Std., 68A, 269, (1964).

108. L. H. Bolz and R. K. Eby; J. Res. Natl. Bur. Std., 69A, 481, (1965).

109. M. I. Bro and B. W. Sandt; U.S. Patent, 2,946,763.

110. Y. Akatsuka, M. Noshiro and Y. Jitsugiri; Reports Res. Lab., Asahi Glass Co. Ltd., 2, 26, (1976).

111. N. G. McCrum; Makromol. Chem., 34, 50, (1959).

112. B. P. Tikhomirov, H. B. Hopfenberg, V. Stannett and J. L. Williams; Makromol. Chem., 118, 177, (1968).

113. A. W. Lawson; J. Chem. Phys., 32, 131, (1960).

114. G. J. van Amerongen; Rubber Chem. Technol., 37, 1065, (1964).

115. J. H. Hildebrand; Proc. Nat. Acad. Sci. U.S., 57, 542, (1967).

116. D. H. Reneker, G. H. Martin, J. D. Barnes and J. P. Colson; Soc. Plast. Eng. Tech. Pap., 20, 214, (1974).

117. A. R. Berens; Polymer, 18, 697, (1977).

118. A. R. Berens and H. B. Hopfenberg; Polymer, 19, 489, (1978).

119. T. Duncan, W. J. Koros and R. M. Felder; J. Appl. Polym. Sci., 28, 209, (1983).

120. H. W. Starkweather; Macromolecules, 10, 1161, (1977).

121. R. L. Scott; J. Phys. Chem., 62, 136, (1958).

122. J. H. Hildebrand, J. M. Prausnitz and R. L. Scott; Regular and Related Solutions, van Nostrand-Reinhold, New York, (1970).